ISSN 2217-8139 (Print)
ISSN 2334-0229 (Online)
UDK: 06.055.2:62-03+620.1+624.001.5(497.1)=861

2016.
GODINA
LIX

GRAĐEVINSKI MATERIJALI I KONSTRUKCIJE

3

BUILDING MATERIALS AND STRUCTURES

ČASOPIS ZA ISTRAŽIVANJA U OBLASTI MATERIJALA I KONSTRUKCIJA
JOURNAL FOR RESEARCH OF MATERIALS AND STRUCTURES

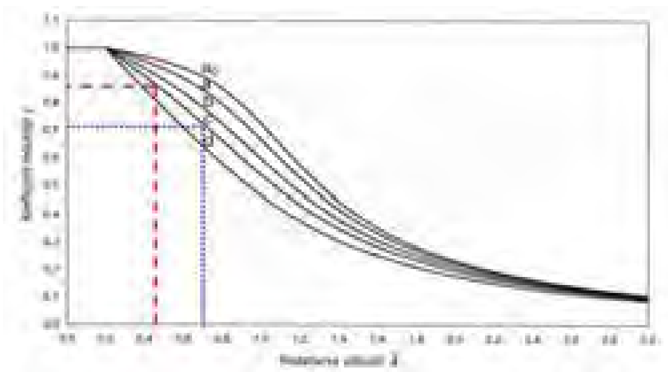

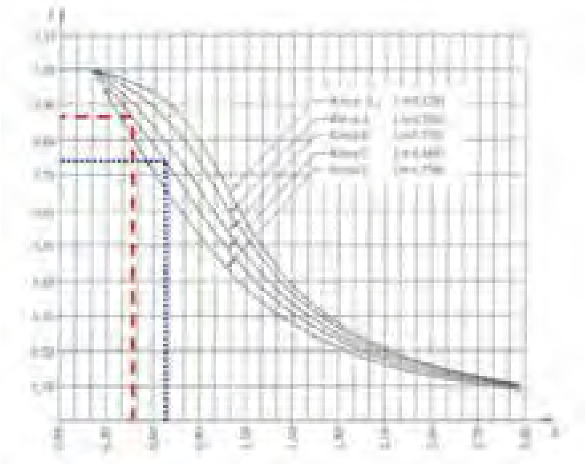

DRUŠTVO ZA ISPITIVANJE I ISTRAŽIVANJE MATERIJALA I KONSTRUKCIJA SRBIJE
SOCIETY FOR MATERIALS AND STRUCTURES TESTING OF SERBIA

DRUŠTVO ZA ISPITIVANJE I ISTRAŽIVANJE MATERIJALA I KONSTRUKCIJA SRBIJE
SOCIETY FOR MATERIALS AND STRUCTURES TESTING OF SERBIA

GRAĐEVINSKI MATERIJALI I KONSTRUKCIJE

BUILDING MATERIALS AND STRUCTURES

ČASOPIS ZA ISTRAŽIVANJA U OBLASTI MATERIJALA I KONSTRUKCIJA
JOURNAL FOR RESEARCH IN THE FIELD OF MATERIALS AND STRUCTURES

PUBLISHER

Society for Materials and Structures Testing of Serbia, 11000 Belgrade, Kneza Milosa 9
Telephone: 381 11/3242-589; e-mail:dimk@ptt.rs, veb sajt: www.dimk.rs

REVIEWERS: All papers were reviewed

KORICE: Određivanje koeficijenta χ prema EC3 i JUS-u za 1.sprat analiziranog okvira s nepomerljivim čvorovima

COVER: Determination of coefficient χ using the EC3 and JUS (first floor of the analyzed non-sway frame)

Financial supports: Mnistry of Scientific and Technological Development of the Republic of Serbia

ISSN 2217-8139 (Print)
ISSN 2334-0229 (Online)

GODINA LIX - 2016.

DRUŠTVO ZA ISPITIVANJE I ISTRAŽIVANJE MATERIJALA I KONSTRUKCIJA SRBIJE
SOCIETY FOR MATERIALS AND STRUCTURES TESTING OF SERBIA

GRAĐEVINSKI MATERIJALI I KONSTRUKCIJE

BUILDING MATERIALS AND STRUCTURES

ČASOPIS ZA ISTRAŽIVANJA U OBLASTI MATERIJALA I KONSTRUKCIJA
JOURNAL FOR RESEARCH IN THE FIELD OF MATERIALS AND STRUCTURES

SADRŽAJ

CONTENTS

CIP - Каталогизација у публикацији
Народна библиотека Србије, Београд

620.1

GRAĐEVINSKI materijali i konstrukcije : časopis za istraživanja u oblasti materijala i konstrukcija = Building Materials and Structures : journal for research of materials and structures / editor-in-chief Radomir Folić. - God. 54, br. 1 (2011)- . - Beograd (Kneza Miloša 9) : Društvo za ispitivanje i istraživanje materijala i konstrukcija Srbije, 2011- (Novi Beograd : Hektor print). - 30 cm

Tromesečno. - Je nastavak: Materijali i konstrukcije = ISSN 0543-0798
ISSN 2217-8139 = Građevinski materijali i konstrukcije
COBISS.SR-ID 188695820

CIP

PROBLEMS AND THEIR SOLUTIONS IN PRACTICAL APPLICATION OF EUROCODES IN SEISMIC DESIGN OF RC STRUCTURES

PROBLEMI I NJIHOVA REŠENJA U PRAKTIČNOJ PRIMENI EVORKODOVA ZA PROJEKTOVANJE AB KONSTRUKCIJA

Jordan MILEV

PREGLEDNI RAD
REVIEW PAPER
UDK: 624.9.042.7
699.841
doi: 10.5937/grmk1603003M

1 INTRODUCTION

The structural Eurocodes are implemented in Bulgaria for seismic design of new buildings. Moreover they are obligatory standard for design of important and significant residential and office buildings. This fact will increase margin of safety of those buildings for sure because Eurocodes are newer and more comprehensive system of structural design standards compared to old Bulgarian codes. However some problems appear in application of those new and advanced standards in Bulgarian design and construction practice.

Most of those problems are already discussed in many references (please see [1]÷[6]). The main goal of this report is to show how those problems are solved in the real application of structural Eurocodes. Special attention is paid to the problems which are developed in using Eurocode 8 in seismic design of reinforced concrete buildings.

2 MAJOR STRUCTURAL PROBLEMS IN APPLICATION OF EUROCODES IN SEISMIC DESIGN OF RC STRUCTURES

The major structural problems in application of Eurocode 8 could be roughly classified as follows:

- More comprehensive design checks, detailing rules, etc. which leads to some solutions which are not typical for the current design and construction practice;
- Requirements for application of some new technologies in execution of building structures such as higher grade concrete, effective splicing of the reinforcement, advanced detailing which ensure stable seismic response of the whole structure, etc.;
- Higher requirements for architectural and functional solutions in order to avoid the unstable and unclear seismic response of structural system of the building i.e. penalties for irregularity in plan and in elevation as well as for the torsionally flexible systems, etc.

There are completely new requirements of Eurocode 8 in comparison it with the old Bulgarian seismic standard. They could be briefly listed as follows:

- New seismic zonation which is based on the current seismic hazard definitions is implemented;
- New limit state is implemented – damage limitation level (DLL);
- Three ductility classes are presented in Eurocode 8 – low, medium, and high – DCL, DCM and DCH;
- Stiffness reduction of structural elements of seismic structure is required;
- Some precise checks for regularity in plan and elevation as well as for torsionally flexible system are required;
- The concept with "primary" and "secondary" seismic elements is implemented;
- The new structural system with "large lightly reinforced walls" is introduced;
- Capacity correction of action effects from the analysis are required;
- Capacity design procedure is applied for seismic design.

Jordan Milev, prof. PhD,
Department of Reinforced Concrete Structures,
University of Architecture, Civil Engineering and Geodesy, Sofia, Bulgaria, j.milev@yoda-bg.com

The seismic analysis of the RC structures according to Eurocode 8 is completely different compared with the old Bulgarian seismic code because of the required by Eurocode 8 capacity design procedure. This procedure requires comprehensive checks for ensuring the corresponding ductility, strength and stiffness of the structure.

The completely new checks for wall type of structures for Bulgarian design practice could be systemized as follows:

- Providing the local ductility by design of special confined boundary elements in the critical zone of the wall which in most of the cases leads to increase of the thickness of wall or application of local widening of the boundary area ("dumbbells") – both of the above solutions are not typical for Bulgarian constructions practice;
- The procedure for calculation of the length of confined boundary elements is too complicated and leads to too long confined boundary elements;
- Confined concrete application for detailing confined boundary elements in the critical zone;
- Different section design checks for shear especially for DCH where the design requirements for shear in compression strut are too high and they could hardly be fulfilled even for typical cases;
- Completely new checks are implemented i.e. sliding shear failure check at the wall base for DCH;
- Vertical web reinforcement shall be taken into account in calculation of flexural resistance of wall sections;
- Composite wall sections consisting of connected or intersecting rectangular segments (L-, T-, U-, I- or similar sections) should be taken as integral units, consisting of a web or webs parallel or approximately parallel to the direction of the acting seismic shear force and a flange or flanges perpendicular or approximately perpendicular to it;
- The detailing rules are more complicated and different comparing with old Bulgarian seismic code;

The differences between old Bulgarian seismic code and Eurocode 8 for the case of frame structures are even more significant. Some new knowledge is required for the structural design engineers to apply Eurocode 8 in the real design practice. The most important new requirements for the seismic design of frame structures which are introduced by Eurocode 8 and are completely new for Bulgarian design practice could be classified as follows:

- Local ductility requirements by the design of suitable critical regions in both beams and columns. These critical regions are detailed by application of confined concrete;
- "Strong" columns – "Weak" beams design concept;
- High requirements for the shear design of beams and columns especially for DCH;
- The detailing rules are much more complicated and difficult for fulfilling. Most problems appear with ensuring the maximum reinforcement ratio for the top beam reinforcement, the maximum diameter limitation of the bars which are bonded in the beam column joints as well as too small distance between stirrups along the splicing length of longitudinal bars in columns and walls;
- Completely new design checks are introduced, i.e. beam-column checks for DCH.

Additionally there are some problems in Eurocode 8 which are not completely clarified, i.e. as follows:

- The procedure for recognition of torsionally flexible system is not presented but it is left to the National Annex;
- The problems with distinguishing primary and secondary elements are incompletely defined;
- It is not completely explained how to reduce the stiffness of members with plastic hinges for the purpose of linear analysis;
- The requirements for ductility checks of composite wall sections are given way too generally.

Moreover the price of structures is slightly increased in comparison with the current Bulgarian practice when the building is designed according to Eurocodes. However higher increase of the building price is expected due to more strict requirements of Eurocode 8 for regularity of the structure which leads to compromising with architectural and functional features of the building.

Particularly for Bulgaria there are some additional problems in application of Eurocode 8 as follows:

- The different theoretical background of Eurocode 8 and the old Bulgarian seismic code;
- Some of the paragraphs of the Bulgarian National Annex are too general and fail to solve the problem they should solve.

Some of the problems defined above are discussed in more details bellow and some proposals for the solutions of some of them are presented (please see [6] for more details).

3 PROBLEMS AND SOLUTIONS IN GENERAL DESIGN OF RC BUILDINGS

3.1 Ductility levels

Eurocode 8 gives the possibility for application of three levels of ductility – low (DCL), medium (DCM) and high (DCH). The code does not recommend application of specific ductility level for different kind of structural types or for different level of seismicity. The only exception is the fact that DCL is not recommended (but it is not prohibited) for the areas with medium and high seismicity. In author's opinion DCL could be effectively applied for the small RC buildings, i.e. one or two--storey houses, etc. Definition of different ductility levels according to Eurocode 8 is given in Fig. 1.

However the DCH is hardly applicable to seismic design of RC wall type of buildings. The main reason for that is reduction of the bearing resistance on compression strut ($\mathbf{V_{Rd,max}}$) in the critical region by taking its value as 40% of the value outside the critical region. This strict requirement leads to the thickness of the wall in critical region which is too high for practical applications. Moreover the high thickness is usually combined with high grade of concrete in this case.

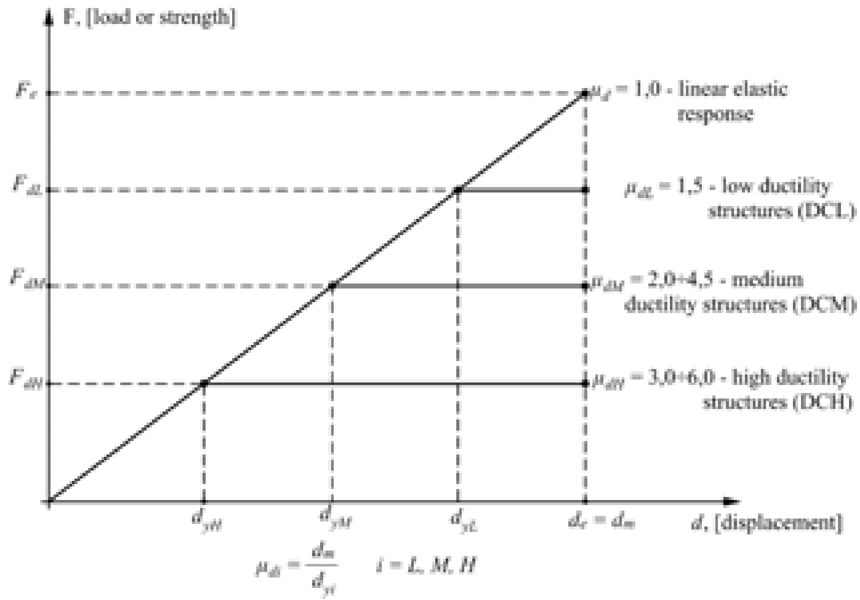

Fig. 1. Ductility levels Low, Medium and High (DCL, DCM and DCH)

3.2 Stiffness correction for linear seismic analysis of RC Structures

According to the requirements of Eurocode 8 the stiffness of the RC members for linear analysis should be reduced. However there are not detailed instructions how exactly to reduce that stiffness. It is proposed in [6] to apply the proposals of the Japanese AIJ Standard for Structural Calculations of RC Structures (from 2010) in order to reduce the stiffness of the structural elements by plastic hinges. The author's proposal based on the above mentioned standard is given in Table 1 and in Figs 2 ÷ 3.

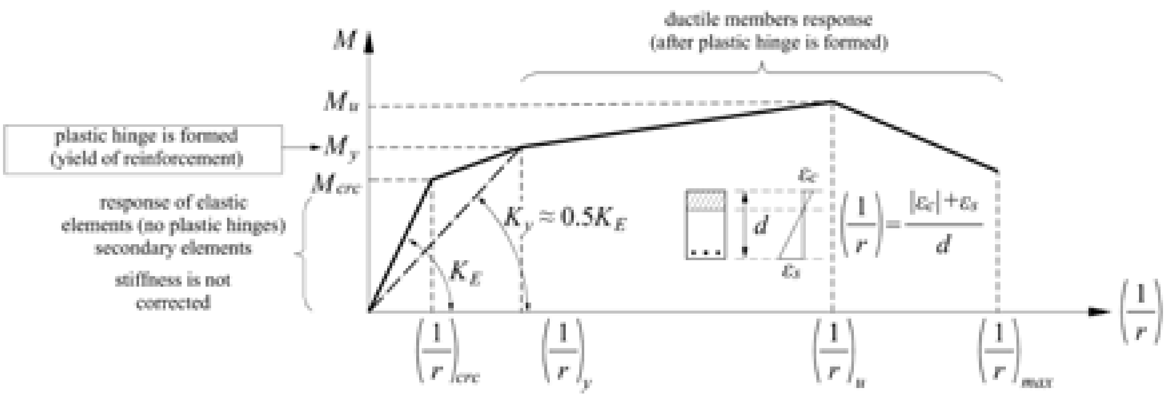

Fig. 2. Moment curvature relationship for RC section

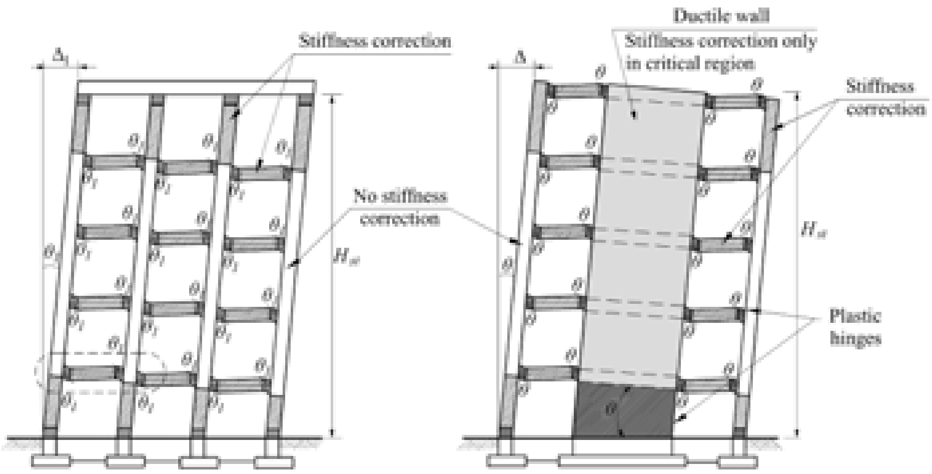

Fig. 3. Stiffness reduction for seismic members with plastic hinges according to Eurocode 8

Table 1. Proposed stiffness reduction for members with plastic hinges according to AIJ

Member		Bending stiffness	Axial stiffness	Shear stiffness
Beams	without plastic hinges	1.0	1.0 (or ∞)	1.0 (or ∞)
	with plastic hinges	0.3÷0.5	1.0 or ∞	0.3÷1.0 (or ∞)
Колони	without plastic hinges	1.0	1.0	1.0 (or ∞)
	with one plastic hinge	0.7	1.0	1.0 (or ∞)
	with two plastic hinge	0.3÷0.5	1.0	1.0 (or ∞)
Structural walls	without plastic hinges	1.0	1.0	0.5÷1.0
	with plastic hinge (stiffnes reduction applied for the hinge region)	0.3÷0.5	1.0	0.3÷0.5
Beam – column joint		-	-	1.0
Plate (floor structure)		0.0	1.0 or ∞	1.0 or ∞

3.3 Recognition of torsionally flexible systems

A lot of attention is paid in Eurocode 8 for recognition and possibly avoiding torsionally flexible systems. The penalty for torsionally flexible system is behaviour factor reduction by about 50% for such systems compared to the wall structures and even much more compared to frame structures. However Eurocode 8 fails to provide clear procedure for recognition of torsionally flexible systems. This problem is left to the National Annexes. The procedure presented below is adopted from [5] and is presented in Fig. 4 . The torsionally flexible systems are extremely dangerous during earthquakes. A heavily damaged building with such system is presented in Fig 5.

It is highly recommended to avoid torsionally flexible systems in practical seismic design of RC structures. A practical example how to avoid torsionally flexible system is presented in Fig. 6 and Fig. 7.

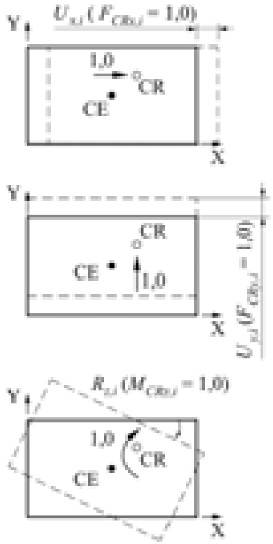

1. Three static load cases are defined for each *i* storey ($F_{CRx,i}$ = 1; $F_{CRy,i}$ = 1; $M_{CRz,i}$ = 1), with loads applied in the centre of rigidity CR;
2. The following displacements and rotations are calculated for each *i* storey:
   a. Displacement $U_{x,i}$ ($F_{CRx,i}$ = 1) at the centre of rigidity along the first principal direction of distribution of horizontal seismic action *X* for load case $F_{CRx,i}$ = 1 (force, equal to 1 with direction *X* and applied in the centre of rigidity CR at story *i*);
   b. Displacement $U_{y,i}$ ($F_{CRy,i}$ = 1) at the centre of rigidity along the second principal direction of distribution of horizontal seismic action *Y* for load case $F_{CRy,i}$ = 1 (force, equal to 1 with direction *Y* and applied in the centre of rigidity CR at story *i*);
   c. Rotation $R_{z,i}$($M_{CRz,i}$ = 1) at the centre of rigidity about vertical axis *Z* for load case $M_{CRz,i}$ = 1 (moment. Equal to 1 and applied in the centre of rigidity CR at story *i*);
3. Stiffnesses $K_{X,i}$ and $K_{Y,i}$ are calculated for each story *i* ,as well as the torsional stiffness $K_{T,i}$ as follows:

$$K_{X,i} = \frac{1}{U_{x,i}(F_{CRx,i} = 1)} \quad K_{Y,i} = \frac{1}{U_{y,i}(F_{CRy,i} = 1)} \quad K_{T,i} = \frac{1}{R_{z,i}(M_{CRz,i} = 1)}$$

4. Torsional radiuses $r_{x,i}$ and $r_{y,i}$ are calculated for each story as follows:

$$r_{x,i} = \sqrt{\frac{K_{T,i}}{K_{Y,i}}} \qquad r_{y,i} = \sqrt{\frac{K_{T,i}}{K_{X,i}}}$$

5. The system fails to be torsionally flexible if the following is verified:

$$r_{x,i} \geq l_{s,i} ; r_{y,i} \geq l_{s,i} ;$$

   a. The radius of gyration of the floor mass in plan $l_{s,i}$ is calculated generally as follows:

$$l_{s,i} = \sqrt{\frac{I_{m,i}}{m_i}}$$

   $I_{m,i}$ polar mass moment of inertia of floor mass m_i about the centre of mass for story *i*;

   m_i floor mass for story *i*

Fig. 4. Recognition of torsionally flexible system

Fig. 5. Heavy damaged office building with torsionally flexible system during the earthquake in Kobe 1995

Fig. 6. The example building as an example for avoiding torsionally flexible system

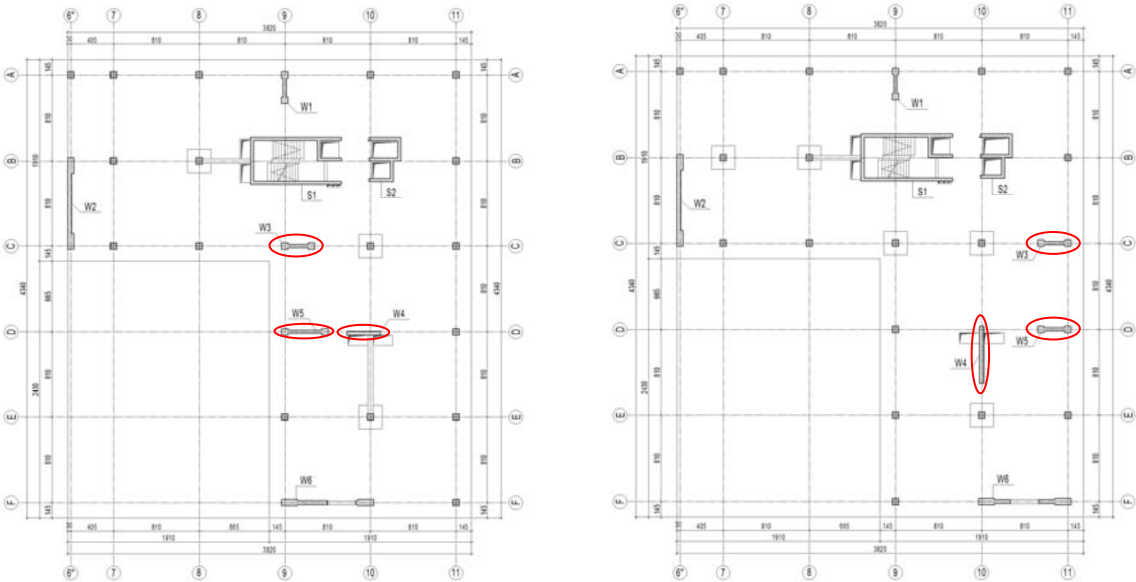

a)Torsionally flexible system *b) Wall system*

Fig. 7. Avoiding torsionally flexible system in the example building

3.4 Capacity correction of the analysis effects

The analysis effects are capacity corrected according to Eurocode 8. A bending moment envelope diagram with consideration for the tension shift is adopted taking into account modelling uncertainties and post-elastic dynamic effects. Moreover, the possible effects of increase in shear forces due to post-yield behaviour, compared to those obtained from analysis, must be considered by implementation of shear force magnification factor. Its value is ε = 1.5 for DCM, while for DCH exact calculations have to be done, taking into account overstrength, flexural capacity and structure response. In frame structures the shear failure mode is avoided by calculating design shear forces based on plastic hinge mechanism for the given member, thus allowing the element to resist the maximal shear force that can be developed before forming the mechanism. Walls correction is presented in Fig 8 ÷ 9 and for the case of frame members – in Figs 10 ÷ 11.

Capacity correction of the analysis forces is very important for seismic shear resistance of beams, columns and shear walls. Some appalling examples of shear failure in columns from past earthquakes are presented in Fig. 12.

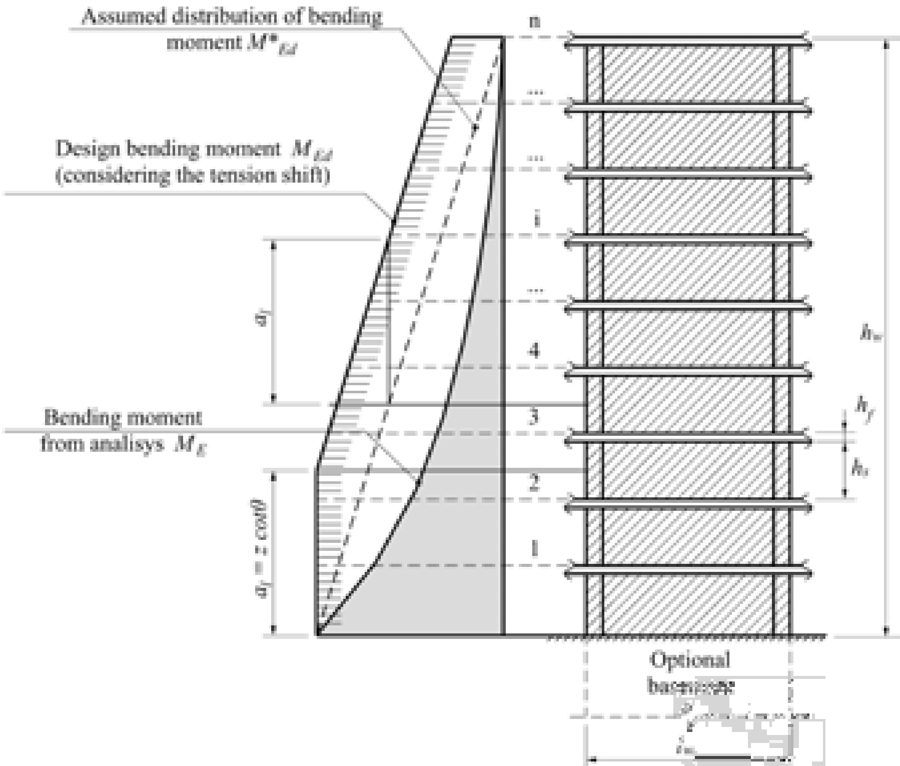

Fig. 8. Capacity corrected diagram of bending moments for a ductile wall

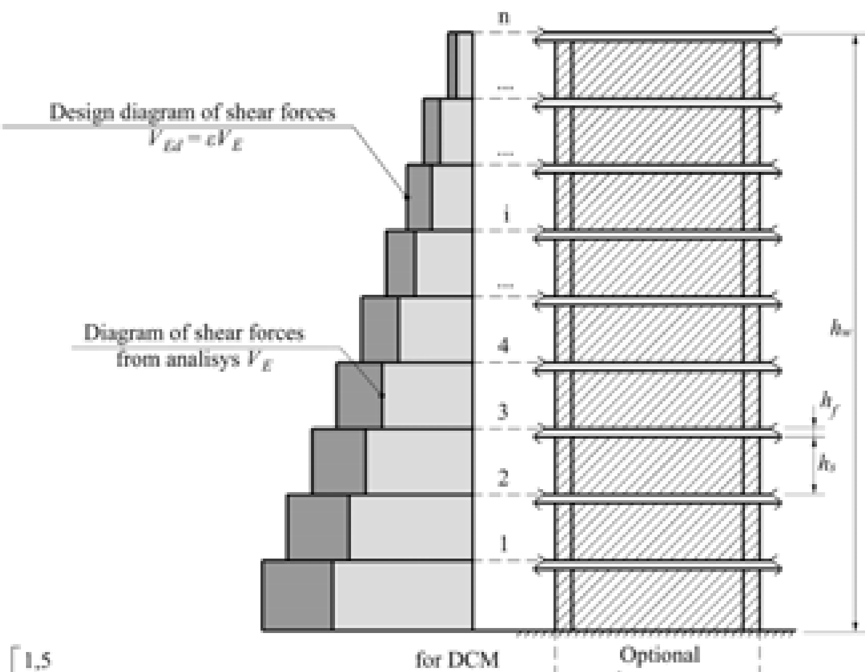

$$\varepsilon = \begin{cases} 1,5 & \text{for DCM} \\ q\sqrt{\left[\dfrac{\gamma_{Rd}}{q}\cdot\dfrac{M_{Rd}}{M_{Ed}}\right]^2 + 0,1\left[\dfrac{S_e(T_C)}{S_e(T_1)}\right]^2} \le q & \text{for DCH} \end{cases}$$

Fig. 9. Capacity corrected diagram of shear forces for a ductile wall

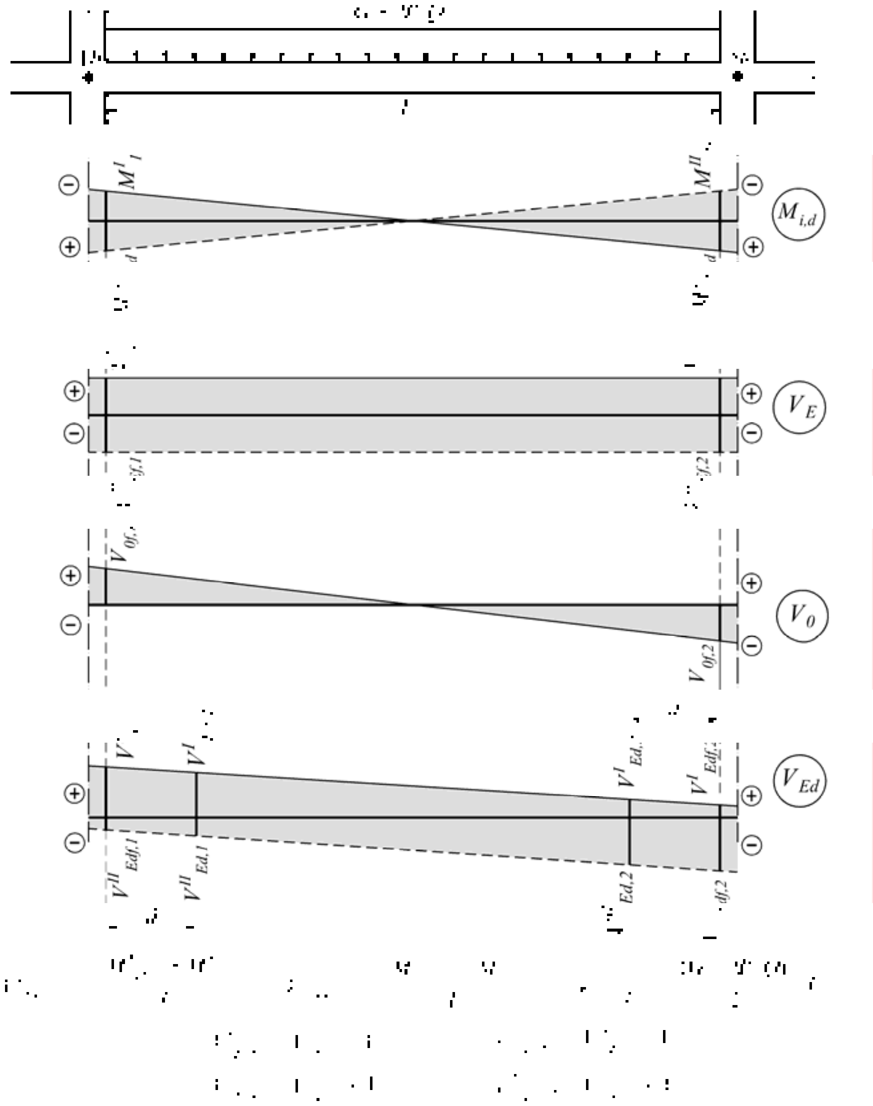

Fig. 10. Calculation of shear forces for beams, based on capacity design rules

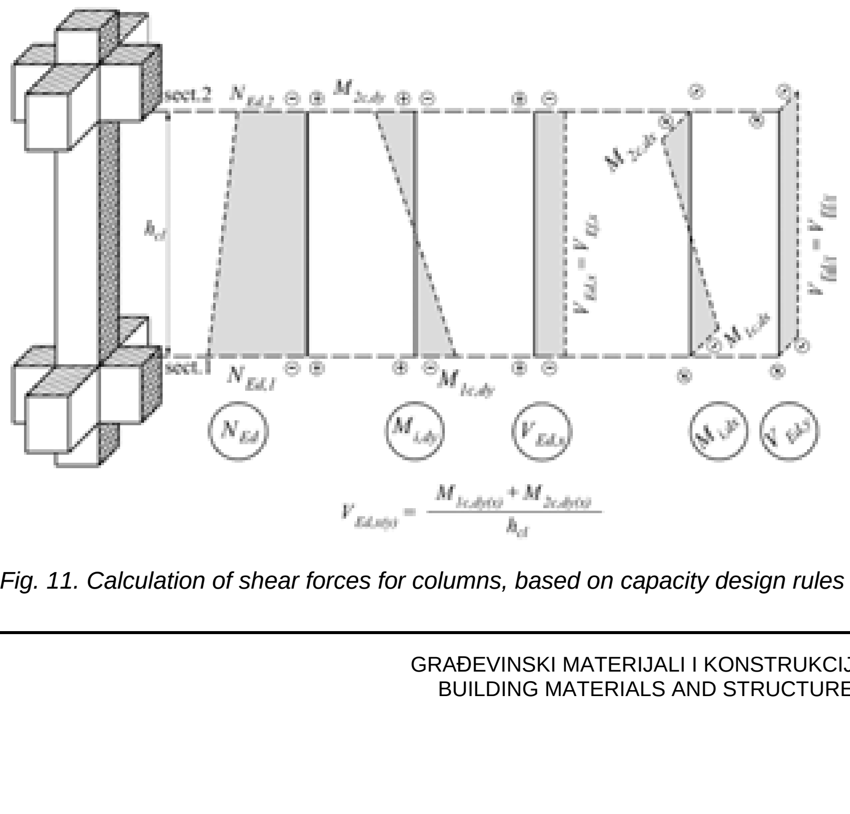

Fig. 11. Calculation of shear forces for columns, based on capacity design rules

a) Kobe 1995 *b) Turkey 1999*

Fig. 12. Shear failure of columns due to insufficient shear resistance

3.5 Wall structures with large lightly reinforced walls

Eurocode 8 defines a new type of wall for Bulgarian construction practice - Large lightly reinforced wall (LLRW), which could be applied in the wall type of structures. That type of wall effectively dissipates energy by rocking effect. However Eurocode 8 fails to completely take into account the favourable effect of rocking and therefore the behaviour factor of structural systems as well in which LLRW is included which is probably too low. The definition of LLRW and systems in which such walls are included are presented in Figs 13 ÷ 15.

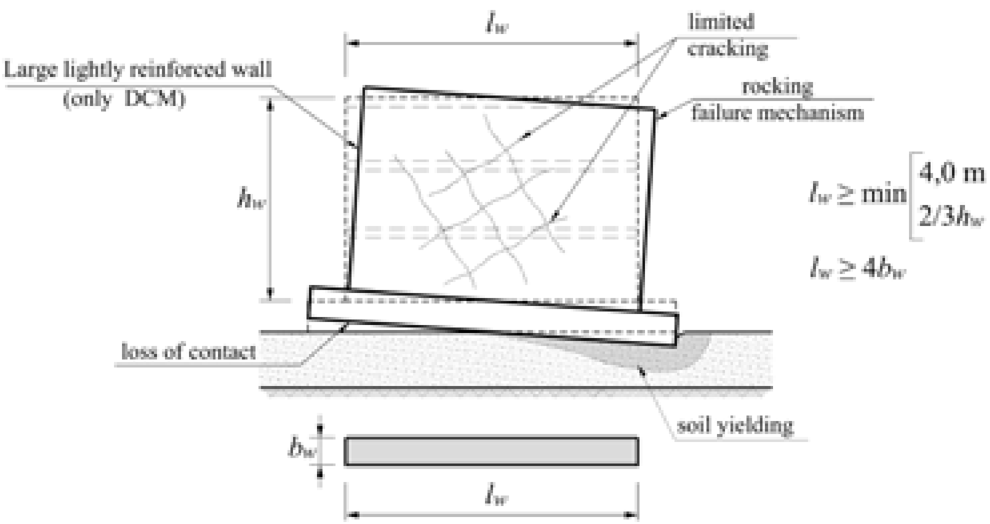

Fig. 13. Failure mechanism of large lightly reinforced walls

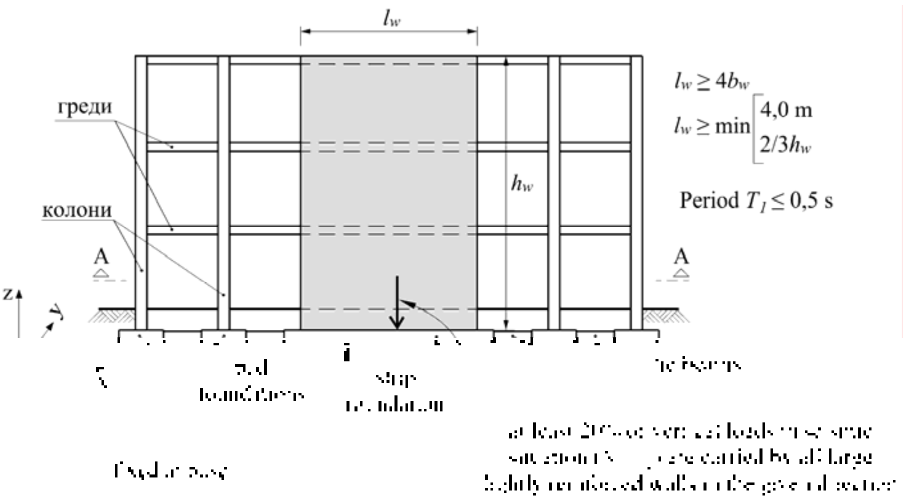

Fig. 14. Vertical section of a typical LLRW system

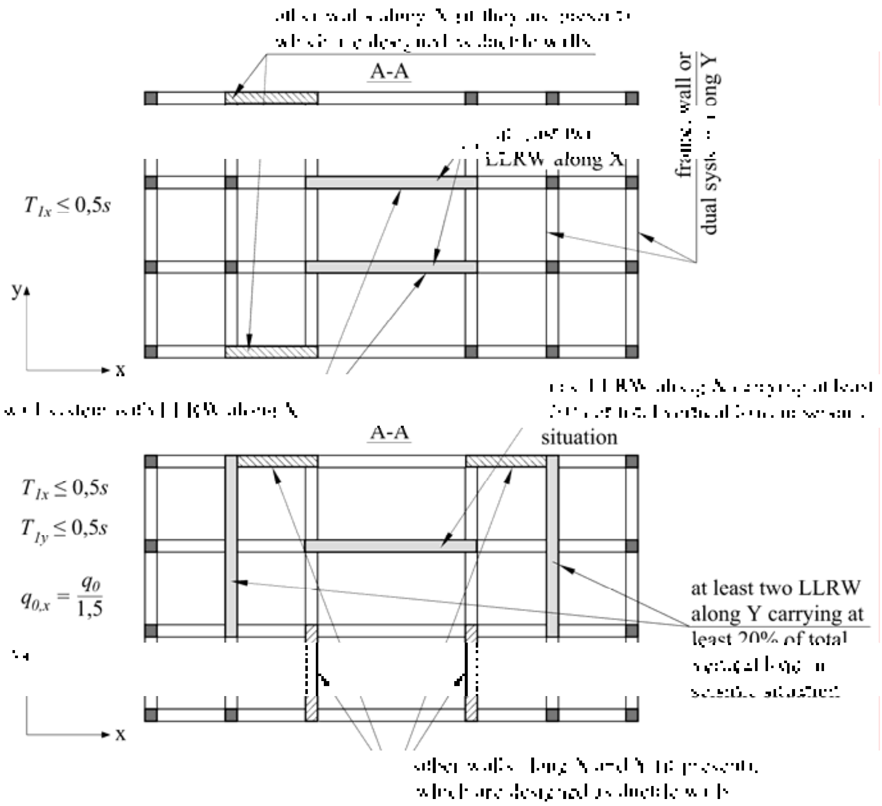

Fig. 15. Plan view of structural system LLRW is included

3.6 Primary and secondary seismic elements

The concept of primary and secondary elements is implemented in Eurocode 8.The secondary elements are not a part of the seismic structure. Their strength and rigidity could be neglected during the seismic analysis. However the whole contribution of the secondary elements to the rigidity of the structure for horizontal loading should not exceed 15% of the rigidity of all primary elements. Typical examples for secondary elements are the columns of RC wall type of buildings with flat slabs. Those elements and their connections should be designed to resist the vertical loading when they are subjected to the most unfavourable displacements by the seismic action. It is disallowed to classify some elements as secondary ones if they change structural type from torsionally flexible into some other. However Eurocode 8 provides some unclear instructions how to calculate the action effects of secondary elements in seismic design situation. A proposal for calculation of action effects in columns of RC wall type of buildings with flat slabs in seismic design situation is given in Fig 16.

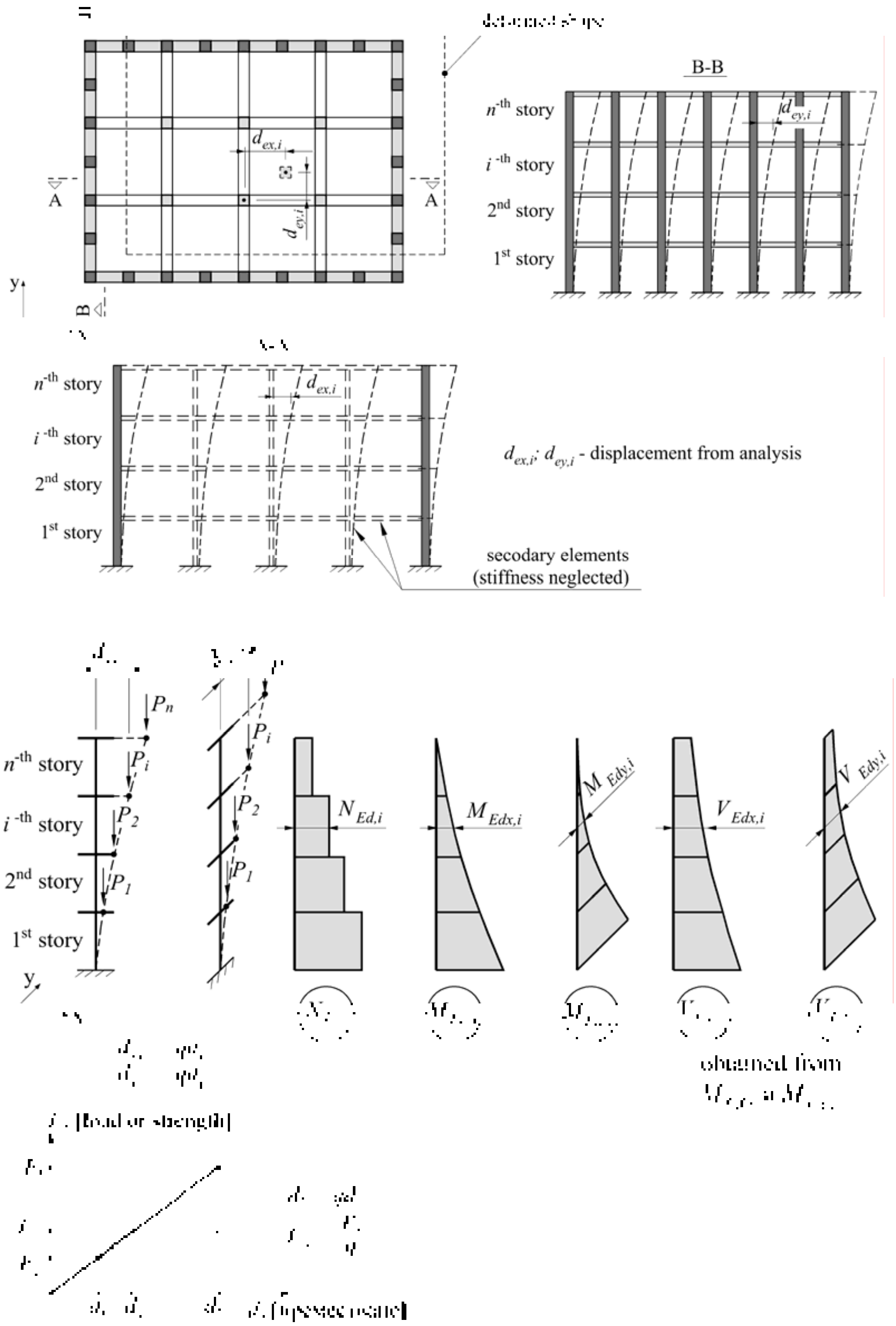

Fig. 16. Example of calculation of design action effects in secondary elements according to Eurocode 8

4 PROBLEMS AND SOLUTIONS IN THE DESIGN OF RC WALL STRUCTURES

4.1 Shear design and commentary on the inclination of the compression strut

One of the major difficulties for application of DCH for the wall type of structures is too strict requirements for the shear resistance check on compression strut. The definition of this check is presented in Fig. 17. The Eurocode 8 has very high requirements for shear design of walls. An example of shear wall reinforcement of the example building presented in Fig.6 is shown in Fig. 18. However the underestimating of shear design of walls leads to the collapse as that presented in Fig. 19.

$$V_{Ed,i} \leq \begin{cases} V_{Rd,\max} = 0{,}5\alpha_{cw} b_{wo}\, z\, v_1 f_{cd} & \text{- above critical region} \\ V_{Rd,\max} = 0{,}2\alpha_{cw} b_{wo}\, z\, v_1 f_{cd} & \text{- in critical region} \end{cases}$$

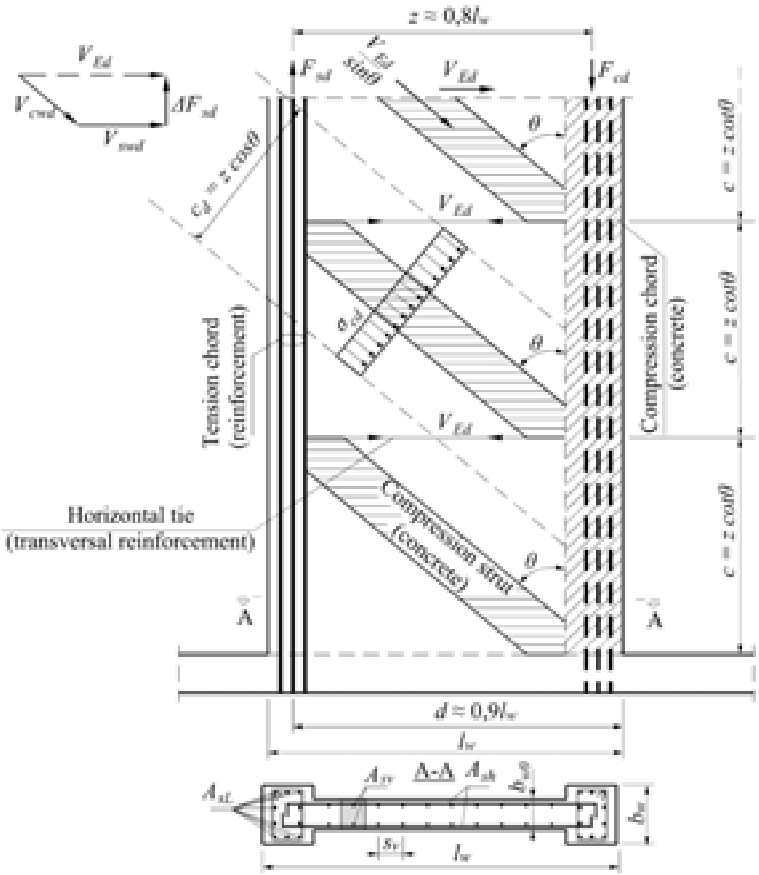

Fig. 17. Truss model for shear design of walls

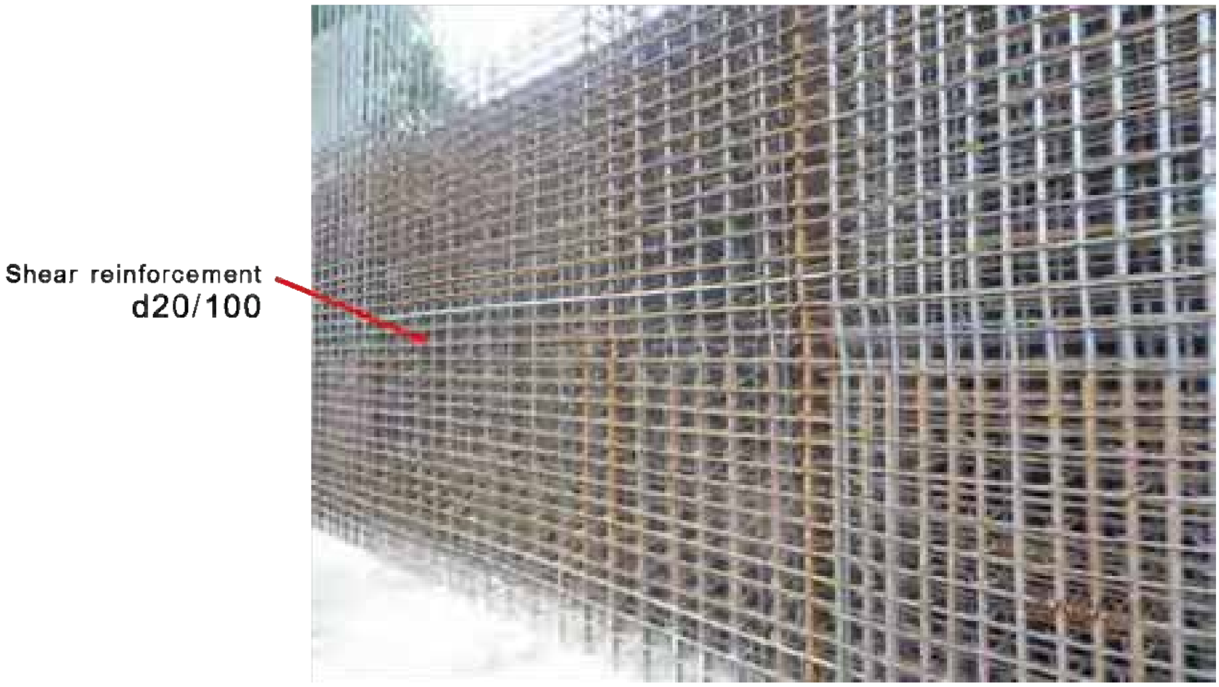

Fig. 18. Shear reinforcement in a wall designed according to Eurocode 8

Fig. 19. Heavy damaged shear wall during the earthquake in Turkey 1999

4.2 Local ductility requirements and checks

Local ductility of ductile walls is ensured by providing the confined boundary elements in the critical zone of the wall. However the procedure for calculation of the length of confined boundary elements is complicated and is partly clear in Eurocode 8 even for the case of walls with rectangular cross section. In author's opinion the procedure is iterative even for the simple cases. Some proposals for procedures for local ductility calculations for walls with rectangular and composite section are given bellow in Figs 20 ÷ 21. An example of confining reinforcement for wall structures with composite cross section designed according to Eurocode 8 is shown on Fig. 22.

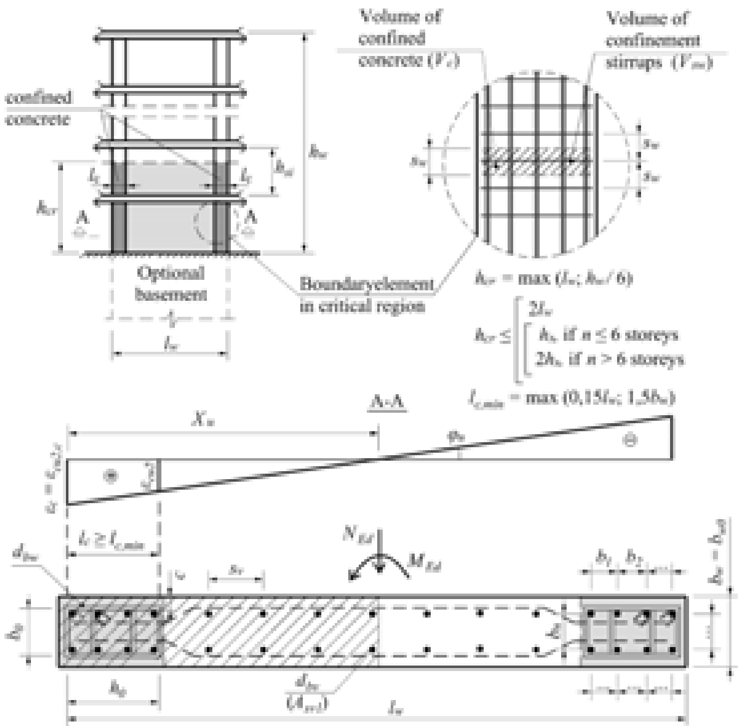

1. $X_u = (v_d + \omega_v)\frac{l_w b_{wo}}{b_o}$;
2. The length of the boundary element is assumed and confinement reinforcement is detailed;
3. $\varepsilon_{cu2,c} = 0.0035 + 0.1\alpha\omega_{wd}$
4. $l_c = X_u\left(1 - \frac{\varepsilon_{cu2}}{\varepsilon_{cu2,c}}\right)$
5. $l_c \geq l_{c,\min} = \max\begin{bmatrix} 0.15 l_w \\ 1.5 b_w \end{bmatrix}$

Steps from 1. to 5. are repeated if required

Fig. 20. Calculation of the length of boundary elements based on the requirements for local ductility

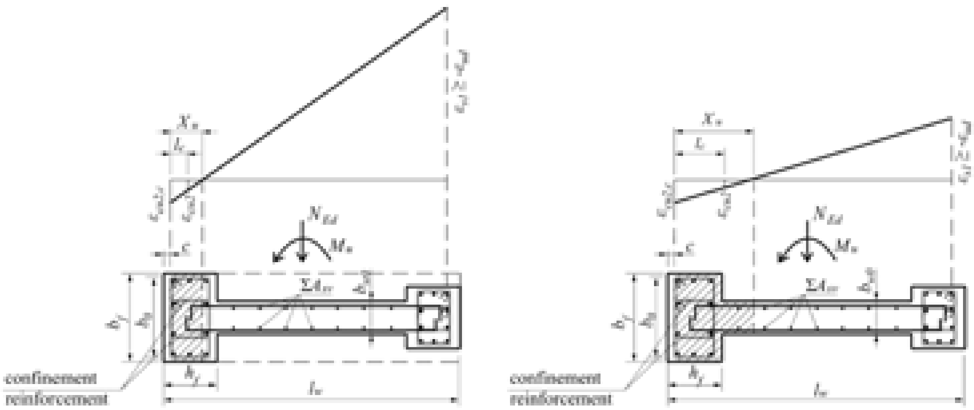

1. $X_u = (v_d + \omega_v)\frac{l_w b_{wo}}{b_o}$;

2.1 If $X_u \leq h_f$ the above procedure for rectangular section is applied assuming $b_w = b_f$

2.2 If $X_u > h_f$ the following iterative solution is proposed:

a) Confinement reinforcement is detailed and boundary elements length is assumed;

b) Equilibrium state at yield curvature is inspected and x_y and ϕ_y are calculated;

c) Equilibrium state at maximum curvature is inspected and x_y and ϕ_y are calculated;

d) Curvature ductility ratio μ is determined

$$\mu_\phi = \frac{\phi_u}{\phi_y} \geq \begin{cases} 2q_o\left(\frac{M_{Ed}}{M_{Rd}}\right)_{\max} - 1 & \text{ако } T_1 \geq T_C \\ 1 + 2(q_0 - 1)T_C/T_1\left(\frac{M_{Ed}}{M_{Rd}}\right)_{\max} & \text{ако } T_1 < T_C \end{cases}$$

e) Steps from a) to d) are repeated if required

Fig. 21. Fulfilment of local ductility requirements for composite wall sections

Fig. 22. The confining reinforcement of wall with composite section designed according to Eurocode 8 (note the example building presented on Fig. 6 and Fig.7

4.3 Detailing requirements

The detailing requirements of Eurocode 8 for ductile walls are given in Figs. 23 ÷ 24. Some special attention should be paid to detailing confined boundary elements in critical zone. An example for detailing shear walls with dumbbell cross-section is presented in Fig. 25. That shear wall is designed according to Eurocode 8 and it is from the example building shown in Fig. 6 and Fig. 7.

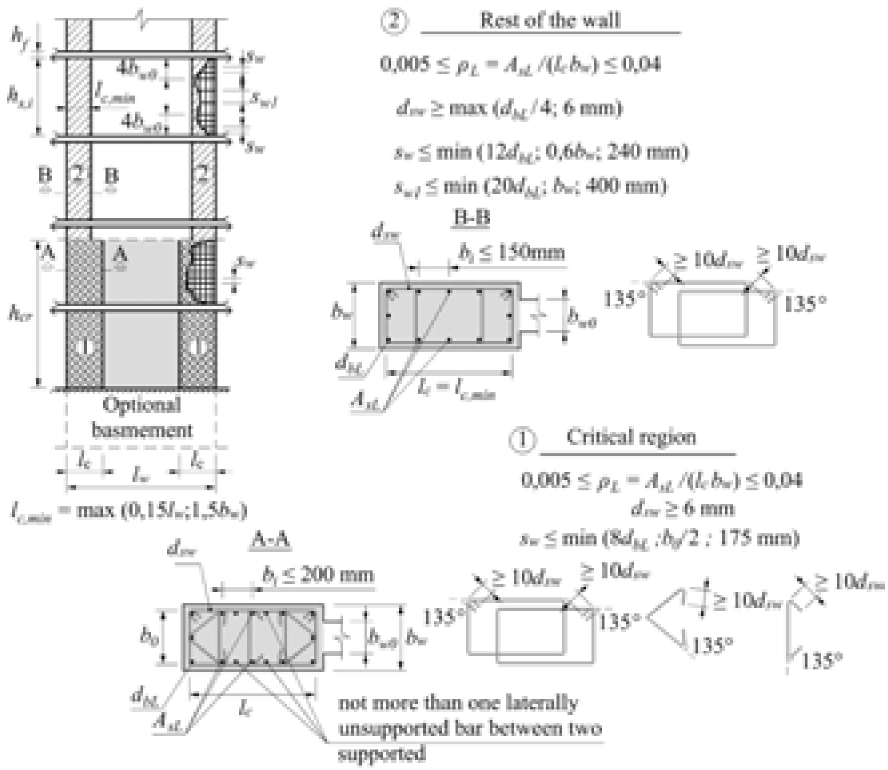

Fig. 23. Reinforcement detailing requirements for DCM

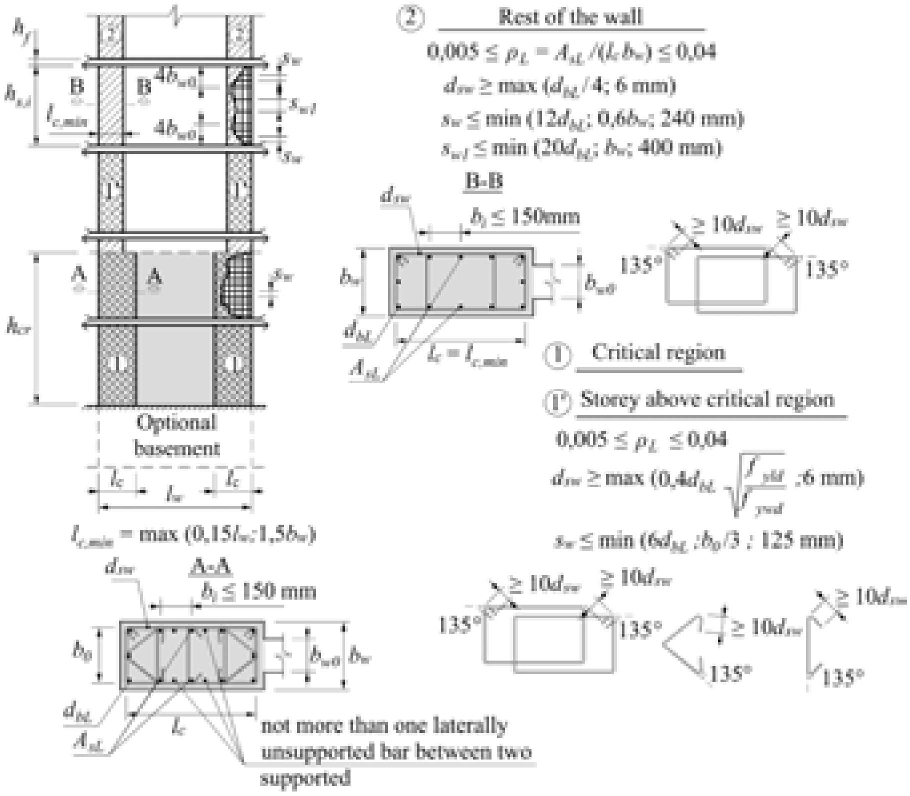

Fig. 24. Reinforcement detailing requirements for DCH

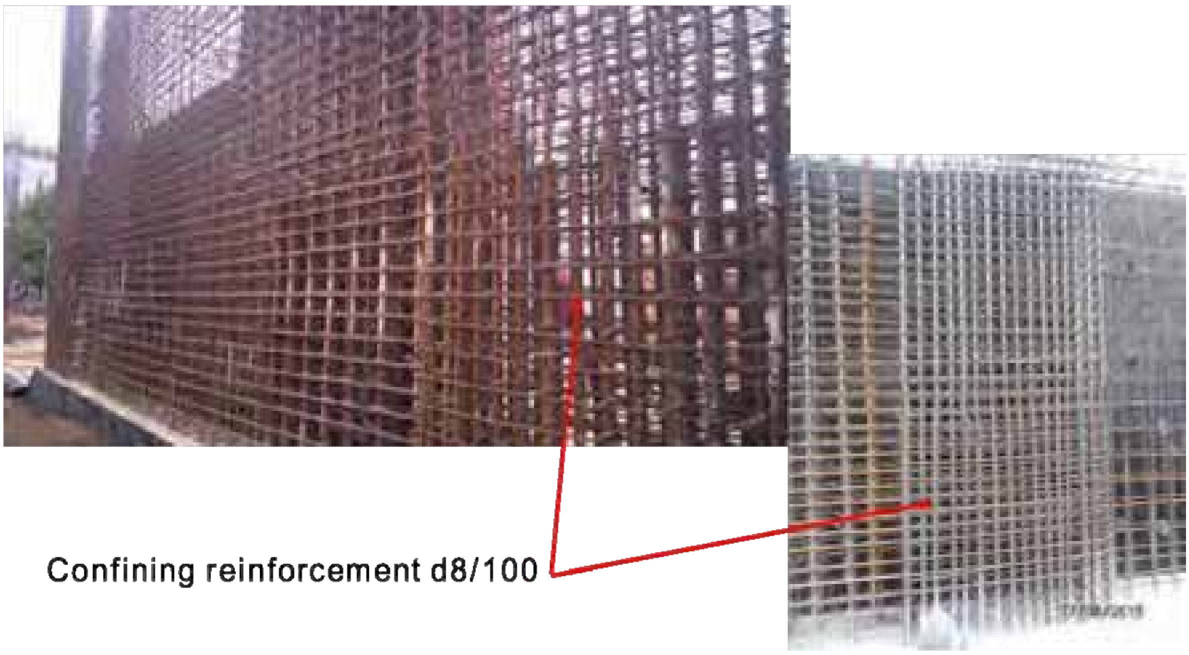

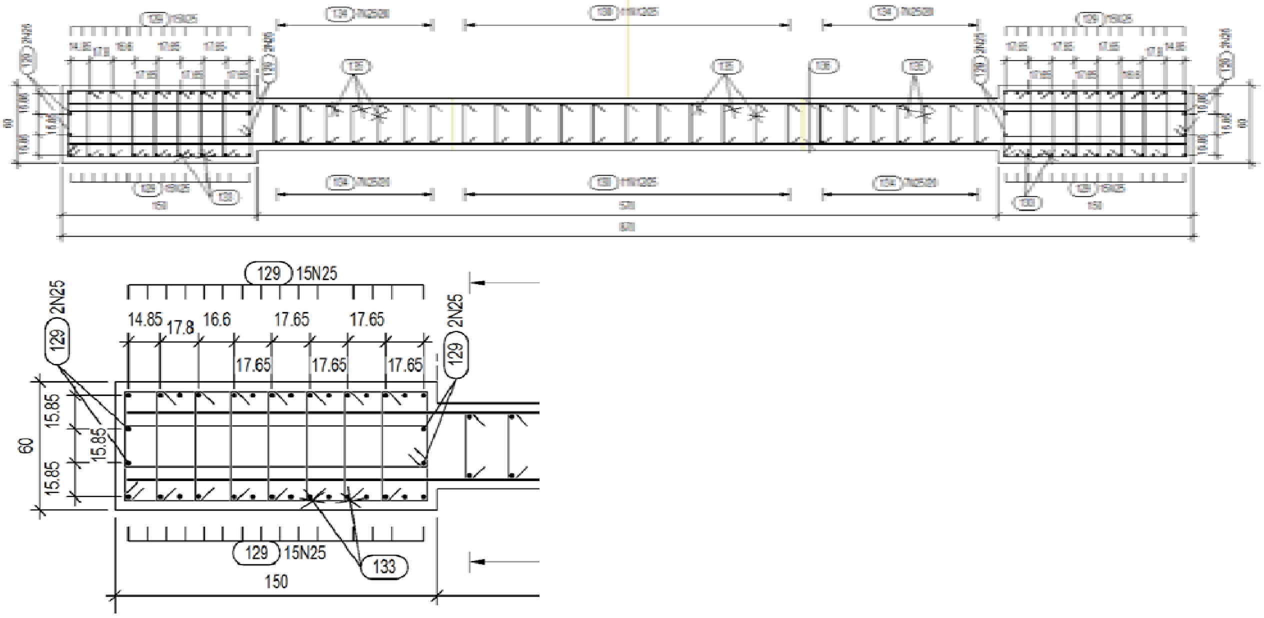

Fig. 25. An example for detailing shear wall with dumbbell cross section designed and detailed according to Eurocode 8

5 PROBLEMS AND SOLUTIONS IN THE DESIGN OF RC FRAME STRUCTURES

5.1 Strong columns-weak beams design philosophy

The "strong columns – weak beams" concept is major issue in seismic design of frame structures according to Eurocode8. That concept is presented in Figs. 26 ÷ 27.

The fulfilment of the capacity design rule "strong columns – weak beams" is very important for seismic design of frame structures. An example of braking that rule and its consequences are presented in Fig. 28 – a total collapse of building.

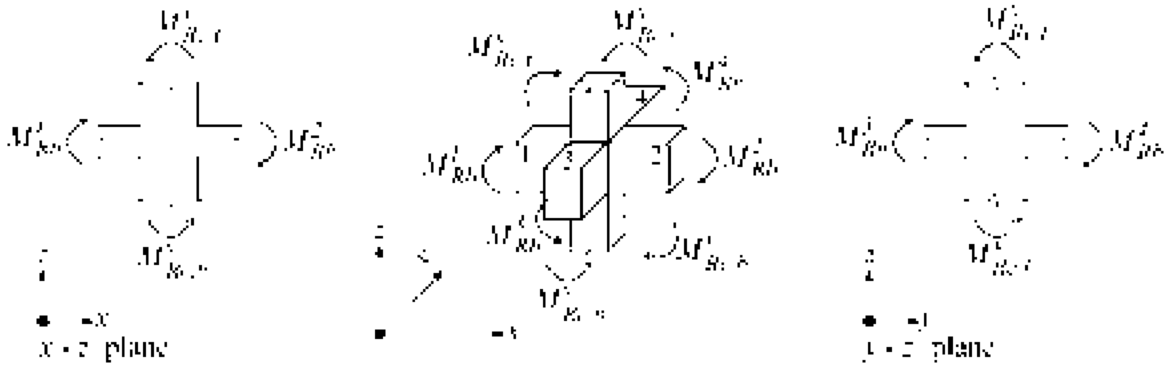

$$\left(M^{y}_{Rc,b} + M^{y}_{Rc,t}\right) \geq 1.3\left(M^{1}_{Rb} + M^{2}_{Rb}\right) \qquad \left(M^{x}_{Rc,b} + M^{x}_{Rc,t}\right) \geq 1.3\left(M^{3}_{Rb} + M^{4}_{Rb}\right)$$

Fig. 26. Verification of "weak beams strong columns" requirement in beam column joints

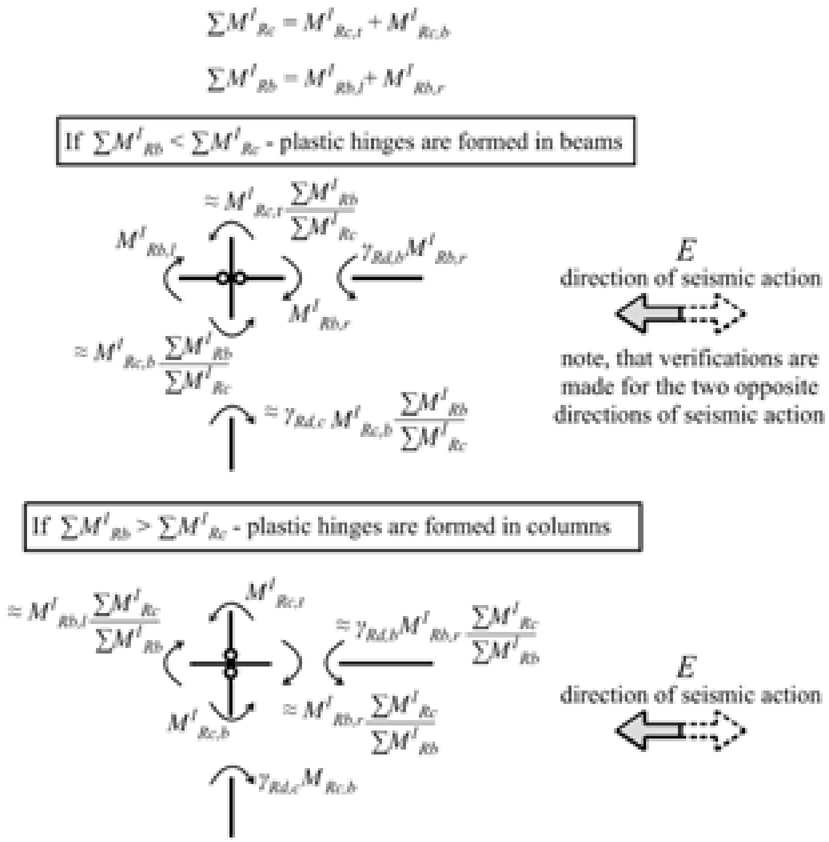

Fig. 27. Calculation of end section moments in beams and columns depending on location of plastic hinges

Fig. 28. Total collapse of a building due to "week columns-strong beams" – Turkey 1999

5.2 Local ductility requirements and checks

Eurocode 8 is the comprehensive seismic code which has local ductility checks for columns which is based on the quantity of confining stirrups as well as on properties of the confined concrete. The procedure of Eurocode 8 for the ductility checks of primary columns of frame structures is presented on Fig. 29.

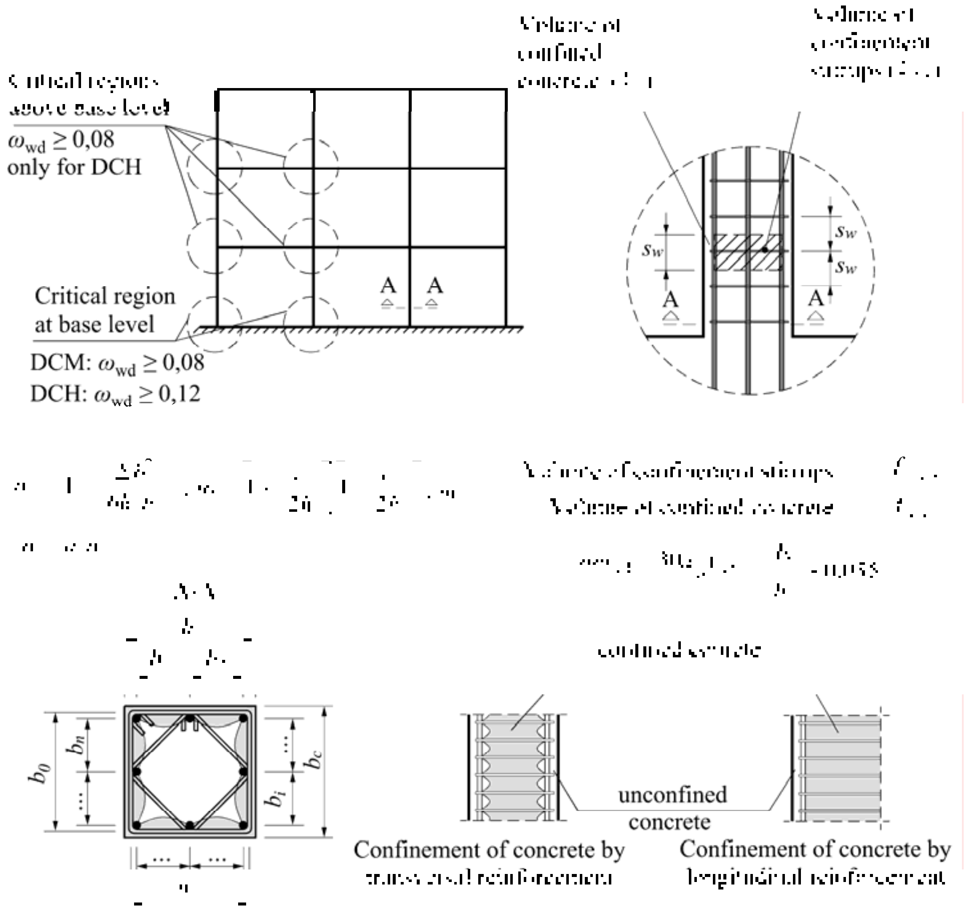

Fig. 29. Local ductility requirements for columns in seismic MRF

5.3 Detailing requirements

The detailing requirements of Eurocode 8 for primary beams and columns are given in Figs. 30 ÷ 33. Some special attention should be paid to the reinforcement ratio of top beam reinforcement and diameter limitation on longitudinal bars which are bonded in beam-column joints.

It is very important to ensure 135^o hook for the stirrups in the beams, columns and walls. The experience of past earthquakes shows that damages are usually initiated from places where 90^o stirrups hooks are applied (please see Fig. 34).

For the case of columns the major problems are close clear distance between longitudinal bars especially in the lapping length as well as required distance between stirrups in the splicing length of longitudinal bars (see Fig. 35). The problem could be solved by splicing devices. However some special tests are required for them. An example of application of such devices is presented in Fig. 36. The building in which the devices were applied was designed and detailed according to Eurocodes.

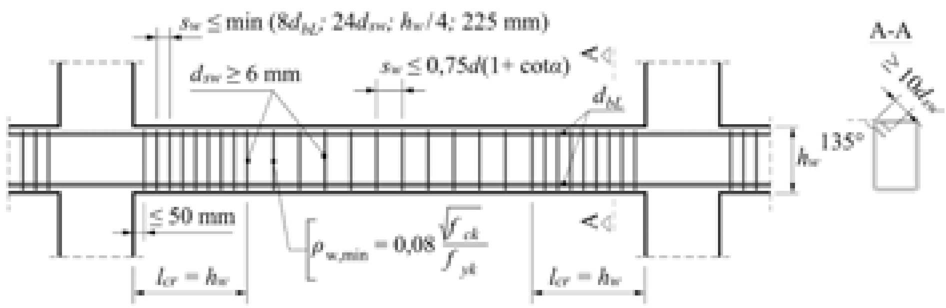

Fig. 30. Transversal reinforcement detailing requirements for beams in seismic MRF – DCM

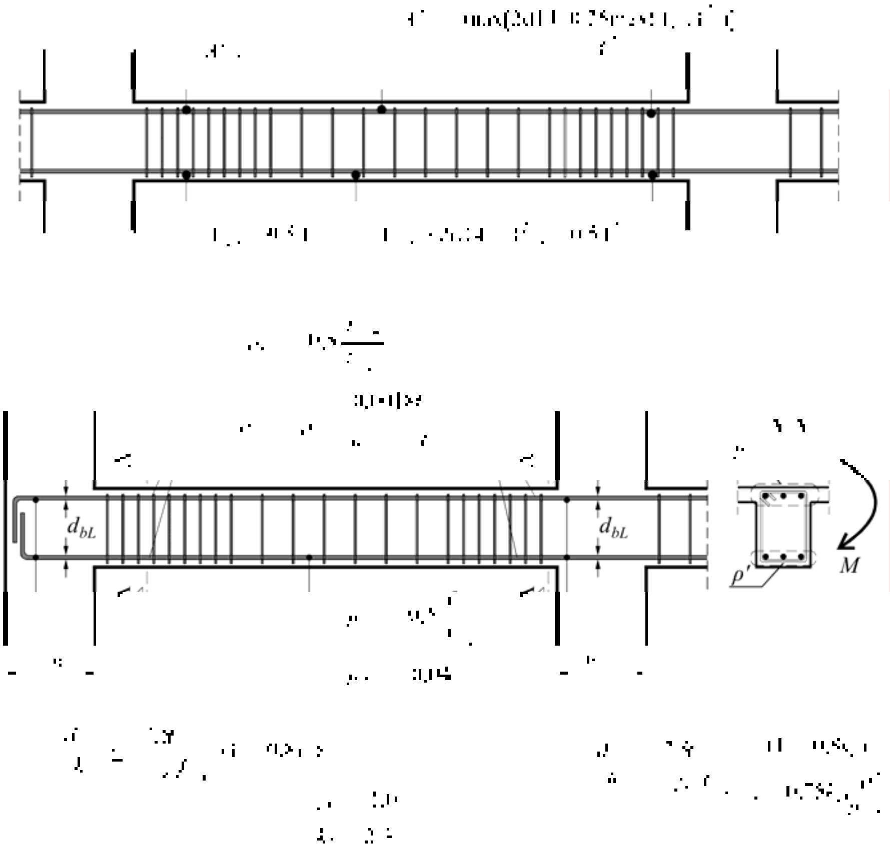

Fig. 31. Longitudinal reinforcement detailing requirements for beams in seismic MRF – DCM

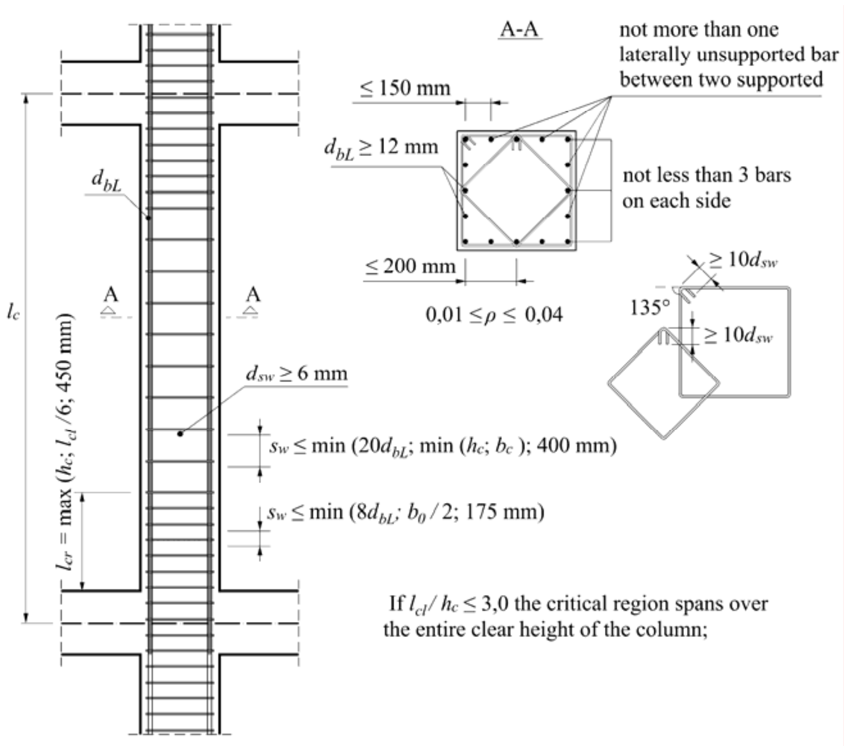

Fig. 32. Reinforcement detailing requirements for columns in seismic MRF – DCM

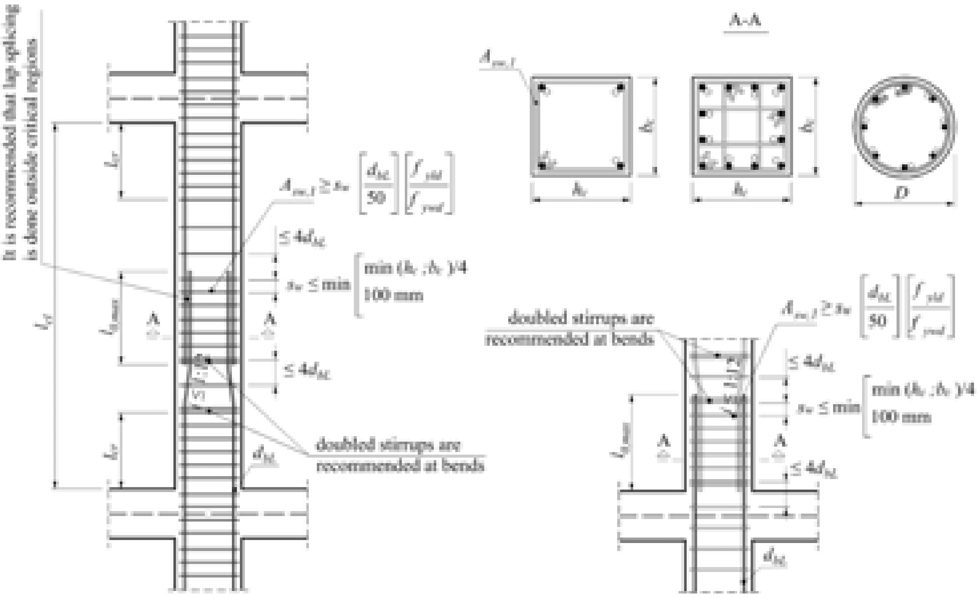

Fig. 33. Transversal reinforcement detailing requirements over the splicing length of the longitudinal reinforcement

Fig. 34. Initiation of column failure due to 90^o hooks of stirrups – Turkey 1999

Fig. 35. Problems with clear space between both longitudinal and transverse reinforcement in lapping length of longitudinal bars (the structure was designed according to Eurocodes)

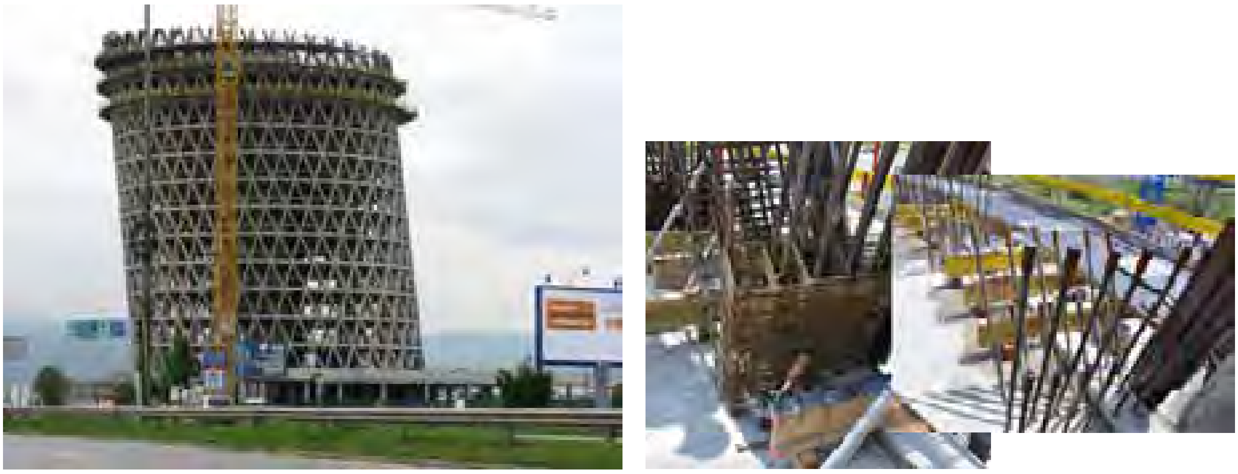

Fig. 36. Application of splicing devices for longitudinal bars in a RC building designed and detailed according to Eurocodes

6 CONCLUSIONS

On the basis of the study presented herein the following conclusions could be drawn:

Eurocode 8 is a code which is based on advanced theoretical background following the latest developments in the research on seismic design of buildings;

- It is necessary to ensure that structural engineers correctly implement new features of Eurocode 8 such as capacity design procedure, primary and secondary elements concept, new types of structural elements as large lightly reinforced walls, local ductility requirements for the different RC elements, etc.;
- It is expected that Eurocode 8 will ensure more stable and reliable seismic behaviour of buildings compared to old Bulgarian seismic code;
- It is possible that building structures which are designed by the Eurocodes will be slightly more expensive than those designed according to old Bulgarian seismic code;
- It is supposed that the major part of the existing buildings in Bulgaria fail to meet the strict requirements of Eurocode 8 and special attention should be made during their retrofit and reconstruction;
- There are some problems in the Bulgarian National Annexes and in the Eurocode 8 itself that should be solved.

7 REFERENCES

[1] Elghazouli, A., (Editor), Seismic Design of Buildings to Eurocode 8, Spoon Press, 2009;

[2] Fardis, M., at al, Designers Guide to EN 1998-1 and EN 1998-5. Eurocode 8: Design of Structures for Earthquake Resistance, Tomas Telford, 2005; [Fardis];

[3] Moehle, J., Seismic Design of Reinforced Concrete Buildings, McGrawHill, 2014

[4] Paulay, T., Priestley, M.J.N., Seismic Design of Reinforced Concrete and Masonry Buildings, John Wiley & sons, Inc, 1992

[5] P. Bisch, E. Carvalho, H. Degee, P. Fajfar, M. Fardis, P. Franchin, M. Kreslin, A. Pecker, P. Pinto, A. Plumier, H. Somja, G. Tsionis, Eurocode 8: Seismic Design of Buildings.Worked examples, Lisbon, 2011;

[6] Milev, J., Seismic Design of Reinforced Concrete Structures, KIIP Sofia, 2012 (in Bulgarian)

SUMMARY

PROBLEMS AND THEIR SOLUTIONS IN PRACTICAL APPLICATION OF EUROCODES IN SEISMIC DESIGN OF RC STRUCTURES

Jordan Milev

The main purpose of the paper is to present practical application of Eurocodes in the field of RC structures design. The selected examples represent the main problems in practical application of Eurocodes for seismic analysis and design of RC Structures in Bulgarian construction practice. The analysis is focused on some structural and economic problems as well as on some contradictions in Eurocode 8 itself. Special attention is paid to the practical solution of the following problems: recognition of torsionally flexible systems, stiffness reduction of RC elements for linear analysis dimensions and detailing of confined boundary areas of shear walls, detailing of wall structures, etc. Those problems appear during the practical design of some buildings in Bulgaria. Several proposals for solving some problems defined in the paper are presented through some practical examples. Some conclusions are made for further application of Eurocode 8 in the design and construction practice. The importance of some rules and procedures in Eurocode 8 is supported by the examples of damaged RC members during the past earthquakes. The problems of Eurocode 8 and their solutions are illustrated through the experience of Bulgarian construction practice.

Key words: seismic design, Eurocode 8, reinforced concrete structures, wall structure, frame structure, local ductility, detailing rules

REZIME

PROBLEMI I NJIHOVA REŠENJA U PRAKTIČNOJ PRIMENI EVORKODOVA ZA PROJEKTOVANJE AB KONSTRUKCIJA

Jordan Milev

Primarni cilj ovog rada je prikaz i analiza praktične primene Evrokodova u projektovanju armiranobetonskoih (AB) konstrukcija. Odabrani primeri ilustuju glavne probleme u praktičnoj primeni Evrokodova za seizmičku analizu i projektovanje AB konstrukcija u građevinskoj praksi Bugarske. Naglasak analize je usmeren na konstrukcijske i ekonomske probleme, kao i na neke kontradiktornosti koje postoje u Evrokodu 8 (EN 1998). Posebna pažnja posvećena je praktičnim rešenjima sledećih praktičnih problema: prepoznavanje torziono fleksibilnih sistema; smanjenje krutosti AB elemenata za linarnu analizu, dimenzionisanje i oblikovanje detalja utegnutih graničnih oblasti smičućih zidova; oblikovanje detalja nosećih zidova i dr. Ovi problemi se javljaju tokom praktičnog projektovanja nekih zgrada u Bugarskoj. Nekoliko predloga za rešavanje problema analiziranih u radu su predstavljeni preko praktičnih primera. Za dalju primenu Evrokoda 8 pri projektovanju i građenju formulisani su odgovarajući zaključci. Značaj pojedinih pravila i procedura u Evrokodu 8 su propraćeni primerima AB elemenata oštećenih tokom prethodnih zamljotresa. Problemi vezani za Evrokod 8 i njihovo rešavanje su ilustrovani primerima i iskustvima iz praktične primene u Bugarskoj.

Ključne reči: aseizmičko projektovanje, Evrokod 8 (EN 1998), armiranobetonske konstrukcije, noseći zidovi, okvirne konstrukcije, lokalna duktilnost, pravila oblikovanja detalja

NELINEARNA ANALIZA STABILNOSTI OKVIRNIH NOSAČA

NONLINEAR STABILITY ANALYSIS OF THE FRAME STRUCTURES

Stanko ĆORIĆ
Stanko BRČIĆ

ORIGINALNI NAUČNI RAD
ORIGINAL SCIENTIFIC PAPER
UDK: 624.072.7.046
doi: 10.5937/grmk1603027C

1 UVOD

Problemi gubitka stabilnosti armiranobetonskih, a još više čeličnih konstrukcija, veoma su aktuelni, a posebno imajući u vidu želje projektanata da grade atraktivne objekte velikih visina i raspona, odnosno velike vitkosti. Proračun ovakvih objekata, posebno iz aspekta analize njihove stabilnosti, zahteva primenu složenih numeričkih modela. Iako postoji značajan broj radova u literaturi, posvećenih raznim problemima stabilnosti konstrukcija, i dalje ima dosta nerešenih ili nedovoljno rešenih problema, posebno kada je reč o ponašanju realnih građevinskih konstrukcija u elasto-plastičnoj oblasti.

Istraživanja u oblasti stabilnosti linijskih nosača, počevši od prvih radova Euler-a krajem osamnaestog veka pa sve donedavno, uglavnom su se bazirala na rešavanju diferencijalnih jednačina izvijanja štapa izvedenih prema teoriji drugog reda. Da bi se taj problem lakše rešio kada su u pitanju složene konstrukcije, istraživači su vršili određena uprošćenja tako da su, na primer, konstrukcije podelili na sisteme štapova s nepomerljivim čvorovima i sisteme štapova s pomerljivim čvorovima. Takođe su posebno izučavali štapove sa elastičnim uklještenjima na jednom ili oba kraja, i to u kombinaciji sa elastičnim osloncima ili bez njih. Numerički izrazi i grafički prikaz dobijenih rezultata za kritično opterećenje dati su, na primer, u [1], [12]. Korišćenjem navedenih izraza, na relativno jednostavan način može da se obavi i proračun višespratnih okvira. Metode koje se najčešće koriste u tom slučaju jesu proračun korišćenjem jednačina obrtanja i korišćenjem izraza za rotacionu krutost [1], [17]. Navedeni postupak

dr Stanko Ćorić, dipl. inž. građ, docent, Građevinski fakultet, Univerzitet u Beogradu, Bulevar kralja Aleksandra 73, 11000 Beograd, Srbija, cstanko@grf.bg.ac.rs
dr Stanko Brčić, dipl. inž. građ, redovni profesor, Državni univerzitet u Novom Pazaru, Vuka Karadžića bb, 36300 Novi Pazar, stanko.brcic@gmail.com

1 INTRODUCTION

The problems of instability of reinforced concrete structures and, even more, of steel structures, are very contemporary, particularly having in mind desires of engineers to build attractive tall structures with high slenderness. Design of these structures, especially from the viewpoint of their stability, requires an application of complex numerical models. Although there are a significant number of papers in the literature devoted to the various problems of structural stability, there are still a lot of unsolved or inadequately solved problems, especially in the case of the real behavior of structures in elasto-plastic domain.

Research of the stability of linear structures, starting from the first Euler's investigations at the end of the eighteenth century, until recently, was mainly based on solving the differential equation of buckling according to the second order theory. In order to find simple solutions for the more complex structures, the researchers performed some approximations in their calculation. It means that members which are "isolated" from the structure, with different boundary conditions, were analyzed. Also, separately sway and non-sway structures were considered. Numerical expressions and graphical representation of the obtained results for the critical load can be found, for example in [1], [12]. Such approximations were also used to formulate procedures for calculations of multi-story frames. The most used methods for this type of calculation are slope deflection method and stiffness distribution method, and they can be found in the literature, for example [1], [17]. The above procedures

Stanko Ćorić, Ph.D., assistant professor, University of Belgrade, Faculty of Civil Engineering, Bulevar kralja Aleksandra 73, Belgrade, Serbia, cstanko@grf.bg.ac.rs
Stanko Brčić, Ph.D., full professor, State University of Novi Pazar, Vuka Karadžića bb, 36300 Novi Pazar, Serbia, stanko.brcic@gmail.com

proračuna višespratnog okvira s jednim poljem može da se primeni i kada su u pitanju znatno složenije konstrukcije okvira s više polja. Naime, u ovom slučaju se problem okvira s više polja može svesti na proračun ekvivalentnog okvira s jednim poljem, kao što je prikazano u [22], [23]. U opštem slučaju, zbog različitih dimenzija stubova i rigli, kao i različitog opterećenja, višespratni okviri s više polja ne mogu da se zamene jednim ekvivalentnim okvirom i da se na taj način odredi njihovo kritično opterećenje. Zato su pojedini autori rešenje problema potražili u primeni nekih drugih metoda, kao npr. energetskog postupka [16].

Teorijske osnove proračuna izolovanog štapa bile su baza za donošenje nacionalnih i evropskih propisa o stabilnosti okvirnih nosača [10], [11] i [25]. Međutim, primena ovih propisa ukazala je na to da takav proračun u pojedinim slučajevima dovodi do grešaka, jer je on približan [7]. Usled toga, poslednjih godina radi se na poboljšanju ovih približnih metoda proračuna. Tako se, na primer, navodi analiza [15] koja ima cilj da se poboljšaju ulazni parametri koji definišu krutost okvirnog nosača, a samim tim i tačnije odrede koeficijenti efektivne dužine izvijanja kod višespratnih okvira.

Na kraju ovog uvoda, treba naglasiti primenu metode konačnih elemenata kao najefikasnije metode za numeričku analizu stabilnosti okvirnih nosača. Naime, kao što je poznato, u linearnoj teoriji prvog reda matrica krutosti konačnog elementa zavisi od geometrije elementa i od mehaničkih karakteristika materijala. Kad je u pitanju problem stabilnosti, on ne može da se reši prema teoriji prvog reda i potrebno je sprovesti proračun prema teoriji drugog reda. To ima za posledicu da je neophodno u proračun uvesti matricu krutosti koja zavisi i od aksijalnih sila. Uobičajeno uprošćenje u ovom proračunu prema teoriji drugog reda jeste da se problem aksijalnog naprezanja i problem savijanja štapa definišu nezavisno jedan od drugog. To omogućuje da se i određivanje matrice aksijalne i transverzalne krutosti štapa mogu razmatrati razdvojeno, kao dva međusobno nezavisna problema. Primenom metode konačnih elemenata u analizi stabilnosti linijskih nosača bavili su se mnogi istraživači, kao npr. [14], [2], a takođe je primenjena u savremenim komercijalnim programima za ovu vrstu analize (SAP2000, STAAD…). Treba napomenuti da se standardno rešenje metode konačnih elemenata dobija preko geometrijske matrice krutosti. U ovom radu biće dato rešenje gde su matrice krutosti izvedene korišćenjem interpolacionih funkcija koje se odnose na tačno rešenje diferencijalne jednačine savijanja štapa prema teoriji drugog reda. Takođe, pri proračunu se osim geometrijske uvodi i materijalna (fizička) nelinearnost, pa su matrice krutosti izvedene korišćenjem tangentnog modula elastičnosti koji prati promenu krutosti štapa u neelastičnoj oblasti.

Pristup koji se zasniva na primeni teorije tangentnog modula u poslednje vreme dosta je razmatran u literaturi, i pri tome može da se izdvoji rešenje koje je dato u [24]. Rezultati dobijeni u ovom radu pokazuju da se predloženom analizom stabilnosti u neelastičnoj oblasti može izračunati kritična sila čeličnih okvirnih nosača i na taj način obaviti proračun takvih nosača.

for calculation of one-bay multi-storey frames can be applied for more complex multi-bay frames. Namely, in this case, the calculation of multi-bay framework can be reduced to calculation of equivalent one-bay frame, as it is shown in [22], [23]. Sometimes, the framework because of its irregularity can not be reduced to an equivalent single-bay frame in order to calculate their critical load. In that case, some other procedure, based on the linear elastic analysis, such as energy method [16], are suggested.

Theoretical approach based on the calculation of isolated member was applied in the national and European regulation for the stability of frame structures [10], [11] and [25]. However, the application of these codes shows that such calculation, in some cases, may lead to the substantial errors, because obtained results are approximate [7]. Therefore, in recent years, considerable effort has been made in order to improve these approximate calculation methods. So, for example, the objective of the analysis [15] is to propose improved input parameters for the determination of the effective buckling length coefficient of columns in multi-story frames.

At the end of this introduction, it shoud be emphasized application of the finite element method as the most effective method for numerical analysis of stability of frame structures. Namely, it is well known that in the linear first order theory, stiffness matrix is the function of geometry of the element and the characteristics of the material. However, stability problem can not be solved by the first order theory, and it is necessary to perform calculation according to the second order theory. Therefore, calculation should be performed using the stiffness matrix which depends upon the axial forces in the element. Usual simplification in this calculation according to the second order theory is that the axial loading and bending problems are considered independently from each other. This enables that the determination of the matrix of axial and transverse stiffness of the member can be considered as two separate problems. The finite element method was investigated by many authors, for example [14], [2], and also it is used in modern commercial programs for such kind of analysis (SAP2000, STAAD, …). In the usual approach, the finite element method is based on the geometric stiffness matrix as a part of the tangent stiffness matrix. In this paper it is given solution where stiffness matrix is derived using interpolation functions related to the exact solution of the differential equation of bending of a beam according to the second-order theory. Also, in this analysis, in addition to geometric nonlinearity, the materially (or physically) nonlinear analysis is also taken into account. It means that stiffness matrices are derived using the tangent modulus that is stress dependent and follows changes of the member stiffness in the inelastic domain.

The approach that is based on the application of tangent modulus theory is also discussed in the literature, and solution given in [24] can be specified. The results obtained in this paper show that the proposed inelastic buckling analysis suitably evaluates the critical load and failure modes of steel frames, and can be a good alternative for the evaluation of critical load in the design of steel frames.

2 STABILNOST OKVIRNIH NOSAČA U ELASTO-PLASTIČNOJ OBLASTI

Kao što je poznato, pri izvijanju štapa dolazi do njegovog savijanja usled aksijalne sile. Pri rešavanju problema stabilnosti, diferencijalna jednačina ravnoteže štapa koristi se u obliku:

2 STABILITY OF THE FRAMES IN ELASTO-PLASIC DOMAIN

It is well known that during the member buckling, axial force produces the bending of the member. The basic differential equation of this stability problem is:

$$v^{iv} + k^2 v'' = 0 \quad (1)$$

gde je $k = \sqrt{P / EI}$, *P* je aksijalna sila, *EI* krutost štapa na savijanja, dok *v* predstavlja ugib normalan na prvobitnu (nedeformisanu) osu štapa. Kada se izvijanje dešava u elastičnoj oblasti, modul elastičnosti E ima konstantnu vrednost.

Kao što je već istaknuto, u metodi konačnih elemenata uobičajeno je da se ova diferencijalna jednačina rešava koristeći približno rešenje u obliku polinoma. Međutim, cilj ovog istraživanja je da se dođe do tačnih rešenja problema stabilnosti okvirnih nosača, tako da se ovde koristi tačno rešenje diferencijalne jednačine (1), koje je dato preko trigonometrijskih funkcija:

where *k* is equal to $\sqrt{P / EI}$, *P* is axial force, *EI* is member bending stiffness, and *v* represents lateral deflection. When the buckling occurs within the elastic range, the modulus of elasticity E has a constant value.

As it is well known, in the finite element method it is usual to use approximate polynomial solution for this differential equation. However, the main aim of this instigation is to apply exact solutions on the problem of stability of frame structures. In order to formulate that exact matrix stability analysis, shape functions are used in the trigonometric form, according to the solution of equation (1):

$$v(x) = \alpha_1 + \alpha_2 kx + \alpha_3 \sin(kx) + \alpha_4 \cos(kx) \quad (2)$$

Matrica krutosti koja se dobija po teoriji drugog reda za štap koji je opterećen silom pritiska, odnosno silom zatezanja prikazana je, na primer, u [6].

Numerički primeri u kojima je analizirana primena dobijene matrice krutosti dati su u [7], [6]. Pri tome je kritično opterećenje dobijeno kao koren transcendentne jednačine, koja predstavlja uslov da je determinanta odgovarajuće matrice krutosti jednaka nuli. Iz dobijenih rezultata zaključeno je da se velike greške mogu javiti kada se primenjuje klasična (linearna) metoda konačnih elemenata. Treba napomenuti da ove greške mogu da se smanje ako se broj konačnih elemenata dovoljno poveća. Međutim, problem ovog približnog postupka je u tome što je potrebno stalno vršiti kontrolu da bi se videlo koliki broj konačnih elemenata je potreban da bi se dobilo konvergentno rešenje. Ovo je i razlog zašto su u ovoj analizi korišćene interpolacione funkcije u trigonometrijskom ili hiperboličkom obliku. Glavna prednost takvog pristupa je u tome što daje, uslovno rečeno, tačna rešenja i ukupan broj konačnih elemenata je pet do deset puta manji nego u uobičajenom postupku s primenom geometrijske matrice krutosti. Nedostatak je u tome što umesto problema sopstvenih vrednosti, za čije rešavanje postoje nekoliko dobro poznatih postupaka (npr. iteracije unutar potprostora, Lanczos-ov postupak, itd...) problem izvijanja svodi se na rešavanje transcendentne jednačine koja je funkcija, na veoma komplikovan način, aksijalne sile u stubovima i gredama. Zato je i formulacija odgovarajućih algoritama i kompjuterskog programa za rešavanje ovakve vrste problema jedan od glavnih naučnih doprinosa ovog istraživanja.

Kao što je već rečeno, analiza problema stabilnosti zasniva se na proračunu prema teoriji drugog reda. To znači da se razmatra geometrijski nelinearan problem zato što su uslovi ravnoteže napisani na deformisanoj konfiguraciji nosača, odnosno uzima se u obzir izmenjena geometrija nosača do koje se dolazi usled deformacija nastalih pod zadatim opterećenjem. Kada je u pitanju veličina naprezanja u pojedinim štapovima nosača, pretpostavljeno je da je posredi problem elastične stabilnosti, odnosno da sve vreme do dostizanja

Obtained stiffness matrix for the members subjected to compressive and tension forces can be found, for example, in [6].

Numerical analysis related to this problem is given in [7], [6]. The critical buckling loads are obtained from the roots of the transcendental equation, representing the condition that the determinant of the corresponding stiffness matrix is equal to zero. From the results of performed analysis it was concluded that when the classic (linear) finite element method is used, large errors for values of critical load might be obtained. It should be noted that this errors could be reduced, if the number of member elements in approximate solution is increased. But, the problem of this approximate procedure is also that it is necessary to perform previous control analyses in order to obtain how many finite elements are needed for convergent solution. These arguments present the reason why in this analysis the interpolation polynomials in the form of trigonometric or hyperbolic functions, sometimes known as the stability functions, are used. The main advantage of such an approach is that it gives, conditionally speaking, exact solutions and the total number of finite elements is 5-10 times less than in the usual approach based on the geometric stiffness matrix. Disadvantage is obvious: instead of the generalized eigenvalue problem, for which there are several well established methods (e.g. the subspace iteration, Lanczos method, etc), the buckling problem is reduced to the solution of the transcendental equation which depends, in a very complicated way, upon the normal forces in columns and beams. So, formulation the suitable algorithms and corresponding computer program for solving such kind of problems is one of the main scientific contributions of this analysis.

As it was already mentioned, the stability analysis is performed according to the second order theory. It means that geometrically nonlinear problem is analyzed since the equilibrium conditions are applied on the deformed configuration of the member. Taking into consideration the stress value in the analyzed columns, it is assumed that this is a problem of elastic stability. It kritične sile naponi (σ_{cr}) u svim štapovima ne prelaze granicu proporcionalnosti (σ_p) materijala od koga su napravljeni.

Proračun na bazi teorije elastične stabilnosti široko je primenjen u inženjerskoj praksi, pošto se polazi od toga da se građevinske konstrukcije uglavnom ponašaju elastično kada su izložene svakodnevnim eksploatacionim opterećenjima. Zato je razumljivo da ovaj vid proračuna predstavlja osnovu standarda (propisa) za analizu stabilnosti okvirnih konstrukcija [10], [11] i [25]. On je definisan kroz određivanje tzv. efektivne dužine izvijanja pojedinih štapova okvirnih nosača.

Proračun stabilnosti okvirnih nosača komplikuje se ukoliko pre dostizanja kritičnog opterećenja pojedini štapovi uđu u fazu nelinearnog ponašanja materijala. To znači da se u njima javljaju naponi koji su veći od granice proporcionalnosti. Time ovaj proračun dobija još jedan vid nelinearnosti zato što postaje i materijalno (fizički) nelinearan problem.

Kao što je poznato, polazeći od Euler-ove kritične sile, kritični napon u štapu može se predstaviti u funkciji modula elastičnosti (E) i vitkosti (λ_i):

means that when the critical load is reached, stresses (σ_{cr}) in all columns do not exceed the proportionality limit of the material (σ_p).

Calculation based on the elastic stability theory is widely applied in the engineering practice, because it can be assumed that engineering structures have generally elastic behavior when they are subjected to the usual working loads. Therefore, it is clear that such theory is the basis of the standards for the stability analysis of the frame structures [10], [11] and [25], and this calculation is defined by the determination of the effective buckling length of the compressed columns.

Stability calculation becomes more complicated if, before the critical load is achieved, some compressed members enter into the phase of nonlinear material behavior. It means that stresses in such columns become higher than the proportionality limit. Therefore, such calculation obtains another type of nonlinearity and it becomes also materially (or physically) nonlinear problem.

Taking into consideration well known expression for the Euler's critical force, critical stress in a member may be expressed as a function of the modulus of elasticity (E) and the slenderness ratio (λ_i):

$$\sigma_{cr} = \frac{P_{cr}}{A} = \frac{\pi^2 EI}{l_i^2 A} = \pi^2 \frac{E}{\lambda_i^2} \tag{3}$$

gde su: *A* - površina poprečnog preseka, $i = \sqrt{I/A}$ - poluprečnik elipse inercije i λ_i - vitkost štapa.

Jednačina ove hiperbole važi sve dok je kritični napon manji od granice proporcionalnosti, slika 1. Kada je ovaj napon prekoračen, izvijanje se dešava u plastičnoj oblasti. Proučavanjem stabilnosti štapova koji se izvijaju u plastičnoj oblasti prvi se bavio Bauschinger koji je vršio eksperimentalna istraživanja krajem devetnaestog veka. Na bazi ovih rezultata i sopstvenih istraživanja, Tetmajer je nešto kasnije prvi dao izraz za vezu napona i vitkosti u plastičnoj oblasti. On je predložio linearnu vezu u obliku:

$$\sigma_{cr} = \sigma_v \qquad \text{za} \quad 0 < \lambda < 60$$

$$\sigma_{cr} = C_1 - C_2 \cdot \lambda \qquad \text{za} \quad 60 < \lambda < \lambda_p$$

gde je $\lambda_p = \pi\sqrt{E/\sigma_p}$ vitkost na granici proporcionalnosti.

Grafički prikaz ove veze dat je na slici 1.

U okviru daljih istraživanja u ovoj oblasti ističe se i rad Engesser-a [9] koji uvodi pojam tangentnog modula elastičnosti. Kasnije su se i mnogi drugi naučnici bavili ovom problematikom. Tako su na primer Karman i Shanley izvršili modifikaciju Engesser-ove krive. Neke od najznačajnih krivih izvijanja u plastičnoj oblasti prikazane su na slici 2.

I pored brojnih istraživanja, kako eksperimentalnih tako i teorijskih, problem izvijanja štapova, a posebno okvirnih nosača u elasto-plastičnoj oblasti nije do sada u potpunosti rešen. Tek se s razvojem kompjuterske tehnike stvorila mogućnost za sveobuhvatno rešenje ovog problema. Treba napomenuti da su se ovim problemom u poslednje vreme bavili mnogi autori čiji su rezultati prikazani u [24], [5] i [13].

where: *A* is cross-sectional area, $i = \sqrt{I/A}$ is radius of inertia, and λ_i is slenderness ratio of the member.

Equation (3) is given by hyperbola function and it is valid until the critical stress is less than a proportionality limit, as it is shown in Figure 1. When the critical stress is exceeded, the member is buckling in the plastic range. Many scientists were dealing with this problem. Bauschinger first made an experimental study at the end of the nineteenth century. On the basis of this results and his own research, Tetmajer later suggested expression for the linear relation between stress and slenderness in the plastic domain:

$$\sigma_{cr} = \sigma_v \qquad \text{for} \quad 0 < \lambda < 60$$

$$\sigma_{cr} = C_1 - C_2 \cdot \lambda \qquad \text{for} \quad 60 < \lambda < \lambda_p$$

where $\lambda_p = \pi\sqrt{E/\sigma_p}$ is the slenderness at the proportionality limit.

This linear function is also given in the Figure 1.

Engesser [9] also made the significant contribution by introducing the concept of the tangent modulus. Many other scientists also investigated these problems, as Karman and Shanley who modified Engessers curve. Some of the most significant buckling curves in the plastic domain are given in Figure 2.

Despite numerous experimental and theoretical studies, buckling problem, especially for the frames in the elastic-plastic domain, has not been completely solved. Fast development of computer technology has created the opportunity for a comprehensive solution of this problem. It should be mentioned that this problem recently was investigated by many authors whose results are presented, for example, in [24], [5] and [13].

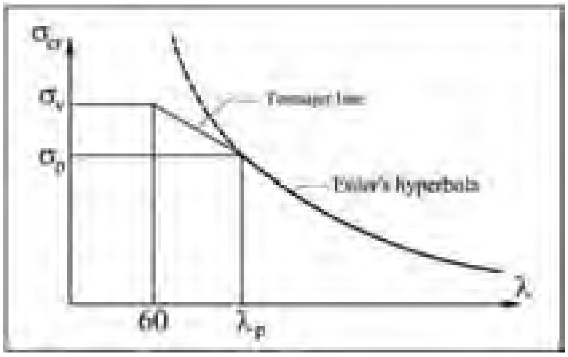

Slika 1. Grafički prikaz Ojlerove hiperbole i Tetmajerove prave
Figure 1. Graphical display of Euler's hyperbola and Tetmajer's line

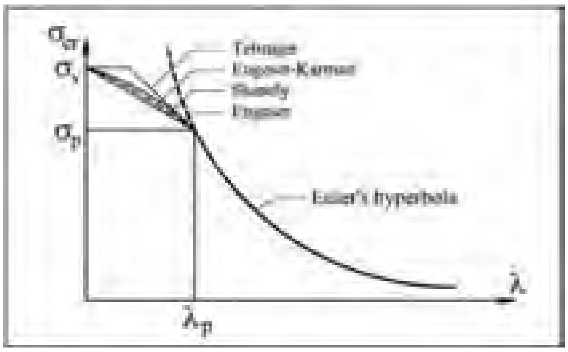

Slika 2. Krive izvijanja u plastičnoj oblasti

Figure 2. Buckling curves in the plastic domain

U ovom radu je primenjena metoda konačnih elemenata kao najefikasnija numerička metoda za rešavanje stabilnosti okvirnih nosača. Kao što je dobro poznato, za određivanje kritičnog opterećenja primenom ove metode koristi se matrična jednačina u obliku:

In this paper, the finite element method as the most efficient numerical method for solving such kind of problems is applied. As it is well known, using this method, the critical load can be obtained from the homogeneous matrix equation as the non-trivial solution:

$$\boldsymbol{K}\boldsymbol{q} = 0 \tag{4}$$

U okviru teorije elastične stabilnosti, matrična jednačina (4) rešava se inkrementalnim postupkom tako što se opterećenje povećava u zadatim inkrementima sve dok se ne dođe do kritične vrednosti iz uslova det ***K***=0. Pri tome, u svakom štapu modul elastičnosti E ima konstantnu vrednost. Međutim, kod elasto-plastične analize postupak proračuna je komplikovaniji. Naime, pri svakom inkrementu opterećenja, u štapovima gde je pređena granica proporcionalnosti, mora da se promeni i krutost štapa, odnosno koristi se novi tangentni modul E_t za taj štap. To znači i da su matrice krutosti koje se koriste u slučaju nelinearnog ponašanja materijala kompleksnije.

Da bi se sproveo proračun stabilnosti u neelastičnoj oblasti, potrebno je poznavati fizičko-mehaničke karakteristike materijala. Kao što je poznato, kada su u pitanju građevinski materijali poput čelika i betona, veza između napona i deformacije iznad granice proporcionalnosti postaje nelinearna. Na bazi eksperimentalnih istraživanja može se doći do ove zavisnosti, tj. dijagrama koji prikazuju vezu između napona i deformacija sve do nivoa naprezanja kada dolazi do iscrpljenja nosivosti materijala, odnosno loma nosećih elemenata konstrukcije. Tipičan dijagram, kada je u pitanju građevinski čelik, prikazan je na slici 3.

This problem can be solved by an incremental process, by increasing the load at the specified increments until the critical value is reached, i.e. until det ***K*** = 0. In the case of elastic stability problem, the modulus of elasticity E has a constant value. But, elastoplastic analysis is more complicated. For the structural member where the proportionality limit is exceeded, for each new load increment the member stiffness has to be changed and the corresponding tangent modulus Et should be used for that member. It means that the stiffness matrices applied in the case of non-linear material behavior are more complex.

In order to implement the calculation of stability in inelastic range, it is necessary to know the physical and mechanical properties of materials. As it is well know, for the building materials (steel, concrete, ...) the relationship between stress and strain above the proportionality limit becomes nonlinear. On the basis of experimental results it is possible to obtain this diagram, which represents the relationship between stress and strain before the load bearing capacity is so reduced that the fracture of structure elements occurs. Typical stress-strain diagram of structural steel is given in Figure 3.

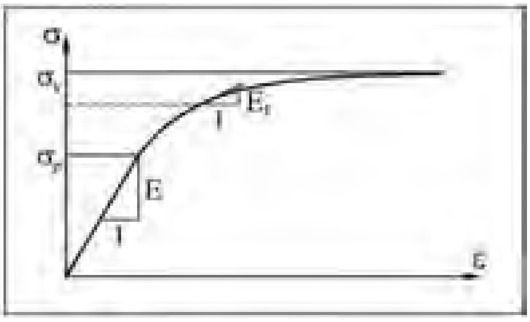

Slika 3. σ-ε dijagram čelika
Figure 3. Stress-strain diagram of structural steel

Ovaj dijagram pretstavlja vezu između napona σ i deformacije ε aksijalno pritisnutog štapa, gde je sa σ_p obeležen napon na granici proporcionalnosti, a sa σ_v napon tečenja. Do granice proporcionalnosti modul elastičnosti E ima konstantnu vrednost i funkcija je samo vrste materijala. Sa daljim rastom opterećenja, ovaj modul postaje i funkcija nivoa naprezanja $E_t = f(\sigma)$ i naziva se tangentni modul [4]. Za razliku od E koji zavisi od karakteristika materijala, E_t je u funkciji i napona.

Na bazi eksperimentalnih istraživanja, jedna od najčešće korišćenih veza između ova dva modula, kada je u pitanju građevinski čelik, može se usvojiti u obliku [19], [8]:

This diagram shows the relationship between stress σ and strain ε of the axially loaded member, where σ_p is the stress at the proportionality limit and σ_v is the yield stress. Below a proportionality limit, modulus of elasticity E is constant and it is function only of the material properties. Above this point, inelastic behavior occurs with a gradually decreasing resistance of material, measured by the tangent modulus E_t [4]. While E is only a function of the type of material, E_t is a stress dependent function.

On the basis of experimental research, one of the most used expressions that describe relationship between these two modules, for the structural steel, is given in the form [19], [8]:

$$E_t = 4E \cdot \left[\frac{\sigma}{\sigma_v} \left(1 - \frac{\sigma}{\sigma_v} \right) \right] \tag{5}$$

Ovo je empirijski izraz koji pokazuje ponašanje čeličnih stubova u neelastičnoj oblasti. Ova zavisnost je korišćena pri formiranju programa ALIN za nelinearnu elasto-plastičnu analizu okvirnih nosača.

Matrice krutosti kod nelinearnog ponašanja materijala imaju formalno isti oblik kao i pri linearnom ponašanju materijala, ali se suštinski bitno razlikuju zato što se u svim članovima umesto ω javlja ω_t, a umesto konstantnog modula elastičnosti E javlja se tangentni modul E_t koji zavisi od nivoa naprezanja u elementu. Tako za slučaj štapa tipa „k", koji je opterećen silom pritiska, imamo:

This is an empirical expression designed to represent the behavior of structural steel columns in the inelastic range. This expression was used in this analysis for developing program ALIN for the nonlinear elastic-plastic analysis of frame structures.

Stiffness matrix for nonlinear material behavior has the same form as for the linear behavior of the material, but they are essentially very different. Namely, the difference is primarily in the fact that constant modulus E is replaced by stress dependent tangent modulus E_t, and value ω is replaced by ω_t. So, for the member of the so-called type "k" (i.e. clamped at both ends), subjected to compressive force, stiffness matrix is:

$$\boldsymbol{K} = \frac{E_t I}{l^3 \Delta_t} \begin{bmatrix} \omega_t^3 \sin\omega_t & \omega_t^2 l(1-\cos\omega_t) & -\omega_t^3 \sin\omega_t & \omega_t^2 l(1-\cos\omega_t) \\ & \omega_t l^2(\sin\omega_t - \omega_t\cos\omega_t) & -\omega_t^2 l(1-\cos\omega_t) & \omega_t l^2(\omega_t - \sin\omega_t) \\ & & \omega_t^3 \sin\omega_t & -\omega_t^2 l(1-\cos\omega_t) \\ & symm. & & \omega_t l^2(\sin\omega_t - \omega_t\cos\omega_t) \end{bmatrix} \tag{6}$$

gde je:

where:

$$E_t = 4E \cdot \left[\frac{P_{cr,i}}{A \cdot \sigma_v} \cdot \left(1 - \frac{P_{cr,i}}{A \cdot \sigma_v} \right) \right] \tag{7}$$

$$\omega_t = \sqrt{\frac{P_{cr,i}}{E_t \cdot I}} \cdot l = \frac{1}{2} A\sigma_v\, l \cdot \sqrt{\frac{1}{EI\left(A\sigma_v - P_{cr,i}\right)}} \tag{8}$$

$$\Delta_t = 2 \cdot \left(1 - cos\omega_t\right) - \omega_t \cdot sin\omega_t \tag{9}$$

Matrica krutosti za štap tipa „g", kao i matrice krutosti za štapove koji su izloženi sili zatezanja prikazani su u [6].

Stiffness matrices of the member of the type "g" (i.e. hinged at one end and clamped at the other), and stiffness matrices for the members subjected to tension force are given in [6].

3 PROGRAM ALIN ZA ANALIZU STABILNOSTI NOSAČA

Numerička analiza u ovom radu je obavljena primenom programa koji je napisan u C++ programskom

3 PROGRAM ALIN FOR STABILITY ANALYSIS OF FRAME STRUCTURES

The numerical analysis in this paper is performed using the code, developed in the C++ programming jeziku. Program je nazvan ALIN i namenjen je kompleksnoj analizi linijskih nosača u ravni i prostoru. Osnovne mogućnosti ovog programa jesu analiza po teoriji prvog reda i linearizovanoj teoriji drugog reda (geometrijski nelinearna analiza), dinamička analiza, kao i analiza stabilnosti, odnosno proračun kritičnog opterećenja u elastičnoj i neelastičnoj oblasti. Detaljan opis i razvoj ovog programa pre svega je prikazan u [26], a takođe i u [6]. Treba istaći da se jedan od glavnih ciljeva ove analize sastoji u formiranju programa ALIN u delu koji omogućuje efikasno rešavanje problema stabilnosti u elasto-plastičnoj oblasti primenom „tačnih” izraza za matrice krutosti koje su izvedene u prethodnom poglavlju.

4 ISTRAŽIVANJE STABILNOSTI OKVIRNIH NOSAČA PRIMENOM PROGRAMA ALIN

4.1 Ponašanje okvirnih konstrukcija u elasto-plastičnoj oblasti

Proračun stabilnosti okvirnih nosača u elasto-plastičnoj oblasti, zbog svoje složenosti, nije zastupljen u svakodnevnim inženjerskim proračunima. Zato se ni u postojećim standardima ne traži ovaj vid proračuna. Naime, određivanje kritične sile, odnosno kritičnog napona u plastičnoj oblasti za štapove okvirnog nosača obavlja se na bazi proračuna u elastičnoj oblasti i korišćenjem empirijskih izraza i krivih koje su dobijene na osnovu brojnih eksperimentalnih istraživanja ponašanja izolovanih štapova u plastičnoj oblasti. Ovde će se pokazati da se primenom programa ALIN može uspešno obaviti proračun stabilnosti okvirnih nosača i u elasto-plastičnoj oblasti. To s jedne strane omogućuje inženjerima da korišćenjem ovakvih kompjuterskih programa povećaju tačnost svojih proračuna i sagledaju stvarno ponašanje okvirnih nosača u elasto-plastičnoj oblasti. S druge strane, primena ovog načina proračuna treba da bude impuls za osavremenjivanje postojećih standarda u delu koji se odnosi na neelastično ponašanje ramovskih konstrukcija.

U nastavku je prikazan numerički primer šestospratnog okvira s tri polja (tj. četiri reda stubova), slika 4. Razmatran je slučaj ukliještenog okvira s pomerljivim i nepomerljivim čvorovima. Analizirano je opterećenje koje deluje na svakom spratu, tj. slučaj kada se aksijalna sila u stubovima skokovito povećava gledajući odozgo ka dole.

Za okvirne nosače u ovoj analizi usvojeno je da su od čelika s karakteristikama: $E = 210{,}000{,}000$ kN/m^2 i $\sigma_v = 240{,}000$ kN/m^2. Iz izraza za tangentni modul (5) izračunava se vrednost napona na granici proporcionalnosti: $\sigma_p = 0.5 \cdot \sigma_v = 120{,}000$ kN/m^2. Ovaj odnos napona u granici proporcionalnosti preporučuje se u [19], [8]. Za stubove i grede analiziranih okvira usvojeno je nekoliko različitih poprečnih preseka, pri čemu je uzeto da je $I_{grede} = 0{,}5 \cdot I_{stuba}$.

Na početku treba reći da su detaljni rezultati analize stabilnosti okvira s pomerljivim čvorovima (slika 4a) dati u [6]. U tabeli 1 prikazani su samo rezultati za kritično opterećenje za slučajeve različitih poprečnih preseka nosača na slici 4a i 4b.

language. The program is named ALIN and it enables the complex plane and space analysis of linear frames. The basic possibilities of this program are analysis according to the first and the second order theory, dynamic analysis and stability analysis, i.e. calculation of the critical load in the elastic and inelastic domains. The detailed description of this code can be found in [26], [6]. It should be emphasized that one of the main goals of this analysis was development of the part of program ALIN, which provides efficient solutions of stability problems in elastic-plastic domain. Those solutions are obtained using the "exact" expressions of the stiffness matrix which are presented in this paper.

4 INVESTIGATION OF THE STABILITY OF FRAME STRUCTURES USING THE PROGRAM ALIN

4.1 Behavior of the frame structures in elasto-plastic domain

Calculation of the stability of frames in the elasto-plastic domain, because of its complexity, is not used by engineers in the standard engineering stability analysis. It is the main reason why the current standards of frame stability analysis do not require this type of calculation. The determination of the critical load and the critical stress in the plastic field, for the analyzed members, usually is performed on the basis of the calculation in elastic domain and applying the empirical expressions and curves. That expressions and curves are obtained from a number of experimental studies related to the behavior of isolated members in the plastic field. In this paper it will be shown that calculation of the stability of frames in the elasto-plastic domain can be performed more successfully using the program ALIN. That allows engineers to use this computer program in order to increase the accuracy of their calculations and to consider the real behavior of the frame structures in elasto-plastic domain. On the other hand, the application of this numerical method may give the stimulus for the innovation of actual standards in the part related to the inelastic behavior of frame structures.

In the following, numerical example of six-story three-bay sway and non-sway frame is presented (Figure 4). The frame is clamped at the base, and concentrated load P is imposed on each column at each story. Since the axial force in columns is not constant, the elastic-plastic stability analysis can lead to the different behavior of the columns in the different floors.

In this analysis steel with characteristic: $E = 210{,}000{,}000$ kN/m^2 and $\sigma_v = 240{,}000$ kN/ m^2 is used. From the tangent modulus expression (5), proportional limit is obtained as $\sigma_p = 0.5 \cdot \sigma_v = 120{,}000$ kN/m^2 [19], [8]. Several different cross-sections are used for columns and girders of the analyzed frames, where it is assumed that $I_{gird} = 0{,}5 \cdot I_{col}$.

It should be noted that the detailed results of the stability analysis of the sway frame (Figure 4a) are given in [6]. Table 1 presents only the values of the critical load for all five analyzed cross-sections for both analyzed frames.

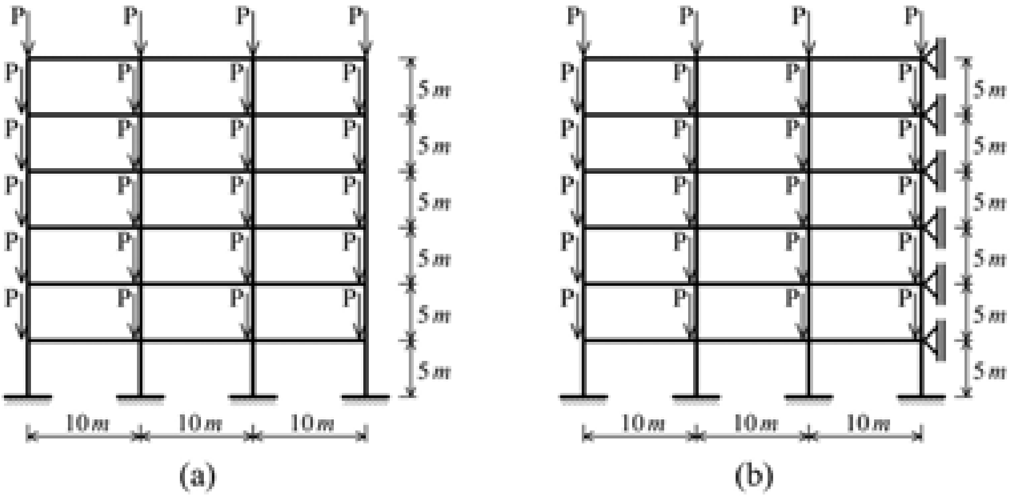

Slika 4. Numerički primer – šestospratni okvir s pomerljivim i nepomerljivim čvorovima
Figure 4. Numerical examples – six-story three-bay sway and non-sway frames

Tabela 1. Vrednosti kritične sile za okvire sa slike 4a i 4b - P_{cr}(kN)
Table 1. Values of critical load for the frames presented in Figure 4a and 4b - P_{cr}(kN)

	2[12	2[16	2[20	2[26	2[30
Sl.4a *Fig. 4a*	$P_{cr,el}$=26,01	$P_{cr,el}$=52,28	$P_{cr,el}$=96,41	$P_{cr,inel}$=209,39	$P_{cr,inel}$=307,58
Sl.4b *Fig. 4b*	$P_{cr,inel}$=113,67	$P_{cr,inel}$=176,35	$P_{cr,inel}$=243,19	$P_{cr,inel}$=372,07	$P_{cr,inel}$=457,51

Iz navedenih rezultata može se zaključiti da se pomerljivi okviri većim delom izvijaju u elastičnoj oblasti. Međutim, za razliku od njih, sistemi s nepomerljivim čvorovima izvijaju se uglavnom u neelastičnoj oblasti. Tako se tokom proračuna u programu ALIN konstantna vrednost modula elastičnosti zamenjuje tangentnim modulom koji je u funkciji nivoa opterećenja u stubovima.

Vrednosti modula E i E_t u trenutku izvijanja prikazani su u tabeli 2. Jasno je da što su stubovi krući, oni primaju veće opterećenje, tako da su im vrednosti tangentnog modula manje. U tabeli 2 prikazani su rezultati za tri najopterećenije etaže zadatog okvirnog nosača.

This numerical example illustrates the difference in the stability analysis of braced and unbraced frames in the elastic-plastic field. In contrast to unbraced frames, braced frame structures buckle in inelastic domain. So, in the calculation using the code ALIN, constant modulus E is replaced by stress dependent tangent modulus E_t.

Values of the modulus E and E_t at the moment of buckling are given in Table 2. It is clear that as the columns are stiffer, they can be more loaded and their values of the tangent modulus are lower. Results for the three most loaded floors of the analyzed frames are given in Table 2.

Tabela 2. Vrednosti tangentnog modula za okvire sa slike 4b - E_t(kN/m^2)
Table 2. Values of tangent modulus for the frame given in Figure 4b - E_t(kN/m^2)

	3. sprat *3rd floor*	2. sprat *2^{nc} floor*	1. sprat *1st floor*
2[8	E = 210,000,000	E_t = 208,233,739	E_t = 189,812,194
2[12	E_t = 207,252,644	E_t = 177,569,958	E_t = 115,288,933
2[16	E_t = 199,401,275	E_t = 150,828,451	E_t = 62,886,369
2[20	E_t = 195,939,666	E_t = 140,944,179	E_t = 44,356,530
2[26	E_t = 193,075,450	E_t = 133,169,928	E_t = 29,994,653
2[30	E_t = 192,045,713	E_t = 130,444,186	E_t = 24,997,478

4.2 Određivanje dužine izvijanja i nosivosti pritisnutih štapova okvirnih nosača

4.2.1 Određivanje dužine izvijanja pritisnutog štapa

Ispitivanje uzroka kolapsa pojedinih građevinskih konstrukcija, posebno kada su u pitanju čelične konstrukcije, pokazalo je da je često do toga dolazilo usled loma pritisnutih elemenata konstrukcije. Ovi elementi doživeli su „prevremeni” lom tako da se i pre dostizanja dopuštenih napona iscrpela njihova nosivost. Može se generalno reći da kod najvećeg broja pritisnutih čeličnih štapova granična nosivost nije uslovljena kriterijumom nosivosti, već kriterijumom stabilnosti.

Proračun na bazi teorije elastične stabilnosti široko je primenjen u inženjerskoj praksi, pošto se polazi od toga da se građevinske konstrukcije uglavnom ponašaju elastično kada su izložene svakodnevnim eksploatacionim opterećenjima, pa i u slučaju kada opterećenje dostigne kritičnu vrednost. Naime, u želji da se projektuju vitke građevinske konstrukcije, često se dešava da se grade nosači velike visine i male krutosti, pa se izvijanje nosača dešava u elastičnoj oblasti. Zato je razumljivo da ovaj vid proračuna predstavlja osnovu standarda (propisa) za analizu stabilnosti okvirnih konstrukcija. On je definisan određivanjem tzv. efektivne dužine izvijanja pojedinih štapova okvirnih nosača.

Fizički gledano, dužina izvijanja je dužina zamenjujućeg obostrano zglobno oslonjenog štapa konstantnog preseka, opterećenog konstantnom normalnom silom. Kritična sila ima oblik:

4.2 Determination of the effective buckling length of the compressed members and determination of the load-bearing capacity of the compressed member

4.2.1 Determination of the effective buckling length of the compressed members

Investigation of the causes of the collapse of some building structures, especially made of steel, found out that collapse often occurred due to the failure of the compressed structural elements. It was found that failure of some elements happened in a way that before the allowable stress was reached, the member load-bearing capacity was exhausted. Generally it can be said that for the most of the compressed steel members, ultimate bearing capacity is determined by the stability criterion.

Calculation based on the theory of elastic stability is widely applied in engineering practice. It is because it can be assumed that building structures generally have elastic behavior when they are subjected to standard exploitation load, even in the case when the critical load is reached. Namely, in order to design structures with high slenderness, designers often make tall structures with low stiffness, so buckling occurs in the elastic domain. Therefore it is reasonable that this type of elastic calculation is the basis of the regulations for the stability analysis of frame structures. Such calculation procedure is defined through the determination of the effective buckling length of frame columns.

From the physical point of view, “effective buckling length” is a length of the equivalent member with constant cross-section that is pined at the both ends and is subjected to the compressive axial force. Critical force is defined by:

$$P_{cr} = \frac{\pi^2 EI}{(\beta \cdot l)^2} \tag{10}$$

i jednaka je kritičnoj sili posmatranog štapa proizvoljnih karakteristika. Matematički gledano, dužina izvijanja je rastojanje između susednih realnih ili fiktivnih prevojnih tačaka izvijenog štapa.

Dužina izvijanja prikazuje se pomoću proizvoda koeficijenta dužine izvijanja „β” i stvarne dužine štapa „*l* ”:

and it is equal to the critical force of the analyzed member with arbitrary characteristics. From the mathematical (geometrical) point of view, “effective buckling length” is a distance between inflection points of the bended member.

The effective buckling length is given as the product of the column's effective length factor „β“ and the geometric length of the column „*l* “:

$$l_i = \beta \cdot l \tag{11}$$

Postupak određivanja efektivne dužine za štapove okvirnih konstrukcija prikazan je u JUS standardima [25], kao i evropskim normama EC3 za čelične konstrukcije [10], [11]. Na bazi tako određenih dužina izvijanja dalje se obavlja proračun aksijalno pritisnutih štapova korišćenjem tzv. krivih izvijanja. Na slici 5 prikazane su dužine izvijanja štapova s različitim uslovima oslanjanja. Na osnovu tako određene dužine izvijanja iz jednačine (10) nalazi se i veličina kritične sile.

Procedure for calculation of the effective buckling length for the members in steel frame structures is given in national JUS standards [25] and European regulations EC3 [10], [11]. On the basis of such obtained buckling lengths, the calculation based on the buckling curves is applied for the axially compressed members. Effective buckling lengths for the members with different boundary conditions are shown in Figure 5. According to obtained buckling lengths, critical load is derived from the equation (10).

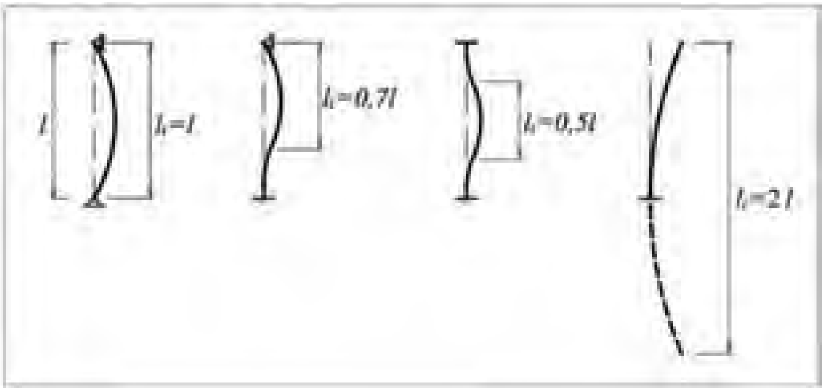

Slika 5. Dužina izvijanja štapova u funkciji uslova oslanjanja
Figure 5. Effective buckling lengths in function of the boundary conditions

Ovaj pristup proračuna kritične sile preko određivanja dužine izvijanja primenjuje se i pri proračunu pritisnutih štapova okvirnih nosača [21]. Tako na primer, kada se vrši proračun stabilnosti okvirnog nosača sa slike 6a, koristi se izraz (10) i određuje dužina izvijanja, odnosno kritična sila svakog stuba ponaosob. Razlog za ovakav pristup leži u činjenici da se do nedavno smatralo da je proračun stabilnosti kompletne okvirne konstrukcije komplikovan za inženjersku praksu. Zato se u navedenim propisima za proračun stabilnosti okvirnih konstrukcija koriste uprošćene statičke šeme, kao na primer ona koja je prikazana na slici 6b. To praktično znači da se razmatra stub koji je „izdvojen" iz okvira, a koji je elastično uklješten ili oslonjen samo na stubove i grede koji su u njegovoj neposrednoj okolini.

This approach to calculate the critical load, when the effective buckling length is obtained, is applied also to the columns of the frame structures [21]. For example, analysis of the whole frame structure (Figure 6a) is performed using the equation (10), and critical load and effective buckling lengths should be defined for each column individually. The reason for this is the fact that until recently it was considered that global stability analysis of frame structures is too complicated for engineering practice. That is the reason why the codes for the stability analysis of plane frame columns, use simplified static scheme, as presented in Figure 6b. Practically, this means that codes consider only columns which are isolated from the frame structure. These isolated columns are supported only by the adjacent columns and beams. Basically, presence of the other structural elements connected to the considered one is introduced by the corresponding boundary conditions.

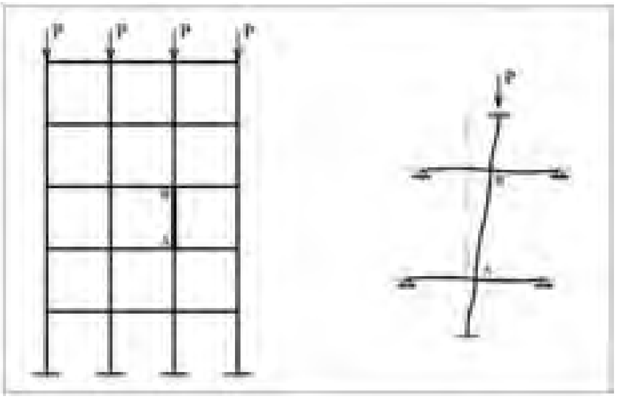

a) b)

Slika 6. Uprošćena statička šema za proračun stabilnosti prema propisima
Figure 6. Simplified static scheme for the stability analysis according to the codes

Ovakav približan, pojednostavljen proračun ima svojih prednosti jer se relativno lako dolazi do rezultata koji su prikazani u vidu odgovarajućih dijagrama i formula. Međutim, postavlja se pitanje da li su takva približna rešenja dovoljno tačna i da li se mogu primeniti na različite slučajeve koji se javljaju u inženjerskoj praksi. Postavlja se i pitanje da li ih i dalje treba koristiti, kada su usled burnog razvoja kompjuterske tehnike i

This approximate, simplified calculation has its advantages because results can be obtained very easily and they are shown by adequate diagrams and approximate formulas. However, very important question is how these approximate solutions are correct and how they can be used for the various examples in engineering practice. Also, there is important question should such solutions still be used, due to the fact that programi za proračun stabilnosti okvirnih nosača postali opšte dostupni.

U ovom radu koristi se metodologija proračuna koja se zasniva na globalnoj analizi stabilnosti okvirne konstrukcije. To podrazumeva da se prvo odredi kritično optereće okvirnog nosača u celini $P_{cr,gl}$, a zatim se na osnovu njega određuju kritične sile za svaki pojedinačni stub P_{cr}. Na osnovu njih dobijaju se koeficijenti efektivne dužine izvijanja pojedinačnih stubova iz izraza:

fast development of computing possibilities is in the progress and the programs for stability analysis of frame structures become generally available.

The methodology of calculation that is used in this paper is related to the global stability analysis of frame structures. This means that critical load for the whole structure ($P_{cr,gl}$) should be calculated first. When this critical load is calculated, the critical load for each column (P_{cr}) can be obtained. Based on these results, effective length factor of individual columns is given by:

$$\beta = \sqrt{\frac{\pi^2 EI}{P_{cr} \cdot l^2}} \tag{12}$$

U slučaju izvijanja u plastičnoj oblasti usvojiće se isti izraz za koeficijent β, s tim što se P_{cr} odnosi na kritičnu silu koja je sračunata na osnovu neelastičnog ponašanja okvira ($P_{cr,inel}$), a modul elastičnosti E više nije konstanta, već je funkcija nivoa naprezanja i zamenjuje se tangentnim modulom E_t :

In the case of buckling in the plastic domain, the expression for the coefficient β has the same form as (12), but critical load (P_{cr}) is related to the critical force that is computed in the inelastic analysis of the frame ($P_{cr,inel}$). Also, modulus of elasticity E is no longer constant, but it is stress dependent and it is replaced by the tangent modulus E_t:

$$\beta = \sqrt{\frac{\pi^2 E_t I}{P_{cr,inel} \cdot l^2}} \tag{13}$$

4.2.2 Određivanje nosivosti pritisnutog štapa

Istraživanja prikazana u ovom radu zasnovana su na pretpostavkama o idealno pravom štapu od idealno homogenog materijala, i koji je idealno centrično opterećen. Jasno je da ove pretpostavke ne mogu biti u potpunosti ispunjene kada je u pitanju realan štap. Zato se od prvih eksperimenata (Bauschinger) pa sve do danas obavljaju intenzivna eksperimentalna istraživanja s ciljem da se što bolje sagleda stvarno ponašanje pritisnutih štapova.

Ova istraživanja ukazala su na brojne nesavršenosti realnih štapova koje izazivaju značajnu disperziju teorijskih i eksperimentalnih rezultata. Osnovni razlozi su mnogi faktori koji utiču na ponašanje i nosivost ovih štapova, kao što su: zaostali naponi, imperfekcije vezane za geometriju i oblik nosača, ekscentričnost pri opterećenju, struktura materijala, istorija opterećenja i drugo. Analizirajući pojedinačno ove faktore, može se konstatovati da, iako se polazi od pretpostavke da je materijal (čelik) idealno homogen, u praksi to nije slučaj. Ova nehomogenost materijala ima za posledicu različite module elastičnosti i granicu razvlačenja po poprečnom preseku nosača.

Jedan od vidova nesavršenosti (imperfekcija) materijala, osim njegove nehomogenosti, jeste i pojava sopstvenih (zaostalih) napona. Oni mogu biti izazvani termičkim uzrocima u toku proizvodnje kada se vrši valjanje ili hlađenje, kao i kasnije tokom procesa zavarivanja. Takođe, zaostali naponi mogu se javiti usled mehaničkih uzroka, kada se vrši ispravljanje limova i slično. Usled ovih zaostalih napona, tokom opterećenja (eksploatacije) dešava se kod centrično opterećenih štapova da se u pojedinim delovima poprečnog preseka formiraju plastične zone, iako središnji napon nije dostigao granicu razvlačenja. Zbog ove pojave smanjena je krutost štapa, pa samim tim i

4.2.2 Determination of the load-bearing capacity of the compressed member

The investigations presented in this paper are based on the assumptions that the members are perfect, which means that they are perfectly straight and geometric imperfections are not taken into account. The load is also perfectly centric. It is clear that these assumptions can not be fully realized for the real members in engineering structures. Therefore, from the first experiments (Bauschinger) up to day, the intensive experimental research has been performed in order to predict the real behavior of compressed members.

Such studies have indicated numerous imperfections of real members that lead to significant dispersion of theoretical and experimental results. These factors that have influence upon the behavior and load-bearing capacity of the observed members are: residual stresses, imperfections related to the geometry and shape of the girder, eccentric load, structure of the material, load histories, etc. Analyzing these factors separately, it can be concluded that, although it is assumed that the steel is ideal homogeneous material, it is not the case in practice. Such material inhomogeneity results in different moduli of elasticity and yield stress over the beam cross-section.

One of the types of material imperfections, besides its inhomogeneity is a phenomenon of residual stresses. They can be caused by thermal effects during production when mill rolling or cooling are performed, and later during the welding process. Also, residual stresses may occur due to mechanical causes, when straightening of steel sheet is performed. Due to these residual stresses, at some parts of the cross section of centrically loaded members, plastic zones might develop even though the normal stress has not reached the yield value. It reduces stiffness of the member, and therefore load bearing njegova nosivost.

Realni nosači u građevinskim konstrukcijama izgrađeni su uvek s manjim ili većim geometrijskim nesavršenostima. Pri njihovoj montaži i formiranju građevinske konstrukcije dolazi do dodatnih imperfekcija ne samo u geometriji nosača već i u nanošenju opterećenja, odnosno pojavi neželjenih ekscentričnosti. Ove nesavršenosti predstavljaju početne deformacije pri izvijanju štapa, koje imaju za posledicu smanjenje granične nosivosti.

Kako bi se definisala stvarna nosivost centrično opterećenih štapova, prišlo se određivanju tzv. krivih izvijanja. Kao rezultat dugotrajnih eksperimentalnih i teorijskih istraživanja u razvijenim zemljama Evrope, došlo se do evropskih krivih izvijanja. Analitičkoj formulaciji ovih krivih najviše su doprineli Perry, Maquoi i Roundal [20], [18]. Ove krive našle su zatim primenu u standardima za proračun čeličnih konstrukcija gotovo svih evropskih zemalja. U evropskim normama one čine deo standarda dat u EC3 [11] i prikazane su na slici 7.

capacity of the member is also reduced.

Real girders in civil engineering structures have been built with more or less geometrical imperfections. In assembly and construction of structures, additional imperfections may appear not only in geometry, but also when the load is applied and the unwanted eccentricity occurs. These imperfections represent the initial strain at buckling of the member and result in reduction of ultimate bearing capacity (critical load).

In order to define the real load bearing capacity of centrically loaded members, it was necessary to determine the so-called "buckling curves". As a result of long-term experimental and theoretical studies, European buckling curves are formulated. Analytical formulation of these curves was contributed most by Perry, Maquoi and Roundal [20], [18]. These curves then were applied in standards for design of steel structures of almost all European countries. In European regulations they are part of the standards given in EC3 [11] and are shown in Figure 7.

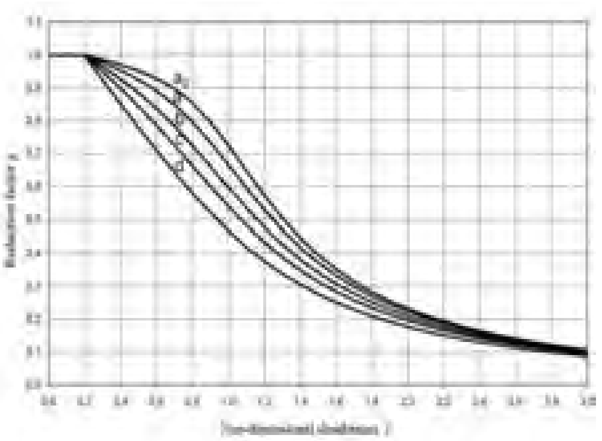

Slika 7. Krive izvijanja prema EC3 (preuzeto iz [11])
Figure 7. Buckling curves according to EC3 (taken from [11])

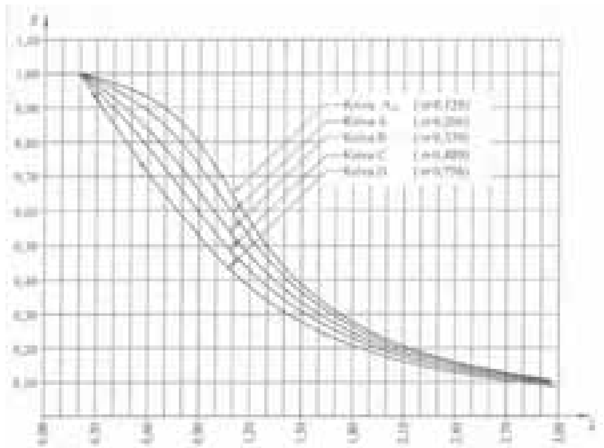

Slika 8. Krive izvijanja prema našim propisima (preuzeto iz [3])
Figure 8. Buckling curves according to JUS (taken from [3])

Naši propisi za proračun centrično opterećenih štapova od čelika takođe se zasnivaju na ovim istraživanjima i odgovaraju evropskim krivama iz standarda EC 3. Te krive su prikazane na slici 8.

Ove krive izvijanja predstavljaju modifikaciju teorijskih krivih izvijanja, jer vode računa o svim imperfekcijama koje se javljaju kod realnih štapova. Pokazalo se da je nemoguće obaviti proveru nosivosti svih pritisnutih elemenata konstrukcije pomoću jedinstvene krive. Naime, mnogo je parametara koji utiču na izvijanja nosača, a to je pre svega početna deformacija štapa, oblik poprečnog preseka, nivo sopstvenih napona, način izrade i debljina delova poprečnog preseka. Da bi se obuhvatili svi ovi aspekti, neophodno je formirati seriju krivih izvijanja za svaki pojedinačni slučaj, kako je to definisano standardom.

Kako se sa slika 7 i 8 vidi, krive izvijanja definišu se preko bezdimenzionalnog koeficijenta otpornosti elementa na izvijanje χ, u funkciji relativne vitkosti $\overline{\lambda}$ i imperfekcija štapa. Naime, da bi se lakše vršio proračun, umesto uobičajene veze između kritičnog napona izvijanja σ_{cr} i vitkosti štapa λ uvodi se zavisnost u

Our national standards for the calculation of centrally loaded steel members (JUS) are also based on these studies, and they are similar to European standards EC 3. These curves are given in Figure 8.

These curves represent a modification of the theoretical buckling curves because they take into account all imperfections that occur in real members. It has proved to be impossible to perform the calculation of load bearing capacity of all compressed structural elements using the single curve. Namely, a lot of parameters have influence on the buckling of girders, primarily: initial deformation of the member, the shape of the cross section, the level of residual stresses, method of fabrication of elements, the thickness of parts of the cross section and so on. In order to cover all these aspects it is necessary to define a series of buckling curves for each case, as it is defined in the standard.

As it can be seen from Figures 7 and 8, buckling curves are defined by reduction factor for relevant buckling mode χ that is the function of appropriate non-dimensional slenderness $\overline{\lambda}$ and imperfection factor of the member. Namely, in order to make calculations bezdimenzionalnom obliku, preko koeficijenata χ i $\bar{\lambda}$. Koeficijent izvijanja χ dobija se kada se kritični napon izvijanja podeli s naponom na granici razvlačenja.

easier, instead of the usual relationship between the critical buckling stress σ_{cr} and member slenderness λ, the relationship in the non-dimensional form is introduced using the coefficients χ and $\bar{\lambda}$. Reduction factor χ is obtained when the critical buckling stress is divided by the stress at the yield point.

$$\chi = \frac{\sigma_{cr}}{\sigma_v} \tag{14}$$

Da bi se očuvala zavisnost, relativna vitkost $\bar{\lambda}$ dobija se tako što se vitkost λ deli s vitkošću na granici razvlačenja:

In order to use these curves, it is necessary that slenderness λ should be divided by the slenderness at the yield point:

$$\bar{\lambda} = \frac{\lambda}{\lambda_v} \tag{15}$$

gde je:

where:

$$\lambda_v = \pi \sqrt{\frac{E}{\sigma_v}} \tag{16}$$

Iz gornjeg izraza vidi se da vitkost na granici razvlačenja zavisi samo od vrste materijala. To znači da koeficijent χ za isti materijal direktno zavisi od vitkosti, odnosno dužine izvijanja štapa. Prema tome, da bi se ove krive izvijanja mogle ispravno koristiti, odnosno da bi davale tačne rezultate, neophodno je tačno odrediti vitkost, odnosno dužinu izvijanja štapa.

Treba napomenuti da su ove krive nastale na osnovu eksperimentalnih istraživanja ponašanja jednog izolovanog štapa s tačno definisanim graničnim uslovima, što je omogućilo i dobijanje tačne teorijske vrednosti kritične sile odnosno dužine izvijanja. Kako se ove krive koriste i za proračun stubova okvirnih nosača, potrebno je za svaki štap okvira tačno proračunati teorijsku vrednost kritične sile odnosno dužinu izvijanja.

Već ranije je u ovom radu napomenuto da donedavno ovaj proračun nije bilo lako sprovesti, pa su u standardima data približna rešenja. U narednom delu rada dokumentovaće se da ta približna rešenja često prouzrokuju greške koje se ne mogu tolerisati. Kada se navedene krive izvijanja koriste za proračun štapova okvirnih nosača, posledica su greške u proračunu njihove nosivosti koje se takođe ne mogu tolerisati, jer se u proračun ulazi s netačnim rezultatima za dužinu izvijanja, odnosno vitkost štapa. Zato je u prethodnom delu rada data metodologija proračuna prema jednačini (12) koja definiše postupak za određivanja tačne vrednosti kritične sile, odnosno dužine izvijanja.

U nastavku će biti prikazani numerički primeri koji ilustruju kakve greške nastaju pri proračunu štapova okvirnih nosača, kada se koriste približna rešenja iz postojećih standarda.

From the expression (16) it can be seen that slenderness at the yield point depends only on the material. It means that the coefficient χ for the same material is directly related to the slenderness, and respectively to the buckling length of the member. Therefore, in order that buckling curves could be used properly and that they would provide accurate results, it is necessary to accurately determine the slenderness and the buckling length of the member.

It should be mentioned that these curves were obtained on the basis of experimental studies of the behavior of an isolated member with clearly defined boundary conditions, so it is possible to calculate the exact theoretical value of the critical buckling load and buckling length. As these curves are used for calculation of columns of the frame structures, it is necessary to calculate accurately the theoretical value of the critical buckling load and buckling length for each member of the frame.

Previously, it was mentioned that until recently, this calculation was not easy to carry out, so the approximate solutions are given in the standards. The following section will present that this approximate solutions often lead to the errors that can not be tolerated. The consequence is that when these buckling curves are used for the calculation of members of frame structures, the substantial errors in the calculation of their load bearing capacity also occurs. The reason for this error is in the fact that calculation uses the incorrect results for the buckling length and slenderness of the member. Therefore, in the previous part of this paper the methodology of calculation according to the equation (12), which defines the procedure for determining the exact value of critical load and corresponding buckling length, is given.

The following section will present the numerical examples that illustrate what kinds of errors are arising in the calculation of members of frame structures, when the approximate solutions from the existing standards are used.

4.2.3 Numerički primer

U ovom delu analiziran je okvirni nosač sa slike 4b.

Kao što je ranije rečeno, u aktuelnim propisima prikazana su rešenja koja se dobijaju analizom elastične stabilnosti. Zato su ta rešenja i upoređena s rezultatima programa ALIN gde je dobijena „elastična” kritična sila, tj. pretpostavljeno je da je modul elastičnosti sve vreme konstantan. Međutim, kao što je već ranije pokazano, kod višespratnih okvirnih nosača s nepomerljivim čvorovima stubovi se često izvijaju u neelastčnom području. Zato je ovde sproveden i taj način proračuna.

Posmatran je primer gde su usvojene dimenzije elemenata kao i ranije: stubovi su visina *l*=5m, a grede dužina 2*l*=10m. Karakteristike materijala su E=210,000,000kN/m^2 i σv=240,000 kN/m^2. Radi poređenja dobijenih rezultata, proračun je sproveden za svih šest do sada analiziranih poprečnih preseka. Vrednosti kritičnog opterećenja i odgovarajućeg tangentnog modula već su prikazane u tabelama 1 i 2. Prikaz rezultata koeficijenata efektivne dužine izvijanja za najopterećenije stubove (na prvoj etaži) dat je u tabeli 3.

4.2.3 Numerical example

The frame with characteristics given in Figure 4b is analyzed in this part.

As previously mentioned, the existing structural codes give solutions that are obtained using the elastic stability analysis. Therefore these solutions are compared with the results obtained using the program ALIN when the elastic critical force is calculated, i.e. when it is assumed that the modulus of elasticity E is constant. However, as already indicated before, non-sway multi-story frames often buckle in inelastic domain, so such kind of analysis also is performed herein.

Characteristics of the material and dimensions of the elements are taken the same as in the previous examples. Calculation is performed for all six considered cross sections. Results of the critical load and tangent modulus values are given in Tables 1 and 2. Table 3 represents results for the effective buckling length coefficient β for the most loaded columns (at the first floor).

Tabela 3. Koeficijent β za stubove 1. sprata analiziranog okvira s nepomerljivim čvorovima
Table 3. Coefficient β for the columns on the first floor of the analyzed non-sway frame

1.sprat *1st floor*	β (EC3)		β (jus)		$β_{EL}$	$β_{INEL}$
	unutr. *inner*	spolj. *outer*	unutr. *inner*	spolj. *outer*		
2[8	0.673	0.686	0.652	0.672	0.751	0.726
2[12						0.635
2[16						0.533
2[20						0.518
2[26						0.509
2[30						0.511

Prvo se može uočiti da kod stubova prvog najopterećenijeg sprata postoji solidno poklapanje rezultata dobijenih primenom propisa i primenom elastične analize, korišćenjem programa ALIN. Međutim, kao što je pokazano u [6], razlika u rezultatima se znatno uvećava kako se analiziraju stubovi na višim spratovima. Kao ilustracija toga, u tabeli 4 prikazane su vrednosti koeficijenta β za unutrašnje stubove analiziranog okvira, gde su rezultati primenom programa ALIN dati samo u slučaju analize u elastičnoj oblasti.

First, it can be noticed that for the columns of the first floor there is a quite well coinciding of the results obtained using the code ALIN, as well as European and national codes for steel structures. However, as it is shown in [6], the differences in the results increase for the columns in the higher floors. As an illustration of this observation, Table 4 gives the values of the coefficient β for the inner columns of the analyzed frame. In this table, the results obtained by code ALIN are given only in case of elastic stability analysis.

Tabela 4. Koeficijent β za unutrašnje stubove okvira sa slike 4b
Table 4. Coefficient β for the inner columns of the frame given in Figure 4b

metod proračuna *calculat. method*		ALIN (elast.)	EC3	differ. (%)	JUS	differ. (%)
sprat *floor*	1	0.751	0.673	-10.3	0.652	-13.1
	2	0.823	0.906	10.0	0.857	4.1
	3	0.920	0.906	-1.5	0.857	-6.9
	4	1.062	0.906	-14.7	0.857	-19.3
	5	1.301	0.906	-30.3	0.857	-34.1
	6	1.840	0.873	-52.5	0.816	-55.6

Razlog za ovakvu razliku u rezultatima je u tome što se proračun prema propisima bazira na analizi izolovanog elementa, tj. uzima se u obzir samo krutost stubova i greda koji su vezani u neposrednoj blizini krajnjih tačaka posmatranog elementa. Takođe, propisi ne uzimaju u obzir veličinu aksijalne sile u elementu.

Iz rezultata u tabeli 3, takođe se jasno vidi kolike se razlike dobijaju kada se proračun vrši u elastičnoj u odnosu na elasto-plastičnu oblast. Zato je u tabeli 5 data detaljnija analiza, odnosno prikazane su vrednosti koeficijenta β za stubove svih etaža ovog nepomerljivog šestospratnog okvirnog nosača.

One of the main reasons for this difference in results is that the calculations according the codes are based on the isolated treatment of considered compressed elements. They only consider stiffness of the other structural elements connected to the considered one. Also, codes do not take into consideration the axial force value in the element.

Results from table 3 also shows what difference in results are obtained when the calculation is performed in elastic and elastic-plastic domain respectively. So, values of the coefficient β for the columns in all stories of the analyzed non-sway six story frame are given in Table 5.

Tabela 5. Vrednosti koeficijenta β za stubove na svim spratovima analiziranog okvira
Table 5. Values of coefficient β for the columns in all stories of the analyzed frame

	β_{el}	2[8	2[12	2[16	2[20	2[26	2[30
$\beta_{in,1}$	0.751	0.726	0.635	0.533	0.518	0.509	0.511
$\beta_{in,2}$	0.823	0.833	0.863	0.905	1.012	1.176	1.278
$\beta_{in,3}$	0.920	0.936	1.042	1.163	1.334	1.583	1.734
$\beta_{in,4}$	1.062	1.080	1.195	1.374	1.592	1.905	2.093
$\beta_{in,5}$	1.301	1.323	1.484	1.557	1.814	2.180	2.398
$\beta_{in,6}$	1.840	1.871	2.098	2.388	2.762	2.424	2.669

Na slici 9 prikazane su krive izvijanja za stubove prve etaže s poprečnim presekom 2[20 (i=0.0589m). Rešenja dobijena na osnovu elastične, odnosno neelastične analize prikazana su tačkastom, odnosno isprekidanom linijom.

Figure 9 represents the buckling curves for the columns of the first floor which have a cross-section 2[20 (i=0.0589m). The solutions obtained on the basis of elastic and inelastic analysis are marked with dotted and dashed line, respectively.

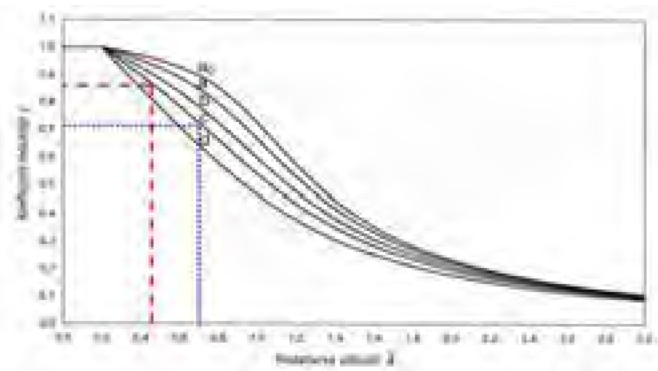

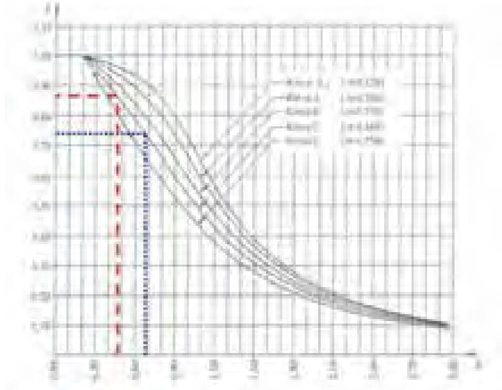

Slika 9. Određivanje koeficijenta χ prema EC3 i JUS-u
za 1.sprat analiziranog okvira s nepomerljivim čvorovima

Figure 9. Determination of coefficient χ using the EC3 and JUS
(first floor of the analyzed non-sway frame)

Očigledno je da se čini značajna greška u proračunu nosivosti stuba, ukoliko se umesto tačne vrednosti za β odnosno $\bar{\lambda}$ koje odgovaraju izvijanju u plastičnoj oblasti koriste vrednosti koje odgovaraju izvijanju u elastičnoj oblasti kako je to definisano postojećim standardima.

It is obvious that significant error in the calculation of the load-bearing capacity of the compressed columns can be made. That happens when, instead of the exact values for β (and the corresponding $\bar{\lambda}$) that are obtained based upon the buckling in plastic domain, the results of elastic analysis are used, as it is defined in the existing structural codes.

5 ZAKLJUČAK

U ovom radu predložen je proračun koji se zasniva na analizi globalne stabilnosti okvirne konstrukcije i – u prvom koraku – određivanju kritične sile za konstrukciju u celini. Zatim se u nastavku određuju kritične sile, odnosno dužina izvijanja pojedinih pritisnutih štapova i to na bazi odnosa između ukupne kritične sile u konstrukciji i normalne sile u pojedinim štapovima.

Predloženi postupak nije nepoznat, ali način kako je on ovde formulisan i sproveden nije do sada primenjen ni u jednom od komercijalnih programa koji se bave stabilnošću okvirnih nosača. Tako se za interpolacione funkcije usvajaju rešenja koja se dobijaju iz diferencijalne jednačine savijanja štapa po teoriji drugog reda. U ovom slučaju je dovoljno da se usvoji samo po jedan konačni element duž svakog štapa u okvirnoj konstrukciji, čime se drastično smanjuje broj nepoznatih, odnosno jednačina u metodi konačnih elemenata. Upravo je i to glavna prednost ovog postupka proračuna i formiranog programa ALIN u odnosu na uobičajeni postupak koji se zasniva na primeni geometrijske matrice krutosti.

U radu je ispitivana tačnost rešenja koja su data u našim JUS i EC3 standardima, a odnose se na dužine izvijanja pritisnutih štapova okvirnih nosača. Primenom predložene metode pokazano je da se u pojedinim slučajevima čine greške ako se koriste postojeći izrazi i dijagrami dati u našim standardima. To znači da je potrebno prići inovaciji ovih standarda na način kako je to, na primer, ovde predloženo, kako bi se inženjerima u praksi omogućio tačniji način proračuna. U tom smislu već su učinjeni koraci za izmenu evropskih standarda (EC3), posebno u delu koji se odnosi na složene deformabilne konstrukcije gde se zahteva proračun po teoriji drugog reda, ali bez navođenja detalja tog proračuna.

Predloženi postupak proračuna u ovom radu korišćen je i za elasto-plastičnu analizu kada se u proračun osim geometrijske uvodi i materijalna nelinearnost. Izvedene su matrice krutosti korišćenjem tangentnog modula elastičnosti koji prati promenu krutosti štapa u neelastičnoj oblasti. Treba istaći da se u napred navedenim standardima kritična sila u plastičnoj oblasti određuje samo približnim proračunom. On se sastoji u tome da se prvo odredi kritična sila kao da se štap izvija u elastičnoj oblasti, a zatim se korišćenjem krivih izvijanja koje su u standardima definisane preko približnih (empirijskih) izraza, određuje kritična sila u plastičnoj oblasti.

Doprinos ove analize sastoji se u tome što se na osnovu formiranog algoritma proračuna koji je implementiran u programu ALIN, može analizirati ponašanje okvirne konstrukcije, ne samo u elastičnoj već i plastičnoj oblasti. Time je omogućeno praćenje fenomena gubitka stabilnosti okvirne konstrukcije i u plastičnoj oblasti i direktno određivanje kritične sile pri njenom kolapsu.

5 CONCLUSIONS

In this paper the global stability analysis of whole frame structure is suggested, and in first step, determination of the critical load for the structure as a whole. Then, the critical load and effective buckling length of each member can be found.

The proposed method is not unknown, but the way how it is formulated and implemented here has not been applied in any of the commercial programs that deal with the stability of frames. The calculation where interpolation functions are derived from the exact solution of the differential equation of bending according to the second order theory is proposed. The advantage of such an approach, which is applied in the program ALIN, is in the fact that only one finite element is needed for each beam or column, so the total number of finite elements is significantly less than in the usual approach based on the geometric stiffness matrix.

The accuracy of the solutions given in JUS and EC3 standards, related to the effective buckling length determination was investigated. Applying the proposed method it was shown that some errors are made when the approximate solutions from the codes are used. That means that there is a need for the innovation of these standards in the part where the effective length of frame columns is considered. It should be emphasized that some steps have already been taken in EC3 standards, in the part related to the complex deformable structures which require the calculation according to second order theory, however, no more details are given in EC3.

The proposed calculation method has been used also for the elasto-plastic analysis when the geometrically non-linear process is followed by development of the material nonlinearity as well. Stiffness matrices are derived using the tangent modulus which is stress dependent and that follows changes of the member stiffness in the inelastic field. These matrices have been implemented in the computer code ALIN. It should be mentioned that in the analyzed standards, a critical force in the plastic domain is determined by the approximate calculation. First, the critical load is calculated when the buckling occurs in elastic domain. Then, using the buckling curves that are defined through the approximate (empirical) expressions, the critical load in plastic domain is determined.

The contribution of this analysis is based upon the calculation algorithm implemented in code ALIN. This algorithm introduces more accurate calculation of buckling not only in elastic, but also in the plastic domain. It allows monitoring of the phenomena of stability loss of the frame structure in the plastic domain and direct determination of the critical force at the moment of buckling.

6 LITERATURA REFERENCES

[1] Allen, H.G., Bulson, P.S.: Backgroung to buckling, McGraw Hill, U.K., 1980.

[2] Bathe K.J.: Finite Element Procedures in Engineering Analysis, Prentice-Hall, 1982

[3] Buđevac D., Marković Z., Bogavac D., Tošić D.: Metalne konstrukcije, Građevinski fakultet Univerziteta u Beogradu, 1999.

[4] Bazant Z.P., Cedolin L.: Stability of Structures, Dover Publications, New York, USA, 2003.

[5] Chen W.F.: Structural stability: from theory to practice, *Engineering Structures*, Vol.22, Iss.2, pp.116–122, 2000.

[6] Ćorić S.: Nelinearna analiza stabilnost okvirnih nosača, doktorska disertacija, Građevinski fakultet Univerziteta u Beogradu, 2013.

[7] Ćorić S.: Prilog određivanju dužina stubova okvirnih nosača, magistarski rad, Građevinski fakultet Univerziteta u Beogradu, 2006.

[8] CRC Japan: Handbook of Structural Stability, Corona, Tokyo, 1971.

[9] Engesser F.: Ueber die Knickfestigkeit Gerader Stabe, Zeistschrift fur Architektur und Ingenieurwesen, 35, 1892.

[10] Eurocode 3, Design of Steel Structures - ENV 1993-1-1: 1992, European Committee for Standardization, 1993.

[11] Eurocode 3, Design of Steel Structures - ENV 1993-1-1: 2005, European Committee for Standardization, 2006.

[12] European Convention for Constructional Steelwork (ECCS): European recommendations for steel structures, 1978.

[13] Farshi B., Kooshesh F.: Buckling analysis of structural steel frames with inelastic effects according to codes, *Journal of Constructional Steel Research*, Vol.65, Iss.10–11, pp.2078–2085, 2009.

[14] Gallagher R.H.: Finite Element Analysis, Prentice-Hall, Inc. New Jersey, 1975.

[15] Gantes C., Mageirou G.: Improves stiffness distribution factors for evaluation of effective buckling lengths in multi-story sway frames, *Engineering Structures*, 2005, Vol. 27, Iss.7, pp.1113–1124.

[16] Horne M.R.: An approximate method for calculating the elastic critical loads of multi-storey plane frames, *Structural Engineer*, 1975.,Vol.56, Iss.6, pp.242–248.

[17] Horne M.R., Merchant W.:The stability of frames, Pergamon, Oxford, 1965.

[18] Massonnet C.E., Maquoi R.: Recent progress in the field of structural stability of steel structures, IABSE, Zurich, Switzerland, 1978.

[19] McGuire W., Gallagher R., Ziemain R.: Matrix Structural Analysis, 2nd edition, John Wiley and Sons, New York, USA, 2000.

[20] Rondal J., Maquoi R.: Single Equation for SSRC Column Strength Curves, *ASCE J.Struct.Div*, Vol.105, No.ST1, pp.247–250, 1979.

[21] Timoshenko S.P., Gere J.M.: Theory of Elastic Stability, New York, McGraw-Hill, 1961.

[22] White D., Hajjar J.:Buckling Models and Stability Design of Steel Frames: a Unified Approach, *Journal of Constructional Steel Research*, 1997, Vol.42, Iss.3, pp.171–207.

[23] White D., Hajjar J.: Accuracy and simplicity of alternative procedures for stability design of steel frames, *Journal of Constructional Steel Research*, 1997., Vol.42, Iss.3, pp. 209–261.

[24] Yoo H., Choi D.H.: New method of inelastic buckling analysis for steel frames, *Journal of Constructional Steel Research*, 2008, Vol.64, Iss.7, pp.1152–1164.

[25] Zarić B., Buđevac D., Stipanić B.: Čelične konstrukcije u građevinarstvu, Građevinska knjiga, Beograd, 2000.

[26] Žugić-Zornija Lj.: Nelinearna analiza mostova sa kosim kablovima, doktorska disertacija, Građevinski fakultet Univerziteta u Beogradu, 2009.

REZIME

NELINEARNA ANALIZA STABILNOSTI OKVIRNIH NOSAČA

Stanko ĆORIĆ
Stanko BRČIĆ

U ovom radu istraživan je fenomen gubitka stabilnosti okvirnih nosača u elasto-plastičnoj oblasti. Numerička analiza je sprovedena primenom metode konačnih elemenata. Matrice krutosti su izvedene korišćenjem trigonometrijskih interpolacionih funkcija koje se odnose na tačno rešenje diferencijalne jednačine savijanja štapa prema teoriji drugog reda. U slučaju kada se izvijanje konstrukcije dešava u plastičnoj oblasti, konstantan modul elastičnosti E u matrici krutosti zamenjen je tangentnim modulom E_t koji prati promenu krutosti štapa u neelastičnoj oblasti i funkcija je nivoa opterećenja u štapu. Za potrebe ove analize formiran je deo računarskog programa ALIN koji može da se koristi za elastičnu i elasto-plastičnu analizu stabilnosti okvirnih konstrukcija. Program je napisan u C++ programskom jeziku. Primenom ovog programa omogućeno je i određivanje kritičnog opterećenja okvirnih nosača u elastičnoj i neelastičnoj oblasti. U ovom istraživanju formiran je i algoritam za proračun dužina izvijanja pritisnutih štapova stubova okvirnih nosača, a koji se bazira na proračunu globalne analize stabilnosti okvirne konstrukcije. Rezultati dobijeni primenom ovog algoritma upoređeni su s rešenjima koja se dobijaju korišćenjem evropskih EC3 i domaćih JUS standarda za okvirne čelične konstrukcije, a koja su približnog karaktera. Na osnovu postupka koji je dat u ovom radu moguće je praćenje fenomena gubitka stabilnosti okvirnog nosača u plastičnoj oblasti i direktno određivanje njegove kritične sile u toj oblasti.

Ključne reči: stabilnost konstrukcija, okvirni nosači, nelinearna analiza, metod konačnih elemenata, tangentni modul

SUMMARY

NONLINEAR STABILITY ANALYSIS OF THE FRAME STRUCTURES

Stanko CORIC
Stanko BRCIC

In this paper the phenomenon of instability of frames in elasto-plastic domain was investigated. Numerical analysis was performed by the finite element method. Stiffness matrices were derived using the trigonometric shape functions related to exact solution of the differential equation of bending according to the second order theory. When the buckling of structure occurs in plastic domain, it is necessary to replace the constant modulus of elasticity E with the tangent modulus E_t. Tangent modulus is stress dependent function and takes into account the changes of the member stiffness in the inelastic range. For the purposes of numerical investigation in this analysis, part of the computer program ALIN was created in a way that this program now can be used for elastic and elasto-plastic stability analysis of frame structures. This program is developed in the C++ programming language. Using this program, it is possible to calculate the critical load of frames in the elastic and inelastic domain. In this analysis, the algorithm for the calculation of buckling lengths of compressed columns of the frames was also established. The algorithm is based on the calculation of the global stability analysis of frame structures. Results obtained using this algorithm were compared with the approximate solutions from the European (EC3) and national (JUS) standards for the steel structures. By the given procedure in this paper it is possible to follow the behavior of the plane frames in plastic domain and to calculate the real critical load in that domain.

Key words: stability of structures, frame structures, nonlinear analysis, finite element method, tangent modulus

METODA DINAMIČKE KRUTOSTI U ANALIZI VIBRACIJA KRUŽNE CILINDRIČNE LJUSKE

DYNAMIC STIFFNESS METHOD IN THE VIBRATION ANALYSIS OF CIRCULAR CYLINDRICAL SHELL

Nevenka KOLAREVIĆ
Marija NEFOVSKA DANILOVIĆ
Mira PETRONIJEVIĆ

ORIGINALNI NAUČNI RAD
ORIGINAL SCIENTIFIC PAPER
UDK: 624.074.43
doi: 10.5937/grmk1603045K

1 UVOD

Ljuske se često koriste kao elementi inženjerskih konstrukcija, naročito u mašinstvu, građevinarstvu, avio i brodskom inženjeringu. Razlog je u tome što ljuske mogu da se koriste za konstrukcije velikih raspona, bez potrebe za međuosloncima, i što ovakve konstrukcije imaju povoljan odnos krutosti i težine. Ljuske se koriste za konstrukcije rezervoara, delova trupova aviona, delova konstrukcija brodova i slično. Tokom životnog veka, odnosno tokom njihove primene, ove konstrukcije izložene su složenim uslovima okruženja koji podrazumevaju najrazličitije granične uslove i opterećenja, kao što su npr. dinamički uticaji velikog intenziteta koji mogu da dovedu do kolapsa konstrukcije. Potpuno poznavanje dinamičkih karakteristika ovih konstruktivnih elemenata od velike je važnosti da bi se obezbedilo sigurno, uspešno i ekonomski isplativo projektovanje.

Metod dinamičke krutosti (MDK), koji u poslednje vreme privlači pažnju sve većeg broja istraživača, predstavlja alternativu metodu konačnih elemenata (MKE) u analizi vibracija. Kao što je poznato, veličina konačnog elementa mora da bude manja od petine talasne dužine koja odgovara najvišoj frekvenciji u analizi da bi se dobili rezultati zadovoljavajuće tačnosti. Zato proračun konstrukcija primenom MKE u oblasti visokih frekvencija, koje se javljaju u akustici ili kod vibracija mašina visokih frekvencija, postaje glomazan i

Nevenka Kolarević, M.Sc, Univerzitet u Beogradu - Građevinski fakultet, Bulevar kralja Aleksandra 73, 11000 Beograd, Srbija, e-mail: nevenka@grf.bg.ac.rs
Docent Dr Marija Nefovska Danilović, Univerzitet u Beogradu - Građevinski fakultet, Bulevar kralja Aleksandra 73, 11000 Beograd, Srbija, e-mail: marija@grf.bg.ac.rs
Prof. Dr Mira Petronijević, Univerzitet u Beogradu - Građevinski fakultet, Bulevar kralja Aleksandra 73, 11000 Beograd, Srbija, e-mail: pmira@grf.bg.ac.rs

1 INTRODUCTION

Shells are often used as elements of engineering structures, particularly in mechanical, civil, aerospace and naval engineering. The reason is that the shells can be used for a large-span structures, without intermediate supports, and because they have a favourable stiffness to weight ratio. Shells are used for the construction of reservoirs, pressure vessels, fuselage, naval vehicles, etc. During their lifetime and exploitation, these structures are subjected to various loadings under complex boundary conditions, such as violent dynamic load, that can lead to collapse of structures. Therefore, a complete knowledge of the dynamic characteristics of these structural elements is very important to ensure a safe, successful and economically feasible design.

The dynamic stiffness method (DSM), which has recently been attracting the attention of a growing number of researchers, is an alternative to the finite element method (FEM) in the vibration and buckling analysis. As known, the size of the finite elements must be less than a fifth of the wavelength corresponding to the highest frequency in the analysis, in order to obtain satisfactory results. Therefore, the analysis of structures by FEM in the high frequencies range, that occur in acoustics and vibrations of machine at high frequencies, becomes cumbersome and time consuming because of the need for condensing the finite element mesh.

Nevenka Kolarević, M.Sc., University of Belgrade - Faculty of Civil Engineering, Bulevar kralja Aleksandra 73, 11000 Belgrade, Serbia, e-mail: nevenka@grf.bg.ac.rs
Assisstent Prof. Marija Nefovska Danilović, PhD., University of Belgrade - Faculty of Civil Engineering, Bulevar kralja Aleksandra 73, 11000 Belgrade, Serbia, e-mail: marija@grf.bg.ac.rs, Prof. Mira Petronijević, PhD., University of Belgrade - Faculty of Civil Engineering, Bulevar kralja Aleksandra 73, 11000 Belgrade, Serbia, e-mail: pmira@grf.bg.ac.rs

dugotrajan zbog potrebe za progušćenjem mreže konačnih elementa.

Dinamička matrica krutosti, koja povezuje sile i pomeranja na granicama elementa, dobija se na osnovu tačnog rešenja parcijalnih diferencijalnih jednačina kojima je definisan problem slobodnih vibracija u frekventnom domenu. Samim tim, matrice krutosti određene na ovaj način jesu tačne, frekventno zavisne i sadrže, pored krutosti, inerciju i prigušenje, pa se elementi zasnovani na tim matricama nazivaju i kontinualni elementi. Njihovom primenom diskretizacija domena je svedena na minimum, odnosno jedan kontinualni element je dovoljan da se opiše ponašanje konstruktivnog elementa konstantnih materijalnih i geometrijskih karakteristika. Globalna dinamička matrica krutosti formira se na sličan način kao i u MKE, s tom razlikom što su u MDK dvodimenzionalni elementi, umesto u čvorovima, spojeni duž kontura. Na taj način, primenom MDK moguća je analiza i konstruktivnih sistema. Na osnovu svega rečenog, može da se zaključi da je MDK spojio prednosti analitičkih i diskretnih-numeričkih (MKE) metoda.

Dinamičke matrice krutosti prvo su bile izvedene za jednodimenzionalne elemente. Na osnovu rešenja problema slobodnih vibracija pravog grednog nosača, koje postoji u zatvorenom obliku, izvedene su dinamičke matrice krutosti po Euler–Bernoulli-jevoj i Timoshenko-ovoj teoriji [1-4]. Casimi*r* [5] je odredio dinamičku matricu krutosti zakrivljene grede, pri čemu je rešenje diferencijalne jednačine odredio numerički. Na isti način, Le Sourne [6] odredio je dinamičku matricu krutosti kružne cilindrične ljuske. Kontinualni elementi formulisani na ovakav način nazivaju se i numerički kontinualni elementi.

Kod pravougaone ploče, problem slobodnih vibracija može da se reši u zatvorenom obliku samo za specijalne granične uslove. Gorman [7] je predložio analitičko rešenje problema slobodnih vibracija pravougaone ploče, koje je nezavisno od graničnih uslova, u obliku sume jednostrukih Fourier-ovih redova. Ovaj metod se naziva metod superpozicije i korišćen je, uz metod projekcije kojim su diskretizovani granični uslovi, za izvođenje dinamičke matrice krutosti pravougaone ploče po Kirchhoff-oj teoriji [8]. Primenom metoda superpozicije i metoda projekcije formulisana je i dinamička matrica krutosti pravougaone ploče za naprezanje u ravni [9], za poprečne vibracije po Mindlin-ovoj teoriji [10], kao i za poprečne vibracije slojevite ploče primenom smičuće teorije višeg reda [11].

Ako je debljina ljuske manja od 1/20 talasne dužine i/ili poluprečnika krivine, teorija tankih ljuski, gde su zanemarene smičuća deformacija i rotaciona inercija, generalno je prihvatljiva. U zavisnosti od pretpostavki učinjenih tokom izvođenja kinematičkih relacija, definisanja presečnih sila i uslova ravnoteže, formulisane su različite teorije tankih ljuski, čiji je pregled dat u knjizi od Leisse-a [12]. U ovom radu je formulisana dinamička matrica krutosti kružne cilindrične ljuske po Flügge-ovoj teoriji. U sistemu parcijalnih diferencijalnih jednačina, kojima je definisan problem slobodnih vibracija, izvodi po vremenu su eliminisani korišćenjem spektralne dekompozicije, dok je tangencionalna koordinata eliminisana primenom rešenja u obliku Fourier-ovog reda. Na taj način je dobijen sistem od tri obične diferencijalne jednačine koje su funkcija samo

The formulation of the dynamic stiffness (DS) matrix, which relates forces and displacements at the boundaries of the element, is based on the exact solutions of the free vibration problem in the frequency domain. Therefore, the stiffness matrices determined in this manner are accurate, frequency dependent, and contain among the stiffness, inertia and damping. Therefore, the elements based on these matrices are called continuous elements. By their usage, the discretization of observed domain is reduced to a minimum, i.e. one continuous element is sufficient to describe behaviour of a structural element of constant material and geometrical properties. The global stiffness matrix is obtained using the assembly procedure in the same way as the FEM, with one exception - in the DSM two dimensional elements, instead at nodes, are connected along the boundary lines. Finally, it can be concluded that the DSM uses advantages of analytical as well as numerical methods (FEM).

The dynamic stiffness matrix was first developed for one-dimensional elements. Based on the closed form solution of the free vibration of a straight beam, the dynamic stiffness matrix according to the Euler-Bernoulli and Timoshenko beam theory was formulated [1-4]. Casimir [5] developed the dynamic stiffness matrix of a curved beam, whereby the differential equations were solved numerically. In the same way, Le Sourne [6] derived the dynamic stiffness matrix of a circular cylindrical shell. Continuous elements formulated in this way are called numerical continuous elements.

For a rectangular plate, the free vibration problem can be solved in a closed form only for special combinations of boundary conditions. Gorman [7] applied the method of superposition and obtained analytical solution for free vibration of a rectangular Kirchhoff plate with arbitrary boundary conditions, in the form of the Fourier series. Casimir [8] used the method of superposition, along with the method of projection for discretization of boundary conditions, and derived dynamic stiffness matrix of a rectangular Kirchhoff plate [8]. In the same manner, continuous rectangular plate elements for the in-plane vibration [9], transverse vibration according to the Mindlin plate theory [10] and transverse vibration of a laminated plate using the higher-order shear deformation theory [11] have been formulated, as well.

Thin shell theory, which neglects shear deformation and rotary inertia, is generally acceptable if the shell thickness is less than $1/20^{th}$ of the wavelength and/or radius of curvature. Depending on the assumptions made in the strain–displacement relations, the force and moment resultant equations and equilibrium equations, various thin shell theories have been formulated. A comprehensive overview of the shell theories is given in the book of Leissa [12]. In this paper the dynamic stiffness matrix of a circular cylindrical shell element according to the Flügge thin shell theory is formulated. In the governing partial differential equations time derivatives are eliminated by using the spectral decomposition, while the circumferential coordinate is eliminated by applying the solution in the form of Fourier series. Therefore, the governing system of three partial differential equations is transformed into the system of three ordinary differential equations, which depends only on the longitudinal coordinate. By expanding the podužne koordinate. Razvijanjem determinante ovog sistema jednačina dobijena je jedna obična diferencijalna jednačina osmog reda s konstantnim koeficijentima, čije je rešenje dobro poznato. Povezivanjem komponenti vektora sila i vektora pomeranja na krajevima ljuske formirana je dinamička matrica krutosti, koja je implementirana u za tu svrhu napisani Matlab [13] program za određivanje sopstvenih vrednosti i oblika oscilovanja kružne cilindrične ljuske. Metod dinamičke krutosti primenjen je u analizi slobodnih vibracija kružne cilindrične ljuske s različitim kombinacijama graničnih uslova, skokovitom promenom debljine, kao i s prstenastim međuosloncima. Putem numeričkih primera izvršena je verifikacija dobijenih rezultata poređenjem s dostupnim analitičkim rešenjima u literaturi, kao i s rezultatima Abaqus-a [14].

determinant of this system of equations, one eighth order ordinary differential equation with constant coefficients is obtained. The solution of this equation is well known. The dynamic stiffness matrix is formulated by relating the force and displacement vectors at the ends of a circular cylindrical shell element. It is implemented in the computer program, written in Matlab [13], for computing natural frequencies and mode shapes of circular cylindrical shell assemblies. The dynamic stiffness method is applied to the free vibrations analysis of circular cylindrical shells with different combinations of boundary conditions, stepped thickness variation and intermediate ring supports. Verification of the obtained results is carried out in comparison with available analytical solutions in the literature, as well as with the results of the Abaqus [13].

2 FORMULACIJA PROBLEMA

Na slici (1) prikazana je zatvorena kružna cilindrična ljuska konstantne debljine *h*, poluprečnika *a* i dužine *L*. Sa u, v i w označena su komponentalna pomeranja srednje površi ljuske.

2 FORMULATION OF THE PROBLEM

Figure (1) shows a closed circular cylindrical shell of constant thickness *h*, radius *a* and length *L*, where *u*, *v* and *w* are the displacements of the mid surface in *x*, φ and *z* directions, respectively.

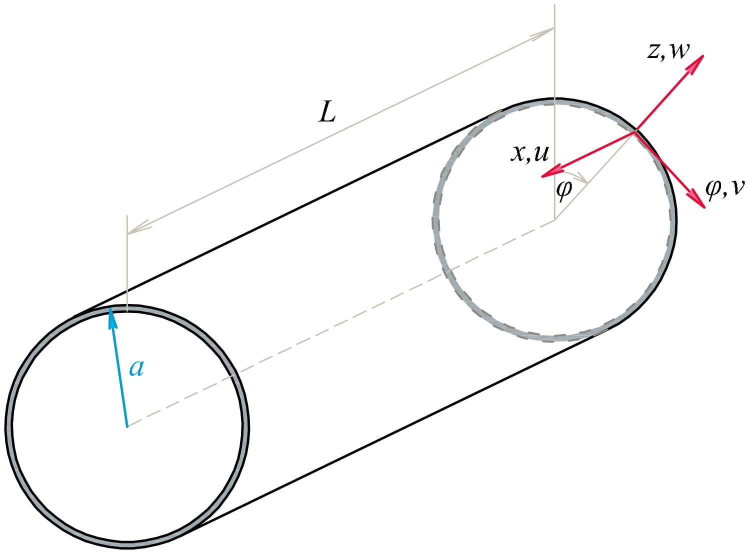

Slika 1. Geometrija i koordinatni sistem zatvorene kružne cilindrične ljuske
Fig. 1. Geometry and coordinate system for a closed circular cylindrical shell

2.1 Osnovne jednačine slobodnih vibracija kružne cilindrične ljuske prema Flügge-ovoj teoriji tankih ljuski

Problem slobodnih vibracija kružne cilindrične ljuske po Flügge-ovoj teoriji definisan je sledećim sistemom parcijalnih diferencijalnih jednačina [12]:

2.1 Governing differential equations for free vibration of a circular cylindrical shell according to the Flügge thin shell theory

The governing differential equations of the Flügge thin shell theory are [12]:

$$\begin{bmatrix} \partial_x^2 + a_1\partial_\varphi^2 + a_2\partial_t^2 & a_3\partial_x\partial_\varphi & a_4\partial_x + a_5\partial_x^3 + a_6\partial_x\partial_\varphi^2 \\ a_3\partial_x\partial_\varphi & a_7\partial_\varphi^2 + a_8\partial_x^2 + a_2\partial_t^2 & a_7\partial_\varphi + a_9\partial_x^2\partial_\varphi \\ a_4\partial_x + a_5\partial_x^3 + a_6\partial_x\partial_\varphi^2 & a_7\partial_\varphi + a_9\partial_x^2\partial_\varphi & \begin{matrix} k\left(\partial_x^4 + 2a_7\partial_x^2\partial_\varphi^2 + a_7{}^2\partial_\varphi^4\right) \\ +a_7 - a_2\partial_t^2 + 2a_{10}\partial_\varphi^2 + a_{10} \end{matrix} \end{bmatrix} \begin{bmatrix} u(x,\varphi,t) \\ v(x,\varphi,t) \\ w(x,\varphi,t) \end{bmatrix} = \begin{bmatrix} 0 \\ 0 \\ 0 \end{bmatrix} \quad (1)$$

gde su sa $u(x,\varphi,t)$, $v(x,\varphi,t)$ i $w(x,\varphi,t)$ označena pomeranja u aksijalnom, tangencijalnom i radijalnom pravcu, $\partial_x = d/dx$, $\partial_\varphi = d/d\varphi$, $\partial_t = d/dt$, $k = h^2/12$ i:

where $u(x,\varphi,t)$, $v(x,\varphi,t)$ and $w(x,\varphi,t)$ denote displacement components in the axial, tangential and radial direction, $\partial_x = d/dx$, $\partial_\varphi = d/d\varphi$, $\partial_t = d/dt$, $k = h^2/12$ and:

$$a_1 = \frac{1-\nu}{2a^2}\left(1+\frac{K}{Da^2}\right) \quad a_2 = -\frac{\rho h}{D} \quad a_3 = \frac{1+\nu}{2a} \quad a_4 = \frac{\nu}{a} \quad a_5 = -\frac{K}{Da}$$
$$a_6 = \frac{1-\nu}{2a^3}\frac{K}{D} \quad a_7 = \frac{1}{a^2} \quad a_8 = \frac{1-\nu}{2}\left(1+\frac{3K}{Da^2}\right) \quad a_9 = \frac{3-\nu}{2}\frac{K}{Da^2} \quad a_{10} = \frac{K}{Da^4} \quad (2)$$

U jednačinama (2) korišćene su sledeće oznake: ν je Poisson-ov koeficijent, $K = Eh^3/12(1-\nu^2)$ je krutost na savijanje ljuske, $D = Eh/(1-\nu^2)$ je krutost u „ravni" ljuske, ρ je gustina mase i E je Young-ov modul elastičnosti.

Izrazi za presečne sile, u funkciji komponentalnih pomeranja, jesu [12]:

In Eqs (2) ν is the Poisson's ratio, $K = Eh^3/12(1-\nu^2)$ is the flexural stiffness, $D = Eh/(1-\nu^2)$ is the stiffness in the mid surface of shell, ρ is the mass density and E is the Young's modulus of elasticity.

The expressions of forces and moments in terms of the displacements are [12]:

$$N_x = D\left[\frac{\partial u}{\partial x} + \frac{\nu}{a}\left(w + \frac{\partial v}{\partial\varphi}\right)\right] - \frac{K}{a}\frac{\partial^2 w}{\partial x^2} \qquad N_\varphi = D\left[\frac{1}{a}\left(w + \frac{\partial v}{\partial\varphi}\right) + \nu\frac{\partial u}{\partial x}\right] + \frac{K}{a^3}\left(\frac{\partial^2 w}{\partial\varphi^2} + w\right)$$
$$N_{x\varphi} = \frac{D(1-\nu)}{2}\left(\frac{1}{a}\frac{\partial u}{\partial\varphi} + \frac{\partial v}{\partial x}\right) + \frac{K(1-\nu)}{2a^2}\left(\frac{\partial v}{\partial x} - \frac{\partial^2 w}{\partial x\partial\varphi}\right)$$
$$N_{\varphi x} = \frac{D(1-\nu)}{2}\left(\frac{1}{a}\frac{\partial u}{\partial\varphi} + \frac{\partial v}{\partial x}\right) + \frac{K(1-\nu)}{2a^2}\left(\frac{1}{a}\frac{\partial u}{\partial\varphi} + \frac{\partial^2 w}{\partial x\partial\varphi}\right) \quad (3)$$
$$M_x = -K\left[\frac{\partial^2 w}{\partial x^2} + \frac{\nu}{a^2}\left(\frac{\partial^2 w}{\partial\varphi^2} - \frac{\partial v}{\partial\varphi}\right) - \frac{1}{a}\frac{\partial u}{\partial x}\right] \qquad M_\varphi = -K\left[\frac{1}{a^2}\left(\frac{\partial^2 w}{\partial\varphi^2} + w\right) + \nu\frac{\partial^2 w}{\partial x^2}\right]$$
$$M_{x\varphi} = -\frac{K(1-\nu)}{a}\left(\frac{\partial^2 w}{\partial x\partial\varphi} - \frac{\partial v}{\partial x}\right) \qquad M_{\varphi x} = -\frac{K(1-\nu)}{2a}\left(2\frac{\partial^2 w}{\partial x\partial\varphi} - \frac{\partial v}{\partial x} + \frac{1}{a}\frac{\partial u}{\partial\varphi}\right)$$

Transverzalne sile Q_x i Q_φ određene su iz uslova ravnoteže:

Shear forces Q_x and Q_φ are determined from the equilibrium conditions:

$$Q_x = \frac{\partial M_x}{\partial x} + \frac{1}{a}\frac{\partial M_{\varphi x}}{\partial\varphi} \qquad Q_\varphi = \frac{1}{a}\frac{\partial M_\varphi}{\partial\varphi} + \frac{\partial M_{x\varphi}}{\partial x} \quad (4)$$

Konvencija o pozitivnim presečnim silama data je na sledećoj slici:

The positive directions of the force and moment resultants are given in the next figure:

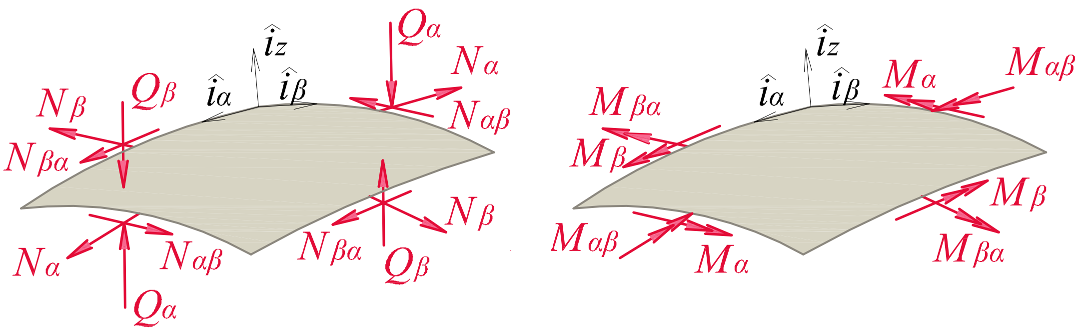

Slika 2. Konvencija o pozitivnim presečnim silama
Fig. 2. Positive directions of the force and moment resultants

2.2 Opšte rešenje problema slobodnih vibracija

Rešenje sistema jednačina (1) pretpostavljeno je u obliku proizvoda dve funkcije, pri čemu je jedna funkcija prostornih koordinata, a druga funkcija vremena:

2.2 General solution of the free vibration problem

By using the method of separation of variables, the general solution of the system of Eqs. (1) is sought in the following form:

$$u(x,\varphi,t)=\hat{u}(x,\varphi)e^{i\omega t} \qquad v(x,\varphi,t)=\hat{v}(x,\varphi)e^{i\omega t} \qquad w(x,\varphi,t)=\hat{w}(x,\varphi)e^{i\omega t} \tag{5}$$

U jednačini (5) ω predstavlja kružnu frekvenciju, dok su $\hat{u}$, $\hat{v}$ i $\hat{w}$ amplitude komponentalnih pomeranja u frekventnom domenu. Zamenom (5) u (1) dobija se:

In Eqs. (5) ω is the circular frequency, while $\hat{u}$, $\hat{v}$ and $\hat{w}$ are the amplitudes of componential displacements. Substituting Eqs. (5) into Eqs. (1) gives:

$$\begin{bmatrix} \partial_x^2+a_1\partial_\varphi^2-a_2\omega^2 & a_3\partial_x\partial_\varphi & a_4\partial_x+a_5\partial_x^3+a_6\partial_x\partial_\varphi^2 \\ a_3\partial_x\partial_\varphi & a_7\partial_\varphi^2+a_8\partial_x^2-a_2\omega^2 & a_7\partial_\varphi+a_9\partial_x^2\partial_\varphi \\ a_4\partial_x+a_5\partial_x^3+a_6\partial_x\partial_\varphi^2 & a_7\partial_\varphi+a_9\partial_x^2\partial_\varphi & \begin{matrix} k\left(\partial_x^4+2a_7\partial_x^2\partial_\varphi^2+a_7{}^2\partial_\varphi^4\right) \\ +a_7+a_2\omega^2+2a_{10}\partial_\varphi^2+a_{10} \end{matrix} \end{bmatrix} \begin{bmatrix} \hat{u}(x,\varphi) \\ \hat{v}(x,\varphi) \\ \hat{w}(x,\varphi) \end{bmatrix} = \begin{bmatrix} 0 \\ 0 \\ 0 \end{bmatrix} \tag{6}$$

Za zatvorenu kružnu cilindričnu ljusku $\hat{u}$, $\hat{v}$ i $\hat{w}$ moraju da zadovolje uslov periodičnosti u tangencijalnom pravcu, pa je rešenje sistema jednačina (6) usvojeno u obliku beskonačnog Fourier-ovog reda:

For a closed circular cylindrical shell, the displacement components $\hat{u}$, $\hat{v}$ and $\hat{w}$ should satisfy periodicity in the tangential direction; therefore the solution of the system of Eqs. (6) can be assumed in the form of infinite Fourier series:

1st part *2nd part*

$$\begin{aligned} \hat{u}(x,\varphi) &= \boxed{\sum_{m=0}^{\infty}U_m(x)\cos(m\varphi)} + \boxed{\sum_{m=1}^{\infty}U_m(x)\sin(m\varphi)} \\ \hat{v}(x,\varphi) &= \boxed{\sum_{m=1}^{\infty}V_m(x)\sin(m\varphi)} + \boxed{\sum_{m=0}^{\infty}V_m(x)\cos(m\varphi)} \\ \hat{w}(x,\varphi) &= \boxed{\sum_{m=0}^{\infty}W_m(x)\cos(m\varphi)} + \boxed{\sum_{m=1}^{\infty}W_m(x)\sin(m\varphi)} \end{aligned} \tag{7}$$

gde m predstavlja ceo broj. U slučaju da granični uslovi ne zavise od koordinate φ rešenja za pojedine harmonike su međusobno nezavisna, pa umesto rešenja u obliku sume, može da se posmatra rešenje samo za m-ti harmonik. U radu će biti prikazano rešenje za asimetrične vibracije ($m \geq 1$), dok rešenje za slučaj rotaciono-simetričnih vibracija ($m=0$) nije razmatrano. Takođe, biće prikazan postupak za rešenje problema

where m is an integer. If the boundary conditions do not depend on φ, the solutions for the different harmonics are uncoupled. Therefore, instead of the solution in the form of the sum, only the solution for the m^{th} harmonic can be considered. In this paper the solution for the asymmetric vibration ($m \geq 1$) will be presented, while the solution for the case of axisymmetric vibration ($m=0$) will not be discussed. Also, only the solution slobodnih vibracija za slučaj kada je usvojen 1. deo rešenja, jednačina (7), dok se rešenje za 2. deo određuje na isti način. Treba istaći da su sopstvene frekvencije koje se dobijaju za 1. i 2. deo rešenja iste, što znači da su kod zatvorene kružne cilindrične ljuske sve sopstvene frekvencije dvostruke.

Izbor trigonometrijskih funkcija u 1. delu rešenja, jednačina (7), omogućava transformaciju sistema jednačina (6) u sistem tri obične diferencijalne jednačine:

procedure for the 1st part of Eq. (7) will be presented, since the solution for the 2nd part can be obtained in the same way. It should be noted that the natural frequencies obtained for the 1st and 2nd part of Eq. (7) are the same, which means that for the closed circular cylindrical shell all the natural frequencies are double.

The choice of trigonometric functions in the 1st part of the solution, Eq. (7), allows transformation of the system of Eqs. (6) into the following system of three ordinary differential equations:

$$\begin{bmatrix} c_{1,m}\partial_x^2 + c_{2,m} & c_{3,m}\partial_x & c_{4,m}\partial_x^3 + c_{5,m}\partial_x \\ -c_{3,m}\partial_x & c_{6,m}\partial_x^2 + c_{7,m} & c_{8,m}\partial_x^2 + c_{9,m} \\ c_{4,m}\partial_x^3 + c_{5,m}\partial_x & -c_{8,m}\partial_x^2 - c_{9,m} & c_{10,m}\partial_x^4 + c_{11,m}\partial_x^2 + c_{12,m} \end{bmatrix} \begin{bmatrix} U_m(x) \\ V_m(x) \\ W_m(x) \end{bmatrix} = \begin{bmatrix} 0 \\ 0 \\ 0 \end{bmatrix} \tag{8}$$

gde su:

where are:

$$\begin{array}{llll} c_{1,m} = 1 & c_{2,m} = -m^2 a_1 - \omega^2 a_2 & c_{3,m} = -m a_3 & c_{4,m} = -a_5 \\ c_{5,m} = a_4 - m^2 a_6 & c_{6,m} = a_8 & c_{7,m} = -m^2 a_7 - \omega^2 a_2 & c_{8,m} = -m a_9 \\ c_{9,m} = -m a_7 & c_{10,m} = k & c_{11,m} = -2km^2 a_7 & c_{12,m} = +a_7 + \omega^2 a_2 + \\ & & & k\left(m^4 a_7{}^2 - 2m^2 a_7 + a_7{}^4\right) \end{array} \tag{9}$$

Razvojem determinante, sistem jednačina (8) svodi se na jednu jednačinu osmog reda, koja važi za sve tri funkcije:

By expanding the determinant of the system (8), the following eighth order differential equation, valid for all three functions, is obtained:

$$\left(\partial_x^8 + a_{1,m}\partial_x^6 + a_{2,m}\partial_x^4 + a_{3,m}\partial_x^2 + a_{4,m}\right)\Psi = 0 \tag{10}$$

gde je $\Psi = U_m(x)$ ili $V_m(x)$ ili $W_m(x)$, a:

where $\Psi = U_m(x)$ or $V_m(x)$ or $W_m(x)$ and:

$$\begin{aligned} a_{1,m} &= \frac{c_{10,m}\left(c_{3,m}^2 + c_{2,m}c_{6,m} + c_{1,m}c_{7,m}\right) + c_{1,m}\left(c_{11,m}c_{6,m} + c_{8,m}^2\right) + 2c_{4,m}\left(c_{3,m}c_{8,m} - c_{5,m}c_{6,m}\right) - c_{4,m}^2 c_{7,m}}{c_{6,m}\left(c_{1,m}c_{10,m} - c_{4,m}^2\right)} \\ a_{2,m} &= \frac{c_{10,m}\left(c_{1,m}c_{5,m} + c_{2,m}c_{7,m}\right) + c_{11,m}\left(c_{3,m}^2 + c_{2,m}c_{6,m} + c_{1,m}c_{7,m}\right) + c_{2,m}c_{8,m}^2 - c_{5,m}^2 c_{6,m}}{c_{6,m}\left(c_{1,m}c_{10,m} - c_{4,m}^2\right)} \\ &+ 2\frac{c_{3,m}\left(c_{5,m}c_{8,m} + c_{4,m}c_{9,m}\right) + c_{1,m}c_{8,m}c_{9,m} - c_{4,m}c_{5,m}c_{7,m}}{c_{6,m}\left(c_{1,m}c_{10,m} - c_{4,m}^2\right)} \\ a_{3,m} &= \frac{c_{7,m}\left(c_{2,m}c_{11,m} - c_{5,m}^2\right) + c_{12,m}\left(c_{3,m}^2 + c_{2,m}c_{6,m} + c_{1,m}c_{7,m}\right) + c_{1,m}c_{9,m}^2 + 2c_{9,m}\left(c_{2,m}c_{8,m} + c_{3,m}c_{5,m}\right)}{c_{6,m}\left(c_{1,m}c_{10,m} - c_{4,m}^2\right)} \\ a_{4,m} &= \frac{c_{2,m}\left(c_{12,m}c_{7,m} + c_{9,m}^2\right)}{c_{6,m}\left(c_{1,m}c_{10,m} - c_{4,m}^2\right)} \end{aligned} \tag{11}$$

Rešenje jednačine (10) usvaja se u obliku $\Psi = e^{rx}$ i dobija se karakteristična jednačina:

The solution of the equation (10) is sought in the form $\Psi = e^{rx}$ and the corresponding characteristic equation is obtained:

$$r^8 + a_{1,m}r^6 + a_{2,m}r^4 + a_{3,m}r^2 + a_{4,m} = 0 \tag{12}$$

Pomoću smene $\mu = r^2$ jednačina (12) redukuje se na sledeću jednačinu četvrtog stepena:

The eight order Eq. (12) can be reduced to the fourth order polynomial by substituting $\mu = r^2$:

$$\mu^4 + a_{1,m}\mu^3 + a_{2,m}\mu^2 + a_{3,m}\mu + a_{4,m} = 0 \tag{13}$$

čiji su koreni označeni sa $\mu_{i,m}$, $i = 1, 2, 3, 4$. Koreni jednačine (12) su:

whose roots are: $\mu_{1,m}$, $\mu_{2,m}$, $\mu_{3,m}$ and $\mu_{4,m}$. The roots of Eq. (12) are defined as:

$r_{1,m}=\sqrt{\mu_{1,m}}$, $r_{2,m}=-\sqrt{\mu_{1,m}}$, $r_{3,m}=\sqrt{\mu_{2,m}}$, $r_{4,m}=-\sqrt{\mu_{2,m}}$, $r_{5,m}=\sqrt{\mu_{3,m}}$, $r_{6,m}=-\sqrt{\mu_{3,m}}$, $r_{7,m}=\sqrt{\mu_{4,m}}$ i $r_{8,m}=-\sqrt{\mu_{4,m}}$.

Rešenja za nepoznate funkcije pomeranja su:

$r_{1,m}=\sqrt{\mu_{1,m}}$, $r_{2,m}=-\sqrt{\mu_{1,m}}$, $r_{3,m}=\sqrt{\mu_{2,m}}$, $r_{4,m}=-\sqrt{\mu_{2,m}}$, $r_{5,m}=\sqrt{\mu_{3,m}}$, $r_{6,m}=-\sqrt{\mu_{3,m}}$, $r_{7,m}=\sqrt{\mu_{4,m}}$ and $r_{8,m}=-\sqrt{\mu_{4,m}}$.

The solutions for unknown functions can be written in the following form:

$$U_m(x)=\sum_{i=1}^{8}A_{i,m}e^{r_{i,m}x}\qquad V_m(x)=\sum_{i=1}^{8}B_{i,m}e^{r_{i,m}x}\qquad W_m(x)=\sum_{i=1}^{8}C_{i,m}e^{r_{i,m}x}\tag{14}$$

pri čemu je samo osam integracionih konstanti, od ukupno 24 ($A_{i,m}, B_{i,m}, C_{i,m}$), međusobno nezavisno.

Ako se integracione konstante $A_{i,m}$ i $B_{i,m}$ izraze u funkciji $C_{i,m}$:

where only eight integration constants, of total 24 ($A_{i,m}, B_{i,m}, C_{i,m}$), are independent. If the integration constants $A_{i,m}$ and $B_{i,m}$ are expressed in terms of $C_{i,m}$:

$$A_{i,m}=\delta_{i,m}C_{i,m}\qquad B_{i,m}=\gamma_{i,m}C_{i,m}\tag{15}$$

gde su $\delta_{i,m}$ i $\gamma_{i,m}$ koeficijenti koji predstavljaju odnos amplituda aksijalnog i radijalnog, odnosno tangencijalnog i radijalnog pomeranja:

where $\delta_{i,m}$ and $\gamma_{i,m}$ are coefficients that represent the ratio of amplitudes of axial-radial and tangential-radial displacements respectively:

$$\begin{aligned}\delta_{i,m}&=\frac{\left(c_{9,m}+c_{8,m}\left(r_{i,m}\right)^2\right)^2+\left(c_{7,m}+c_{6,m}\left(r_{i,m}\right)^2\right)\left(c_{12,m}+c_{11,m}\left(r_{i,m}\right)^2+c_{10,m}\left(r_{i,m}\right)^4\right)}{r_{i,m}\left(c_{5,m}+c_{4,m}\left(r_{i,m}\right)^2\right)\left(c_{7,m}+c_{6,m}\left(r_{i,m}\right)^2\right)-c_{3,m}r_{i,m}\left(c_{9,m}+c_{8,m}\left(r_{i,m}\right)^2\right)}\\ \gamma_{i,m}&=\frac{c_{12,m}c_{3,m}+c_{5,m}c_{9,m}+\left(c_{11,m}c_{3,m}+c_{5,m}c_{8,m}+c_{4,m}c_{9,m}\right)\left(r_{i,m}\right)^2+\left(c_{10,m}c_{3,m}+c_{4,m}c_{8,m}\right)\left(r_{i,m}\right)^4}{c_{5,m}c_{7,m}-c_{3,m}c_{9,m}+\left(c_{5,m}c_{6,m}+c_{4,m}c_{7,m}-c_{3,m}c_{8,m}\right)\left(r_{i,m}\right)^2+c_{4,m}c_{6,m}\left(r_{i,m}\right)^4}\end{aligned}\tag{16}$$

dobijaju se analitički izrazi za komponentalna pomeranja kružne cilindrične ljuske u obliku:

the analytical expressions for displacement components are obtained in the following form:

$$\begin{aligned}\hat{u}(x,\varphi)&=\sum_{m=1}^{M}\left(\sum_{i=1}^{8}\delta_{i,m}C_{i,m}e^{r_{i,m}x}\right)\cos(m\varphi)\\ \hat{v}(x,\varphi)&=\sum_{m=1}^{M}\left(\sum_{i=1}^{8}\gamma_{i,m}C_{i,m}e^{r_{i,m}x}\right)\sin(m\varphi)\\ \hat{w}(x,\varphi)&=\sum_{m=1}^{M}\left(\sum_{i=1}^{8}C_{i,m}e^{r_{i,m}x}\right)\cos(m\varphi)\end{aligned}\tag{17}$$

Zamenom izraza (17) u jednačine (3) i (4) dobijaju se izrazi za presečne sile.

By substituting Eq. (17) into Eqs. (3) and (4), the expressions for forces and moments can be obtained, as well.

3 DINAMIČKA MATRICA KRUTOSTI $\mathbf{K}_{Dm}$

Vektor pomeranja $\hat{\mathbf{q}}$ i vektor sila $\hat{\mathbf{Q}}$ sadrže pomeranja i rotacije, odnosno sile i momente, na konturama ljuske $x=0$ i $x=L$:

3 DYNAMIC STIFFNESS MATRIX $\mathbf{K}_{Dm}$

The displacement vector $\hat{\mathbf{q}}$ and the force vector $\hat{\mathbf{Q}}$, contain the displacements and rotations, i.e. the forces and moments at the boundaries $x=0$ and $x=L$, respectively:

$$\begin{aligned}\hat{\mathbf{q}}^T&=\left[\hat{u}(0,\varphi)\ \hat{v}(0,\varphi)\ \hat{w}(0,\varphi)\ \hat{\psi}_\varphi(0,\varphi)\ \hat{u}(L,\varphi)\ \hat{v}(L,\varphi)\ \hat{w}(L,\varphi)\ \hat{\psi}_\varphi(L,\varphi)\right]\\ \hat{\mathbf{Q}}^T&=\left[-\hat{N}_x(0,\varphi)\ -\hat{\hat{N}}_{x\varphi}(0,\varphi)\ -\hat{\hat{Q}}_x(0,\varphi)\ -\hat{M}_x(0,\varphi)\ \hat{N}_x(L,\varphi)\ \hat{\hat{N}}_{x\varphi}(L,\varphi)\ \hat{\hat{Q}}_x(L,\varphi)\ \hat{M}_x(L,\varphi)\right]\end{aligned}\tag{18}$$

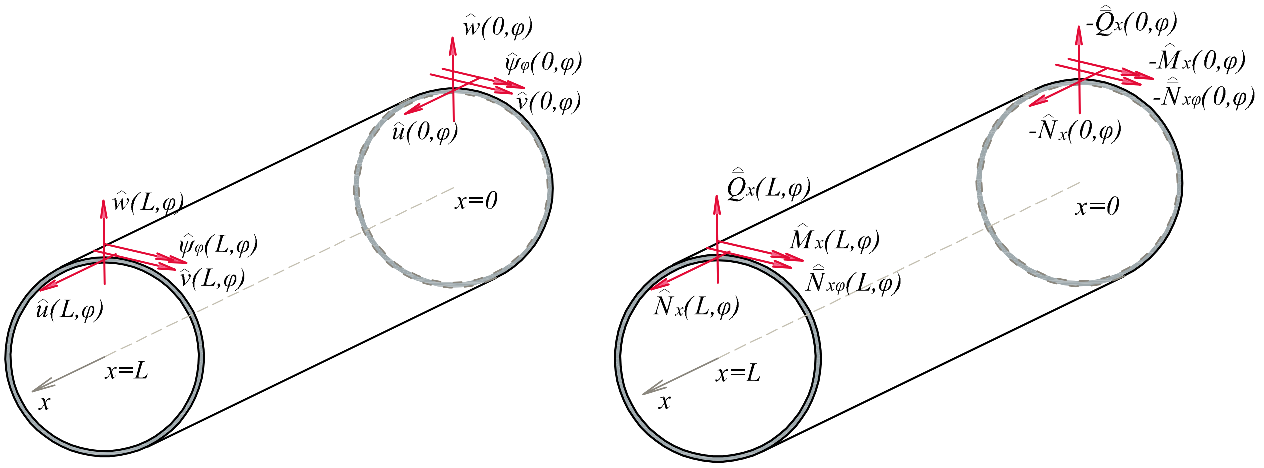

Slika 3. Komponente vektora pomeranja $\hat{\mathbf{q}}$ i vektora sila $\hat{\mathbf{Q}}$

Fig. 3. Components of the displacement and force vectors

Komponente vektora pomeranja $\hat{\mathbf{q}}$ i sila $\hat{\mathbf{Q}}$ prikazane su na slici (3) i definisane su sledećim izrazima:

The components of the vectors $\hat{\mathbf{q}}$ and $\hat{\mathbf{Q}}$, shown in Fig. (3) are defined by the following expressions:

$$\begin{aligned}
&\hat{u}(0,\varphi)=U_m(0)\cos(m\varphi) && \hat{u}(L,\varphi)=U_m(L)\cos(m\varphi)\\
&\hat{v}(0,\varphi)=V_m(0)\sin(m\varphi) && \hat{v}(L,\varphi)=V_m(L)\sin(m\varphi)\\
&\hat{w}(0,\varphi)=W_m(0)\cos(m\varphi) && \hat{w}(L,\varphi)=W_m(L)\cos(m\varphi)\\
&\hat{\psi}_\varphi(0,\varphi)=\Psi_{\varphi m}(0)\cos(m\varphi) && \hat{\psi}_\varphi(L,\varphi)=\Psi_{\varphi m}(L)\cos(m\varphi)\\
&\hat{\psi}_\varphi(x,\varphi)=\frac{\partial\hat{w}(x,\varphi)}{\partial x}
\end{aligned} \tag{19}$$

$$\begin{aligned}
&\hat{N}_x(x,\varphi)=\hat{N}_{xm}(x)\cos(m\varphi)=\left(\sum_{i=1}^{8}C_{i,m}N_{xi,m}e^{r_{im}x}\right)\cos(m\varphi)\\
&N_{xi,m}=\frac{D\nu\left(1+m\gamma_{i,m}\right)+aDr_{i,m}\delta_{i,m}-Kr_{i,m}^2}{a}\\
&\hat{\hat{N}}_{x\varphi}(x,\varphi)=\hat{N}_{x\varphi}+\frac{\hat{M}_{x\varphi}}{a}=\hat{\hat{N}}_{x\varphi m}(x)\sin(m\varphi)=\left(\sum_{i=1}^{8}C_{im}\bar{N}_{x\varphi i,m}e^{r_{im}x}\right)\sin(m\varphi)\\
&\bar{N}_{x\varphi i,m}=\frac{(1-\nu)\left[-aD\delta_{i,m}m+a^2D\gamma_{i,m}r_{i,m}+3Kr_{i,m}\left(\gamma_{i,m}+m\right)\right]}{2a^2}\\
&\hat{\hat{Q}}_x(x,\varphi)=\hat{Q}_x+\frac{1}{a}\frac{\partial\hat{M}_{x\varphi}}{\partial\varphi}=\hat{\hat{Q}}_{xm}(x)\cos(m\varphi)=\left(\sum_{i=1}^{8}C_{i,m}\bar{Q}_{xi,m}e^{r_{im}x}\right)\cos(m\varphi)\\
&\bar{Q}_{xi,m}=\frac{K\left[(1-\nu)\delta_{i,m}m^2+2a^2r_{i,m}^2\left(\delta_{i,m}-ar_{i,m}\right)\right]}{2a^3}+\frac{Kmr_{i,m}\left[(3-\nu)\gamma_{i,m}+2m(2-\nu)\right]}{2a^2}\\
&\hat{M}_x(x,\varphi)=\hat{M}_{xm}(x)\cos(m\varphi)=\left(\sum_{i=1}^{8}C_{i,m}M_{xi,m}e^{r_{im}x}\right)\cos(m\varphi)\\
&M_{xi,m}=\frac{K\left[m\nu\left(\gamma_{i,m}+m\right)+ar_{i,m}\delta_{i,m}-a^2r_{i,m}^2\right]}{a^2}
\end{aligned} \tag{20}$$

Vektori pomeranja $\hat{\mathbf{q}}_m$ i sila $\hat{\mathbf{Q}}_m$ koji sadrže amplitude pomeranja i rotacija, odnosno presečnih sila za $x=0$ i $x=L$ za *m*-ti harmonik su:

The new displacement and force vector, namely $\hat{\mathbf{q}}_m$ and $\hat{\mathbf{Q}}_m$, that contain the amplitudes of displacements and rotations, i.e. forces, on the boundaries $x=0$ and $x=L$ for m[th] harmonic are:

$$\left(\hat{\mathbf{q}}_m\right)^T = \left[U_m(0)\;\; V_m(0)\;\; W_m(0)\;\; \Psi_{\varphi m}(0)\;\; U_m(L)\;\; V_m(L)\;\; W_m(L)\;\; \Psi_{\varphi m}(L)\right]_{8x1}$$
$$\left(\hat{\mathbf{Q}}_m\right)^T = \left[-\hat{N}_{xm}(0)\;\; -\hat{\bar{N}}_{x\varphi m}(0)\;\; -\hat{\bar{Q}}_{xm}(0)\;\; -\hat{M}_{xm}(0)\;\; \hat{N}_{xm}(L)\;\; \hat{\bar{N}}_{x\varphi m}(L)\;\; \hat{\bar{Q}}_{xm}(L)\;\; \hat{M}_{xm}(L)\right]_{8x1} \quad (21)$$

Veza između vektora $\hat{\mathbf{q}}_m$ i vektora integracionih konstanti $\mathbf{C}_m$ uspostavlja se preko matrice $\mathbf{D}_m$, odnosno veza između vektora $\hat{\mathbf{Q}}_m$ i vektora integracionih konstanti se uspostavlja preko matrice $\mathbf{F}_m$, na sledeći način:

The vector $\hat{\mathbf{q}}_m$ is related to the vector of integration constants $\mathbf{C}_m$ by the matrix $\mathbf{D}_m$, while the vectors $\hat{\mathbf{Q}}_m$ and $\mathbf{C}_m$ are related through the matrix $\mathbf{F}_m$, as follows:

$$\hat{\mathbf{q}}_m = \mathbf{D}_m \mathbf{C}_m \quad (22)$$

$$\hat{\mathbf{Q}}_m = \mathbf{F}_m \mathbf{C}_m \quad (23)$$

gde su vektori integracionih konstanti $\mathbf{C}_m$ i matrice $\mathbf{D}_m$ i $\mathbf{F}_m$ jednake:

where the vector of integration constants $\mathbf{C}_m$ and matrices $\mathbf{D}_m$ and $\mathbf{F}_m$ are:

$$\mathbf{C}_m = \begin{bmatrix} C_{1,m} \\ C_{2,m} \\ C_{3,m} \\ C_{4,m} \\ C_{5,m} \\ C_{6,m} \\ C_{7,m} \\ C_{8,m} \end{bmatrix} \quad \mathbf{D}_m = \begin{bmatrix} \delta_{1,m} & \dots & \delta_{8,m} \\ \gamma_{1,m} & \dots & \gamma_{8,m} \\ 1 & \dots & 1 \\ -r_{1,m} & \dots & -r_{8,m} \\ \delta_{1,m}\cdot e^{r_{1,m}L} & \dots & \delta_{8,m}\cdot e^{r_{8,m}L} \\ \gamma_{1,m}\cdot e^{r_{1,m}L} & \dots & \gamma_{8,m}\cdot e^{r_{8,m}L} \\ e^{r_{1,m}L} & \dots & e^{r_{8,m}L} \\ -r_{1,m}\cdot e^{r_{1,m}L} & \dots & -r_{8,m}\cdot e^{r_{8,m}L} \end{bmatrix}_{8x8} \quad \mathbf{F}_m = \begin{bmatrix} -N_{x1,m} & \dots & -N_{x8,m} \\ -\bar{N}_{x\varphi 1,m} & \dots & -\bar{N}_{x\varphi 8,m} \\ -\bar{Q}_{x1,m} & \dots & -\bar{Q}_{x8,m} \\ -M_{x1,m} & \dots & -M_{x8,m} \\ N_{x1,m}\cdot e^{r_{1,m}L} & \dots & N_{x8,m}\cdot e^{r_{8,m}L} \\ \bar{N}_{x\varphi 1,m}\cdot e^{r_{1,m}L} & \dots & \bar{N}_{x\varphi 8,m}\cdot e^{r_{8,m}L} \\ \bar{Q}_{x1,m}\cdot e^{r_{1,m}L} & \dots & \bar{Q}_{x8,m}\cdot e^{r_{8,m}L} \\ M_{x1,m}\cdot e^{r_{1,m}L} & \dots & M_{x8,m}\cdot e^{r_{8,m}L} \end{bmatrix}_{8x8} \quad (24)$$

Ako se iz jednačine (32) izrazi $\mathbf{C}_m$ u funkciji od $\hat{\mathbf{q}}_m$ i zameni u jednačinu (33) dobija se veza između vektora $\hat{\mathbf{Q}}_m$ i $\hat{\mathbf{q}}_m$:

If vector $\mathbf{C}_m$ is expressed from the Eqs. (32) as a function of $\hat{\mathbf{q}}_m$ and replaced in the Eq. (33), the relation between vectors $\hat{\mathbf{Q}}_m$ and $\hat{\mathbf{q}}_m$ is obtained in the following form:

$$\hat{\mathbf{Q}}_m = \mathbf{K}_{Dm} \hat{\mathbf{q}}_m \quad (25)$$

gde je $\mathbf{K}_{Dm} = \mathbf{F}_m \left(\mathbf{D}_m\right)^{-1}$ dinamička matrica krutosti kružne cilindrične ljuske za *m*-ti harmonik. Red matrice $\mathbf{K}_{Dm}$ je 8.

where $\mathbf{K}_{Dm} = \mathbf{F}_m \left(\mathbf{D}_m\right)^{-1}$ is the dynamic stiffness matrix of the circular cylindrical shells element for the m^{th} harmonic. The size of the matrix $\mathbf{K}_{Dm}$ is 8.

4 GRANIČNI USLOVI, SOPSTVENE FREKVENCIJE I OBLICI OSCILOVANJA

Kada je određena dinamička matrica krutosti kontinualnog elementa kružne cilindrične ljuske, globalna dinamička matrica krutosti sistema formira se na sličan način kao u MKE, samo što se elementi međusobno spajaju duž kontura, a ne u čvorovima. Na slici (4) prikazano je formiranje globalne matrice krutosti koja se sastoji od dva kontinualna elementa.

4 BOUNDARY CONDITIONS, NATURAL FREQUENCIES AND MODE SHAPES

When the dynamic stiffness matrix is determined, a global DS matrix of the structure can be obtained. The procedure is similar to that of FEM, except that continuous elements are connected at the boundaries, instead at nodes. Fig. (4) shows schematically the assembly procedure of two-element structure.

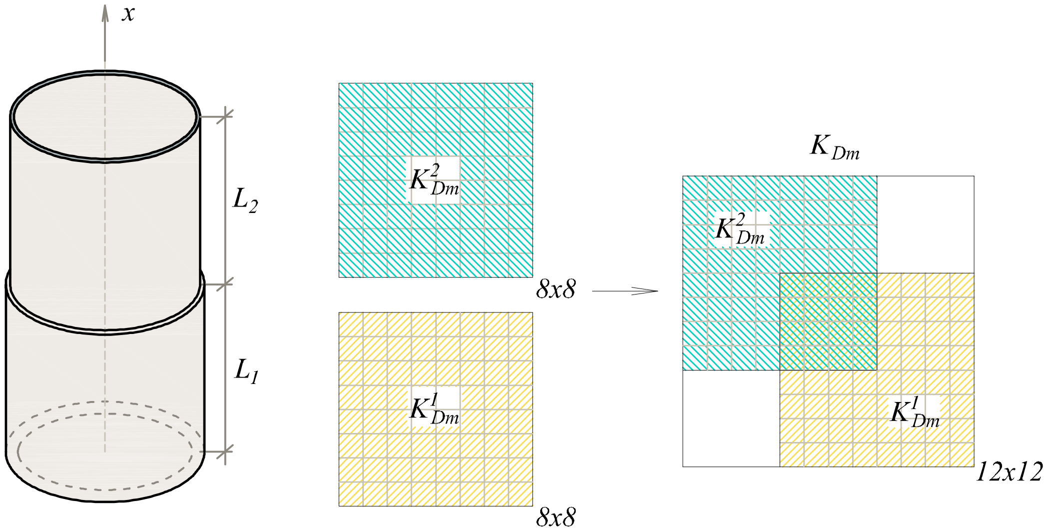

Slika 4. Formiranje globalne dinamičke matrice krutosti $\mathbf{K}_{Dm}$

Fig. 4. Assembly procedure of two-element structure

Kada je određena dinamička matrica krutosti sistema, granični uslovi se apliciraju brisanjem vrsta i kolona koje odgovaraju sprečenim pomeranjima. U numeričkim primerima biće prikazana rešenja samo za najčešće korišćene granične uslove:

- *slobodna kontura F*: sva tri komponentalna pomeranja i rotacija $\hat{\psi}_{\varphi}$ su različiti od nule,
- *shear diaphragm SD*: $v = w = 0$,
- *uklještena kontura C*: $u = v = w = \psi_{\varphi} = 0$.

Za slučaj kružno cilindrične ljuske uklještene na oba kraja (*C-C* granični uslovi) došlo bi do brisanja svih vrsta i kolona u matrici krutosti, pa za ovu kombinaciju graničnih uslova treba da se koriste najmanje dva kontinualna elementa.

Na slici (5) šematski je prikazano apliciranje izabranih graničnih uslova.

When the global dynamic stiffness matrix is determined, the boundary conditions are applied by removing the rows and columns that correspond to the constrained displacements and rotations. In the numerical examples only the results for the most commonly used boundary conditions will be presented:

- *free F*: componential displacements and rotation $\hat{\psi}_{\varphi}$ are different from zero,
- *shear diaphragm SD*: $v = w = 0$,
- *clamped C*: $u = v = w = \psi_{\varphi} = 0$.

If a circular cylindrical shell with *C-C* boundary conditions is modelled with one continuous element, all rows and columns have to be deleted. Thus, for this combination of boundary conditions minimum two continuous elements have to be used.

The application of defined boundary conditions is shown in Fig. 5.

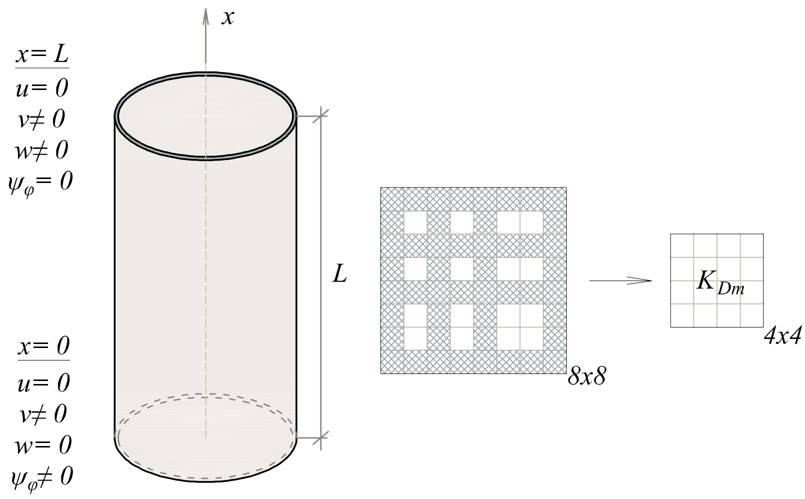

Slika 5. Apliciranje prikazanih graničnih uslova

Fig. 5. Application of the presented boundary conditions

Sopstvene frekvencije dobijaju se iz uslova da je $\det(\mathbf{K}_{Dm})=0$. Dinamička matrica krutosti je transcendentna, tako da se frekvencije za koje je $\det(\mathbf{K}_{Dm})=0$ dobijaju tehnikama pretraživanja. Za određivanje svojstvenih frekvencija, u radu su umesto nula determinante $\mathbf{K}_{Dm}$ traženi pikovi (peak) izraza $1/\log\det(\mathbf{K}_{Dm})$[15]. Za tu svrhu je napisan kôd u programu *Matlab*.

Kada su određene sopstvene frekvencije, oblici oscilovanja dobijaju se na poznat način. Oblici oscilovanja ljuski nemaju prave čvorne linije, tj. linije na površi duž kojih su sva tri komponentalna pomeranja jednaka nuli. Umesto njih će se javiti čvorne linije duž kojih su dva pomeranja jednaka nuli, a treće pomeranje ima maksimalnu vrednost. U slučaju rotaciono-simetričnih vibracija (*m*=0) aksijalna, torziona i radijalna komponenta pomeranja potpuno su razdvojene, tako da se za svaku od njih dobijaju nezavisne čvorne linije.

5 NUMERIČKI PRIMERI

Verifikacija izvedenih tačnih dinamičkih matrica krutosti po Flügge-ovoj teoriji izvršena je upoređivanjem sopstvenih frekvencija dobijenih primenom Matlab programa s rešenjima dostupnim u literaturi, kao i s rezultatima programa Abaqus, na četiri primera. U svim primerima usvojena vrednost Poisson-ovog koeficijenta je ν = 0.3.

Primer 5.1

U ovom primeru je određeno prvih devet sopstvenih frekvencija u (*Hz*) za ljusku sa *C-C* graničnim uslovima i karakteristikama: $E=210\ GPa$, $\rho=78000\ kg/m^3$, $L=20\ m$, $a=1\ m$ i $h=0.01\ m$. U Tabeli 1 data su rešenja dobijena primenom MDK po Flügge-ovoj teoriji, rezultati Zhang-a [16], kao i rezultati dobijeni pomoću programa Abaqus. Zhang je koristio Love–Timoshenko teoriju tankih ljuski, [17], i metod prostiranja talasa (*wave propagation approach*). Talasni broj u pravcu x-ose odredio je aproksimativno, kao talasni broj odgovarajuće grede sa sličnim graničnim uslovima. Za proračun u programu Abaqus korišćena su dva različita tipa konačnog elementa: *STRI3* (ravan konačni element sa šest čvorova) i *S4R* (konačni element ljuske sa četiri čvora koji uzima u obzir deformaciju smicanja). Znak “-“ u tabeli znači da je Zhang preskočio petu sopstvenu frekvenciju. Primenom samo jednog kontinualnog elementa dobijeno je slaganje s rezultatima MKE analize, gde je primenjeno 50526 *S4R*, odnosno 101052 *STRI3* konačnih elemenata.

The natural frequencies are obtained from the condition that $\det(\mathbf{K}_{Dm})=0$. Since the dynamic stiffness matrix is transcendent matrix, the natural frequencies are obtained using searching techniques. In this paper instead of finding zeros of the determinant $\mathbf{K}_{Dm}$, the peaks of the expression $1/\log\det(\mathbf{K}_{Dm})$ [15] are sought. Therefore, a computer program written in Matlab has been used.

When the exact natural frequencies are determined, the corresponding mode shapes are computed routinely. The mode shapes do not have true nodal lines, i.e. lines on the surface of a shell for which all displacement components are zero, but have lines along which two of displacement components are zero and the third has maximum values. In the case of axisymmetric vibration, the axial, circumferential and radial displacements are uncoupled, giving distinct nodal lines.

5 NUMERICAL RESULTS

The dynamic stiffness matrix based on the Flügge thin shell theory, formulated above, is verified through four numerical examples. The exact natural frequencies computed by the DSM are compared with the available analytical solution in the literature, as well as with the results from *Abaqus*. The adopted value of Poisson ratio ν is 0.3 in all examples.

Example 5.1

In this example, the first nine natural frequencies (*Hz*) of a circular cylindrical shell with *C-C* boundary conditions and the following properties: $E=210\ GPa$, $\rho=78000\ kg/m^3$, $L=20\ m$, $a=1\ m$ and $h=0.01\ m$, are determined. Table 1 shows the results obtained by the *DSM* according to the Flügge thin shell theory, the results of Zhang [16], as well as the results obtained by Abaqus. Zhang used the Love-Timoshenko thin shell theory [17] and the *wave propagation* approach. The axial wave number is determined approximately as the wave number of an equivalent beam with similar boundary conditions. For the Abaqus models, two different finite elements are used: *STRI3* (flat element with six nodes) and *S4R* (4-node, quadrilateral shell element with reduced integration and a large-strain formulation). The sign "-" in the table means that Zhang missed the fifth natural frequency. By applying a single continuous element, total agreement with the results of FEM analysis has been obtained. The total number of elements in the FE model was 50526 for S4R elements, i.e. 101052 for STRI3 elements.

*Tabela 1. Prvih devet sopstvenih frekvencija u (*Hz*) za kružnu cilindričnu ljusku sa* C-C *graničnim uslovima:*
$E = 210\ GPa\ \ \rho = 78000\ \ kg/m^3$, $L = 20\ m$, $a = 1\ m$, $h = 0.01\ m$, $\nu = 0.3$

Table 1. First nine natural frequencies (Hz) for a circular cylindrical shell with C-C boundary conditions:
$E = 210\ GPa\ \ \rho = 78000\ \ kg/m^3$, $L = 20\ m$, $a = 1\ m$, $h = 0.01\ m$, $\nu = 0.3$

ton mode	[16]	*DSM*	*Abaqus*	
			S4R	*STRI3*
1	12.17	12.00	12.00	12.01
2	19.61	19.56	19.60	19.57
3	23.28	23.1	23.13	23.12
4	28.06	27.16	27.16	27.19
5	-	28.30	28.30	28.30
6	31.98	31.47	31.50	31.52
7	36.47	36.42	36.59	36.43
8	37.37	37.28	37.43	37.27
9	39.78	39.59	39.74	39.62

Primer 5.2

U Tabeli 2 prikazane su najniže bezdimenzionalne sopstvene frekvencije $\bar{\omega} = \omega a^2 \sqrt{\rho\left(1-\nu^2\right)/E}$ za kružnu cilindričnu ljusku sa *F-F* graničnim uslovima ($L/a = 20$, $h/a = 0.05$) za usvojeno *m*= 1, 2, 3, 4, 5, 6. Rezultati dobijeni primenom MDK po Flügge-ovoj teoriji, upoređeni su s rezultatima Zxang-a [18], kao i s rešenjima dobijenim pomoću programa Abaqus. Xiang je u svom radu za rešenje problema slobodnih vibracija koristio Goldenveizer–Novozhilov teoriju tankih ljuski ([19], [20]) i *state-space* metod za dobijanje homogenih diferencijalnih jednačina. U Abaqus-u je kružna cilindrična ljuska (*a = 1 m*) modelirana sa 101052 *STRI3* konačnih elemenata. Iz Tabele 2 vidi se dobro slaganje rezultata Xiang-a i MDK sa rezultatima dobijenim pomoću Abaqus-a. Relativna razlika u procentima između prikazanih rešenja govori da su razlike zanemarljive. Na slici (6) prikazani su oblici oscilovanja dobijeni primenom MDK i programa u Matlab-u, koji odgovaraju sopstvenim frekvencijama određenim u Tabeli 2.

Example 5.2

Table 2 shows the first dimensionless natural frequencies $\bar{\omega} = \omega a^2 \sqrt{\rho\left(1-\nu^2\right)/E}$ for a circular cylindrical shell ($L/a = 20$, $h/a = 0.05$) with *F-F* boundary conditions and given *m*= 1,2,3,4,5,6. The results obtained by the DSM based on the Flügge thin shell theory are compared with the exact results of Zhang [18], as well as those obtained by Abaqus. Xhang used the Goldenveizer-Novozhilov thin shell theory ([19], [20]) and the state-space method to obtain the homogenous differential equations. In Abaqus, the circular cylindrical shell of radius *a = 1 m* has been modelled with 101052 STRI3 finite elements. Table 2 shows close agreement between the results obtained by Xhang, DSM and Abaqus. The relative differences between these results are negligible. In Fig. 6. the corresponding mode shapes obtained by the program written in the Matlab are presented.

Tabela 2. Najniža bezdimenzionalna sopstvena frekvencija $\bar{\omega} = \omega a^2 \sqrt{\rho\left(1-\nu^2\right)/E}$ *za usvojeno m kružne cilindrične ljuske sa FF graničnim uslovima:* $L/a = 20$, $h/a = 0.05$, $\nu = 0.3$

Table 2. Fundamental dimensionless natural frequency $\bar{\omega} = \omega a^2 \sqrt{\rho\left(1-\nu^2\right)/E}$ *of a circular cylindrical shell with F-F boundary conditions for a given m:* $L/a = 20$, $h/a = 0.05$, $\nu = 0.3$

m	[18]	Δ% [18] and *Abaqus*	*DSM*	Δ% *DSM* and *Abaqus*	*Abaqus* (*STRI3*)
1	0.035424	0.25	0.0355221	-0.03	0.03551
2	0.038683	0.03	0.0386885	0.01	0.03869
3	0.109366	-0.02	0.1093867	-0.04	0.10934
4	0.209644	-0.09	0.2096895	-0.12	0.20945
5	0.340330	-0.60	0.3390779	-0.23	0.33832
6	0.498824	-0.64	0.4973616	-0.35	0.49563

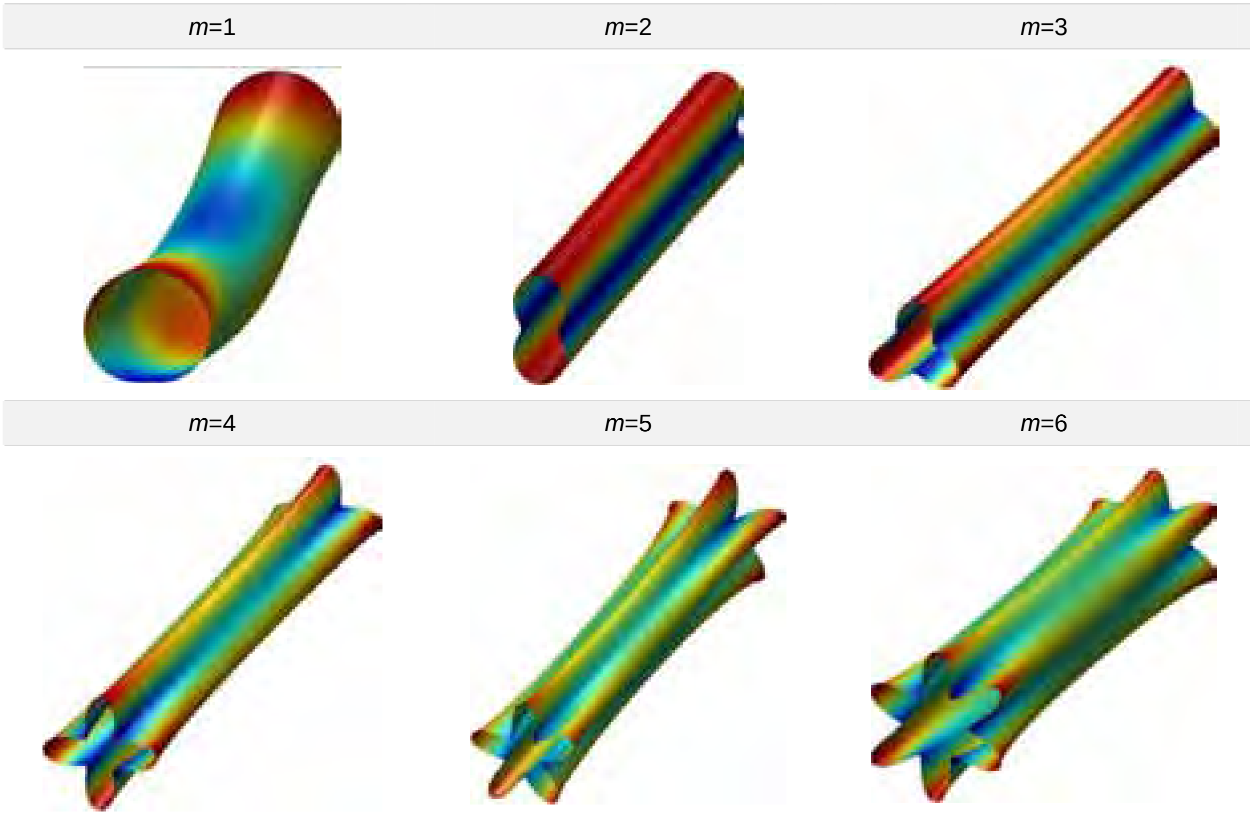

Slika 6. Oblici oscilovanja F-F kružne cilindrične ljuske koji odgovaraju najnižoj sopstvenoj vrednosti za usvojeno m
Figure 6. Fundamental modes shapes for a circular cylindrical shell ($L/a = 20$ *,* $h/a = 0.05$ *,* $\nu = 0.3$ *) with F-F boundary conditions and given m*

Primer 5.3

U okviru ovog primera je demonstrirana primena metode dinamičke krutosti u analizi slobodnih vibracija kružne cilindrične ljuske sa skokovitom promenom debljine. Za usvojeno *m* određene su prve četiri bezdimenzionalne sopstvene frekvencije kružno cilindrične ljuske s jednostepenom promenom debljine i različitim graničnim uslovima. Rešenja dobijena primenom MDK po Flügge-ovoj teoriji upoređena su s rezultatima Zhang-a [21]. Zhang je koristio Flügge-ovu teoriju tankih ljuski, *state-space* metod i metod dekompozicije domena (*domain decomosition method*) da bi postavio uslove ravnoteže i kompatibilnosti na spoju dva segmenta. U Tabeli 3 prikazana su rešenja za ljuske sa sledećim graničnim uslovima i geometrijom: (1) *C-F* granični uslovi, $L/a = 1$ i $m = 1$ i 2, (2) *C-SD* granični uslovi, $L/a = 10$ i $m = 3$ i 4, (3) *C-C* granični uslovi, $L/a = 5$ i $m = 5$ i 6. Za sve ljuske je: $h_1/a = 0.01$, $h_2/h_1 = 0.5$ i $L_1/L = 0.5$, gde su h_1 i L_1 debljina i dužina prvog segmenta ljuske, h_2 je debljina drugog segmenta i L je ukupna dužina ljuske. U Tabeli 3 su, takođe, prikazane i relativne razlike u procentima između ova dve rešenja, koja ne prelaze 0.01 %.

Example 5.3

In this example, the application of the DSM in free vibration analysis of a stepped circular cylindrical shell has been demonstrated. The first four dimensionless natural frequencies of circular cylindrical shells with one-step thickness variation and with *C-F*, *C-SD* and *C-C* boundary conditions are calculated for a given *m*. Then results obtained by the DSM are compared with the results of Zhang [21]. Zhang used the Flügge thin shell theory, the state-space method and domain decomposition method in order to satisfy continuity requirements between shell segments. In Table 3, the results are presented for shells with following boundary conditions and geometry: (1) *C-F* boundary conditions, $L/a = 1$, $m = 1$,2, (2) *C-SD* boundary conditions, $L/a = 10$, $m = 3$,4 and (3) *C-C* boundary conditions, $L/a = 5$, $m = 5$,6. For all the shells applies the following: $h_1/a = 0.01$, $h_2/h_1 = 0.5$ and $L_1/L = 0.5$, where h_1 and L_1 are the thickness and the length of the first segment of the shell, h_2 is the thickness of the second segment and *L* is the total length of the shell. In Table 3 the relative differences in the percentage between the solutions are presented, which do not exceed 0.01%.

Tabela 3. Prve četiri bezdimenzionalne sopstvene frekvencije $\bar{\omega} = \omega a^2 \sqrt{\rho(1-\nu^2)/E}$ *za usvojeno m kružne cilindrične ljuske s jednostepenom promenom debljine:* $h_1/a = 0.01$, $h_2/h_1 = 0.5$, $L_1/L = 0.5$, $\nu = 0.3$

Table 3. First four dimensionless natural frequencies $\bar{\omega} = \omega a^2 \sqrt{\rho(1-\nu^2)/E}$ *of a circular cylindrical shell with one-step thickness variation for a given m:* $h_1/a = 0.01$, $h_2/h_1 = 0.5$, $L_1/L = 0.5$, $\nu = 0.3$

	mode	[21]	*DSM*	Δ% [20] - *DSM*	[21]	*DSM*	Δ% [21] - *DSM*
			$m=1$			$m=2$	
C-F $\frac{L}{a}=1$	1	0.637349	0.637356	0.00	0.409444	0.409447	0.00
	2	0.899615	0.899611	0.00	0.766426	0.766433	0.00
	3	0.948341	0.948335	0.00	0.911952	0.911948	0.00
	4	0.973919	0.973926	0.00	0.954440	0.954443	0.00
			$m=3$			$m=4$	
C-SD $\frac{L}{a}=10$	1	0.073550	0.073553	0.00	0.057247	0.057254	-0.01
	2	0.169777	0.169773	0.00	0.117799	0.117796	0.00
	3	0.275089	0.275093	0.00	0.194529	0.194532	0.00
	4	0.388211	0.388217	0.00	0.283104	0.283104	0.00
			$m=5$			$m=6$	
C-C $\frac{L}{a}=5$	1	0.038185	0.038187	-0.01	0.051992	0.051994	0.00
	2	0.057617	0.057618	0.00	0.064715	0.064712	0.01
	3	0.071696	0.071702	-0.01	0.089501	0.089506	-0.01
	4	0.085486	0.085492	-0.01	0.102022	0.102016	0.01

Primer 5.4

U poslednjem primeru određene su najniže bezdimenzionalne sopstvene frekvencije $\bar{\omega} = \omega a^2 \sqrt{\rho(1-\nu^2)/E}$ za ljusku sa *SD-SD*, *C-C* i *F-F* graničnim uslovima koja ima dva, odnosno tri prstenasta međuoslonca na jednakim rastojanjima. Na mestu prstenastog međuoslonca sprečeno je radijalno pomeranje, tj. $w = 0$. Posmatrani su slučajevi za koje je $L/a =$ 5 i 10 i $h/a =$0.05 i 0.005. Rezultati dobijeni primenom MDK po Flügge-ovoj teoriji upoređeni su s rezultatima Xiang-a [22], koji je koristio Goldenveizer-Novozhilov teoriju tankih ljuski, *state-space* metod i metod dekompozicije domena. Osnovne sopstvene frekvencije, zajedno sa odgovarajućim brojem *m*, date su u Tabeli 4. Relativna razlika u procentima, takođe prikazana u tabeli, ne prelazi 1.18%.

Example 5.4

In the last example, the fundamental dimensionless natural frequencies $\bar{\omega} = \omega a^2 \sqrt{\rho(1-\nu^2)/E}$ for a shell with *SD-SD*, *C-C* and *F-F* boundary conditions and two, i.e. three equally spaced intermediate ring supports are computed. The radial displacement is prevented at the locations of ring supports, i.e. $w = 0$. In the analysis $L/a =$ 5, 10 and $h/a =$0.05, 0.005 are adopted.

The results obtained by the DSM using the Flügge theory are compared with the results of Xiang [22], who used the Goldenveizer-Novozhilov thin shell theory, the state-space technique and the domain decomposition method. Fundamental frequencies, along with the corresponding circumferential number *m*, are given in Table 4. The relative differences in percentage, which is also presented in Table 4, do not exceed 1.18%.

Tabela 4. Najniže bezdimenzionalne sopstvene frekvencije $\bar{\omega} = \omega a^2 \sqrt{\rho\left(1-\nu^2\right)/E}$ za kružnu cilindričnu ljusku sa dva, odnosno tri prstenasta međuoslonca ($w = 0$) na jednakim međusobnim rastojanjima, $\nu = 0.3$

Table 4. Fundamental dimensionless natural frequencies $\bar{\omega} = \omega a^2 \sqrt{\rho\left(1-\nu^2\right)/E}$ of a circular cylindrical shell with two and three equally spaced intermediate ring supports ($w = 0$): $\nu = 0.3$

BC	$\frac{L}{a}$	$\frac{h}{a}$	dva međuoslonca / *2 supports*				tri međuoslonca / *3 supports*			
			[22]	*DSM*	Δ%	*m*	[22]	*DSM*	Δ%	*m*
SD-SD	5	0.005	0.0973340	0.09736141	-0.03	(7)	0.13052900	0.13056499	-0.03	(8)
		0.05	0.3066290	0.30744889	-0.27	(4)	0.39346800	0.39311378	0.09	(1)
	10	0.005	0.04757610	0.04758199	-0.01	(5)	0.06529310	0.06529980	-0.01	(6)
		0.05	0.14468164	0.14504722	-0.25	(3)	0.18596200	0.18648681	-0.28	(3)
C-C	5	0.005	0.10608300	0.10609919	-0.02	(7)	0.13655000	0.13658628	-0.03	(8)
		0.05	0.31320200	0.31385083	-0.21	(3)	0.40571000	0.40674818	-0.26	(4)
	10	0.005	0.05294030	0.05294578	-0.01	(5)	0.06864620	0.06865649	-0.01	(6)
		0.05	0.15388300	0.15425217	-0.24	(3)	0.19404800	0.19454980	-0.26	(3)
F-F	5	0.005	0.04372600	0.04367161	0.12	(5)	0.06023600	0.06017825	0.10	(5)
		0.05	0.11563700	0.11540796	0.20	(1)	0.17655500	0.17631291	0.14	(1)
	10	0.005	0.02093890	0.02091878	0.10	(3)	0.02938180	0.02934511	0.12	(4)
		0.05	0.0551552	0.05450301	1.18	(2)	0.11356600	0.11343547	0.11	(1)

6 ZAKLJUČAK

U ovom radu je formulisana dinamička matrica krutosti elementa kružne cilindrične ljuske. Dinamička matica krutosti određena je na osnovu tačnog rešenja sistema parcijalnih diferencijalnih jednačina kojima je definisan problem slobodnih vibracija po Flügge-ovoj teoriji. Izvedena dinamička matrica krutosti implementirana je u za tu svrhu napisani Matlab program za sračunavanje svojstvenih frekvencija i oblika oscilovanja kružne cilindrične ljuske i sistema kružnih cilindričnih ljuski. Primenom programa određene su svojstvene frekvencije za više karakterističnih primera. Dobijeni rezultati su upoređeni s dostupnim analitičkim rezultatima iz literature, kao i s rezultatima dobijenim primenom metoda konačnih elemenata i programa Abaqus. Analiza rezultata pokazala je odlično slaganje sa analitičkim rešenjima i s rešenjima dobijenim primenom programa Abaqus.

Prednost primene dinamičke matrice krutosti je očigledna: (1) za ljuske konstantnog preseka i s proizvoljnim graničnim uslovima na krajevima, dovoljno je koristiti samo jedan element, izuzev kod obostrano uklještene ljuske gde je potrebno koristiti dva kontinualna elementa; (2) za ljuske promenljive debljine i za ljuske s međuosloncima potreban je samo jedan

6 CONCLUSION

In this paper the dynamic stiffness matrix for a circular cylindrical shell element is formulated. Dynamic stiffness matrix is developed using the exact solution of the governing differential equations of free vibration according to the Flügge thin shell theory. The derived dynamic stiffness matrix is implemented in a Matlab program for calculation of natural frequencies and mode shapes of circular cylindrical shells and circular cylindrical shell assemblies. For several numerical examples natural frequencies are calculated using this program. The obtained results are validated against the available analytical results in the literature, as well as the results of the FE program Abaqus.

The analyses of the obtained results show excellent agreement with analytical solutions as well as the results obtained by Abaqus. The advantage of using the dynamic stiffness matrix is obvious: (1) for shells of constant cross section and arbitrary boundary conditions at the ends, it is sufficient to use only one DS element, except for shells clamped at both side, where it is necessary to apply two continuous elements; (2) for shells with stepped thickness variation and shells with intermediate ring supports it is necessary to apply one element for each segment of the shell. Contrary to the DSM in the element za svaki segment ljuske. Za razliku od MDK u MKE je potrebno mnogo elemenata (preko 100000) da bi se postigla željena tačnost.

Prikazani rezultati demonstrirali su glavnu prednost MDK u odnosu na MKE, a to je značajno smanjenje veličine modela i visoka preciznost rezultata u širokom frekventnom opsegu.

FEM a significant number of elements (over 100000) have to be applied in numerical model in order to achieve the desired accuracy. Presented results demonstrate the main advantages of DSM in comparison with FEM - a significant reduction of the size of model and highly accurate results in a wide frequency range.

ZAHVALNOSTI

Autori izražavaju zahvalnost Vladi Republike Srbije – Ministarstvu prosvete, nauke i tehnološkog razvoja, za finansijsku pomoć u okviru projekta TR-36046.

ACKNOWLEDGEMENTS

The authors are grateful to the Ministry of Science and Technology, Republic of Serbia, for the financial support of this research within the Project TR 36046.

7 LITERATURA REFERENCES

[1] Lunden R, Akesson B. Damped second order Rayleigh Timoshenko beam vibration in space – an exact complex dynamic member stiffness matrix. International Journal of Numerical Methods in Engineering, 1983, 19:431–49.

[2] Leung AYT. Dynamic stiffness and substructures. New-York: Springer; 1993.

[3] Banerjee JR, Williams FW. Coupled bending-torsional dynamic stiffness matrix for Timoshenko beam elements. Computers & Structures, 1992, 42:301–10.

[4] Lee U. Spectral element method in structural dynamics. Incheon, Korea: Inha University Press, 2004.

[5] Casimir JB, Duforet C, Vinh T. Dynamic behavior of structures in large frequency range by continuous element methods. Journal of Sound and Vibration, 2003, 267:1085–106.

[6] Le Sourne H. Developpement d'elements continus de coques axisymetriques et de coudes. Thesis, Universite de Nantes, 1998.

[7] Gorman DJ. Free vibration analysis of the completely free rectangular plate by the method of superposition. Journal of Sound and Vibration, 1978, 437-447.

[8] Casimir JB, Kevorkian S, Vinh T. The dynamic stiffness matrix of two- dimensional elements: application to Kirchhoff's plate continuous elements. Journal of Sound and Vibration, 2005, 287:571-589.

[9] Nefovska-Danilovic M, Petronijevic M. In-plane free vibration and response analysis of isotropic rectangular plates using the dynamic stiffness method. Computers and Structures, 2015, 82-95.

[10] Kolarevic N, Nefovska-Danilovic M, Petronijevic M. Dynamic stiffness elements for free vibration analysis of rectangular Mindlin plate assemblies. Journal of Sound and Vibration, 2015, 84-106.

[11] Kolarevic N, Marjanovic M, Nefovska-Danilovic M, Petronijevic M. Free vibration analysis of plate assemblies using the dynamic stiffness method based on the higher order shear deformation theory. Journal of Sound and Vibration, 2016, 110-132.

[12] Leissa AW. Vibration of shells. Washington, D.C.: US Government Printing Office, 1973.

[13] Matlab MI. The Language of Technical Computing. MATLAB 2011b, 2011.

[14] Abaqus. Users manual. Version 6.9. Providence, RI, USA: DS SIMULIA Corp., 2009.

[15] Doyle JF. Wave propagation in structures. New York: Springer- Verlag, 1997.

[16] Zhang XM. Vibration analysis of thin cylindrical shells using wave propagation approach. Journal of Sound and Vibration, 2001, 397-403.

[17] Timoshenko S. Theory of Plates and Shells. New York: McGraw-Hill, 1959.

[18] Zhang L, Xiang Y, Wei GW. Local adaptive differential quadrature for free vibration analysis of cylindrical shells with various boundary conditions. International Journal of Mechanical Sciences, 2006, 48: 1126–1138.

[19] Goldenveizer L. Theory of Thin Shells. New York: Pergamon Press, 1961.

[20] Novozhilov VV. The Theory of Thin Elastic Shells. Groningen, The Netherlands: P. Noordhoff Lts., 1964.

[21] Zhang L. Exact solutions for vibration of stepped circular cylindrical shells. Journal of Sound and Vibration, 2007, 948-964.

[22] Xiang Y. Exact solutions for vibration of cylindrical shells with intermediate ring supports. International Journal of Mechanical Sciences, 2002, 1907-1924.

REZIME

METODA DINAMIČKE KRUTOSTI U ANALIZI VIBRACIJA KRUŽNE CILINDRIČNE LJUSKE

Nevenka KOLAREVIĆ
Marija NEFOVSKA DANILOVIĆ
Mira PETRONIJEVIĆ

U ovom radu korišćena je metoda dinamičke krutosti za analizu slobodnih vibracija kružne cilindrične ljuske. Dinamička matrica krutosti formulisana je na osnovu tačnog rešenja sistema diferencijalnih jednačina problema slobodnih vibracija po Flügge-ovoj teoriji ljuski. To je frekventno zavisna matrica koja u sebi, pored krutosti, sadrži uticaj inercije i prigušenja. Izvedena dinamička matica krutosti implementirana je u za tu svrhu napisani Matlab program za određivanje sopstvenih frekvencija i oblika oscilovanja kružne cilindrične ljuske. Urađen je niz primera. Rezultati dobijeni primenom dinamičke matrice krutosti upoređeni su s rezultatima dobijenim pomoću komercijalnog programa zasnovanog na metodi konačnih elemenata Abaqus, kao i sa dostupnim analitičkim rezultatima iz literature.

Ključne reči: slobodne vibracije, dinamička matica krutosti, Flügge-ova teorija ljuski

SUMMARY

DYNAMIC STIFFNESS METHOD IN THE VIBRATION ANALYSIS OF CIRCULAR CYLINDRICAL SHELL

Nevenka KOLAREVIC
Marija NEFOVSKA DANILOVIC
Mira PETRONIJEVIC

In this paper the dynamic stiffness method is used for free vibration analysis of a circular cylindrical shell. The dynamic stiffness matrix is formulated on the base of the exact solution for free vibration of a circular cylindrical shell according to the Flügge thin shell theory. The matrix is frequency dependent and, besides the stiffness, includes inertia and damping effects. The derived dynamic stiffness matrix is implemented in the code developed in a Matlab program for computing natural frequencies and mode shapes of a circular cylindrical shell. Several numerical examples are carried out. The obtained results are validated against the results obtained by using the commercial finite element program Abaqus as well as the available analytical solutions from the literature.

Key words: free vibration, circular cylindrical shell, Flügge thin shell theory, dynamic stiffness matrix,

QUADRUPLE SYMMETRIC REAL SIGNALS SPECTRAL EVEN AND ODD DECOMPOSITION

SPEKTRALNA DEKOMPOZICIJA ČETVOROSTRUKO SIMETRIČNIH REALNIH SIGNALA PARNIM I NEPARNIM DELOVIMA SIGNALA

Venelin JIVKOV
Philip PHILIPOFF

ORIGINALNI NAUČNI RAD
ORIGINAL SCIENTIFIC PAPER
UDK: 517.9
517.518.45
doi: 10.5937/grmk1603063J

1 INTRODUCTION

Spectral even and odd decomposition of quadruple symmetric real signals is illustrated in the case of:

1.1 SH (polarized in horizontal plane) wave propagation through multi layered media
[1, 2, 3, 4, 7]

The wave propagation process, at the direction of the axis *x* perpendicular to the investigated multilayered media (fig. 1), could be described by the following equation:

The wave propagation process, at the direction of the axis *x* perpendicular to the investigated multilayered media (fig. 1), could be described by the following equation:

$$\frac{\partial^2 w(x,t)}{\partial t^2} - V_{SH}^2 \frac{\partial^2 w(x,t)}{\partial x^2} = 0 \,, \qquad (1)$$

where $V_{SH} = \sqrt{\frac{\mu}{\rho}}$ is the wave propagation velocity for the shear waves SH, μ=const is the Lame coefficient, ρ=constant represents mass density. The function *w(x,t)* is the anti plane *(X, Y)* component of the displacement vector in the direction parallel to the axis *Z*.

On the boundary between the two neighbouring layers *"i"* and *"i+1"* the corresponding boundary conditions are satisfied. These boundary conditions represent that the unknown displacements and forces (stresses) are continuous:

$$w(x,t)^i_{boundary} = w(x,t)^{i+1}_{boundary} \qquad (2)$$

$$P^i_{boundary} = (\sigma_{ij} n_j)^i_{boundary} = -P^{i+1}_{boundary} = -\ (\sigma_{ij} n_j)^{i+1}_{boundary} \,, \qquad (3)$$

where P^i is the boundary force vector of the corresponding layer, σ_{ij} is the stress tensor, and n_j is the corresponding normal vector. The initial conditions with respect to the displacement and to the first difference are homogeneous. The both functions depend on the spatial variable *x* and time argument *t* in the initial moment *t=0:*

Philip Philipoff, Assistant Professor, PhD, Institute of Mechanics-BAS, acad.G.Bonchev street, 4 bl., phone: +359 888 28 11 75, e-mail: philip.philipoff@gmail.com; philip_philipoff@imbm.bas.bg
Venelin Jivkov, Corresponding Member of BAS, Professor, Senior Doctor of Sciences, Technical University-Sofia, 8 Kliment Ohridsky boulevard, phone: +359 888 65 81 81, e-mail: jivkov@tu-sofia.bg

$$w(x,t)\big|_{t=0} = 0, \qquad \frac{\partial w(x,t)}{\partial t}\Big|_{t=0} = 0. \qquad (4)$$

For the direct problem [1, 2, 3, 4] on the bedrock the displacement boundary condition is given in the mode of the known time function:

$$w(0,t) = X_b(t). \qquad (5)$$

The free surface stresses (force boundary conditions) are homogeneous for the investigated direct and inverse problems [1, 2, 3, 4]:

$$P^{surface} = (\sigma_{ij} n_j)^{surface} = 0. \qquad (6)$$

On the other hand, for the inverse problem [1, 2, 3, 4] on the free surface, the displacement boundary condition is given in the mode of the known time function:

$$w(l,t) = X_s(t) \qquad (7)$$

1.2 Structural mathematical model of the multi layered structure.

The structural model of the multilayer media is shown in fig. 1. The SH Wave Propagation Reflect – Pass Perpendicular Process is illustrated on the fig.1 a. The Block - Diagram Model of the media under investigation is shown in fig.1 b. The Flow Graph of the system signals is shown in the fig.1. c.

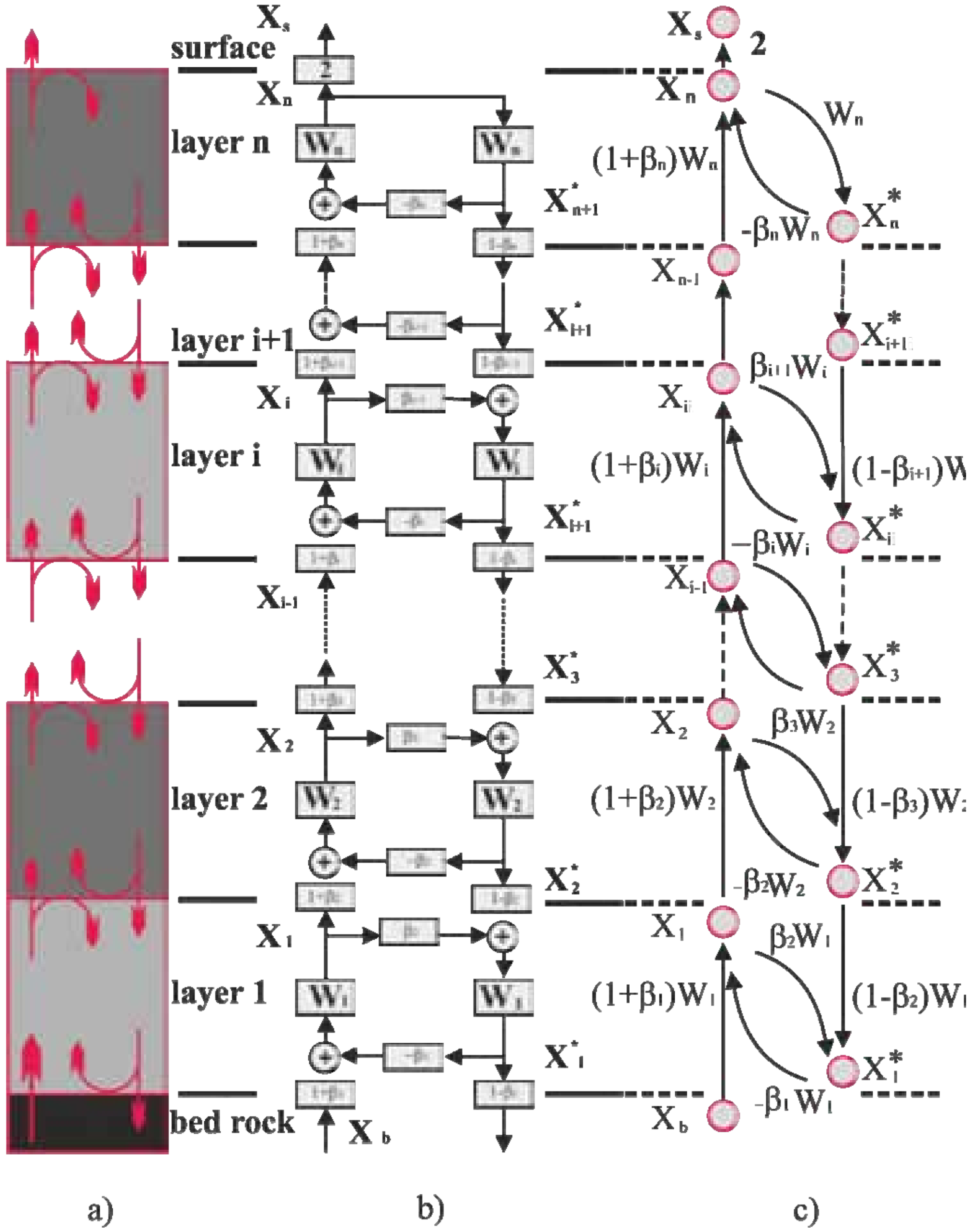

Fig. 1. Multilayered Media Structural Model. a) SH Wave Propagation Reflect – Pass Perpendicular Process. b) Block - Diagram Model. c) Signal Flow Graph.

The above formulated SH wave boundary condition problem (1) - (7) could be solved by a system of differential equations, initial and boundary conditions. This differential system consists of the following elements [1, 2, 3, 4]:

- n equations in the mode (1), one differential equation for each layer, because the velocity function $V(x)$ depending on spatial co-ordinate *x* is discontinued and is a terrace-like type;
- 2(n - 1) boundary conditions in the mode (2), (3);
- surface boundary condition in the mode (6);
- initial conditions in the mode (4),
- and either of boundary conditions (cinematic excitation) (5) for the direct problem or (7) for the inverse problem.

The above formulated wave boundary problem (1)-(7) can be transformed in the complex domain. The solution of the investigated problem (1)-(7) in the complex domain could be obtained by solving the following algebraic system of equations [1, 2, 3, 4]:

$$X_1(s) = W_1(s)\left[\left(1+\beta_1(s)\right)X_b(s) - \beta_1(s)X_1^*(s)\right],$$
$$*** \quad *** \quad ***$$
$$X_i(s) = W_i(s)\left[\left(1+\beta_i(s)\right)X_{i-1}(s) - \beta_i(s)X_i^*(s)\right], \qquad (8)$$
$$*** \quad *** \quad ***$$
$$X_i^*(s) = W_i(s)\left[\beta_{i+1}(s)X_i(s) + \left(1-\beta_{i+1}(s)\right)X_{i+1}^*(s)\right],$$
$$*** \quad *** \quad ***$$
$$X_n^*(s) = W_n(s)\; X_n(s) \; .$$

The unknown variables in the system (8) ($X1, X_2,...,X_i.,...X_n$, X^*_1, X^*_2,..., X^*_i,..., X^*_n) represent the displacements, velocities or accelerations of the media particles under investigation. The coefficients β=β(s)= Re β (s)+ j Im β (s) in the system (8) are reflection and refraction layer ratios (see fig.1 b, fig. 1 c). They are known complex functions of the parameter of integral transformation.

1.3 Transfer function of the multi layered structure.

The connections between the signals in the algebraic system (8) could be visualized by the oriented graph. Similar oriented graph is shown in the fig.1.c. This mathematical description represents a system of 2n algebraic equations. The system of variables, the seismic signals on the both sizes of each layer boundary ($X_1, X_2,...,X_i.,...X_n$, X^*_1, X^*_2,..., X^*_i,..., X^*_n), and the system of coefficients, reflection and refraction layer ratios, are complex-valued. This choice of the system of variables approximates the investigated structural model to the corresponding continuous differential problem. The variables in the above mentioned system (8) ($X_1, X_2,...,X_i.,...X_n$, X^*_1, X^*_2,..., X^*_i,..., X^*_n) for the continuous and discrete problems are identical. The equation (7) together with the used integral transformation of the initial boundary value problem [1, 2, 3, 4] affords the opportunity to solve direct and inverse problem of the engineering seismology [1, 2, 3, 4] in the complex domain. In this system the differential equation (1) takes part only indirectly by the corresponding transfer function of the problem. The function matrix of the system (8) is asymmetric. Based on this fact, the common transfer function of the problem $\Psi(s)$ could be obtained by recurrent elimination of the system parameters. This function physically represents the quotient between images of input and output signals of the geological structure under investigation [1, 2, 3, 4]:

$$\Psi\,(s) = \left\{X_{input}(s)\right\}^{-1}\left\{X_{output}(s)\right\}. \qquad (9)$$

Substituting the analytical complex parameter *"s"* by the numerical imaginary parameter *"jω"* into system of equations (8), it is possible to calculate numerically the formulated direct and inverse problems [1, 2, 3, 4] by means of Fourier integral transformation.

2 QUADRUPLE SYMMETRIC REAL FUNCTIONS.

The coefficients β= β(jϖ)= Re β (ϖ)+ j Im β (ϖ) in the system (8) are reflection and refraction layer ratios according to the Willebrord Snellius (1580–1626) low (see fig.1 b, fig. 1 c). They are known complex functions of the frequency ϖ. The properties of the layers under investigation of structural model in fig.1 [7, 8] are presented in mathematical description (8) by corresponding layer transfer function signed

W_i (jϖ) and corresponding reflection and refraction coefficients signed β_i(jϖ). By suitable selection of the real and imaginary parts of the coefficients β_i (jϖ) can be obtained quadruple symmetric real functions presented in the first quadrant of the fig.2 in a capacity of searched problem solution. In the case of real and imaginary parts of the coefficients β_i according to the conditions of Theorem 1 of the present paper, the signal will be received in the second quadrant. In the case of real and imaginary parts of the coefficients β_i according to the conditions of Theorem 3 of the present paper, the signal will be received in the third quadrant. The signals from third quadrant and from fourth quadrant can be obtained also in the case of real and imaginary parts of the coefficients β_i according to the conditions of Theorems 2 and 4 of the present paper respectively.

The five theorems (they are published as sub conditions in the theorem 2.1 in [5] signed by * and here points) describe the Symmetry - Conjugation relation:

- Theorem 1 (The phenomenon "Symmetry" in the time domain corresponds to the phenomenon "Conjugation" in the frequency domain). The complex Fourier F(jω) spectra of the symmetric real functions in the first and second quadrants are conjugated as well as.
- **Theorem 2.** The complex Fourier F(jω) spectra of the symmetric real functions in the third and fourth quadrants are conjugated respectively.
- Theorem 3 (The phenomenon "Anti Symmetry" in the time domain corresponds to the phenomenon "Anti Conjugation" in the frequency domain). The complex Fourier F(jω) spectra of the anti symmetric real functions in the first and third quadrant are anti conjugated as well as.

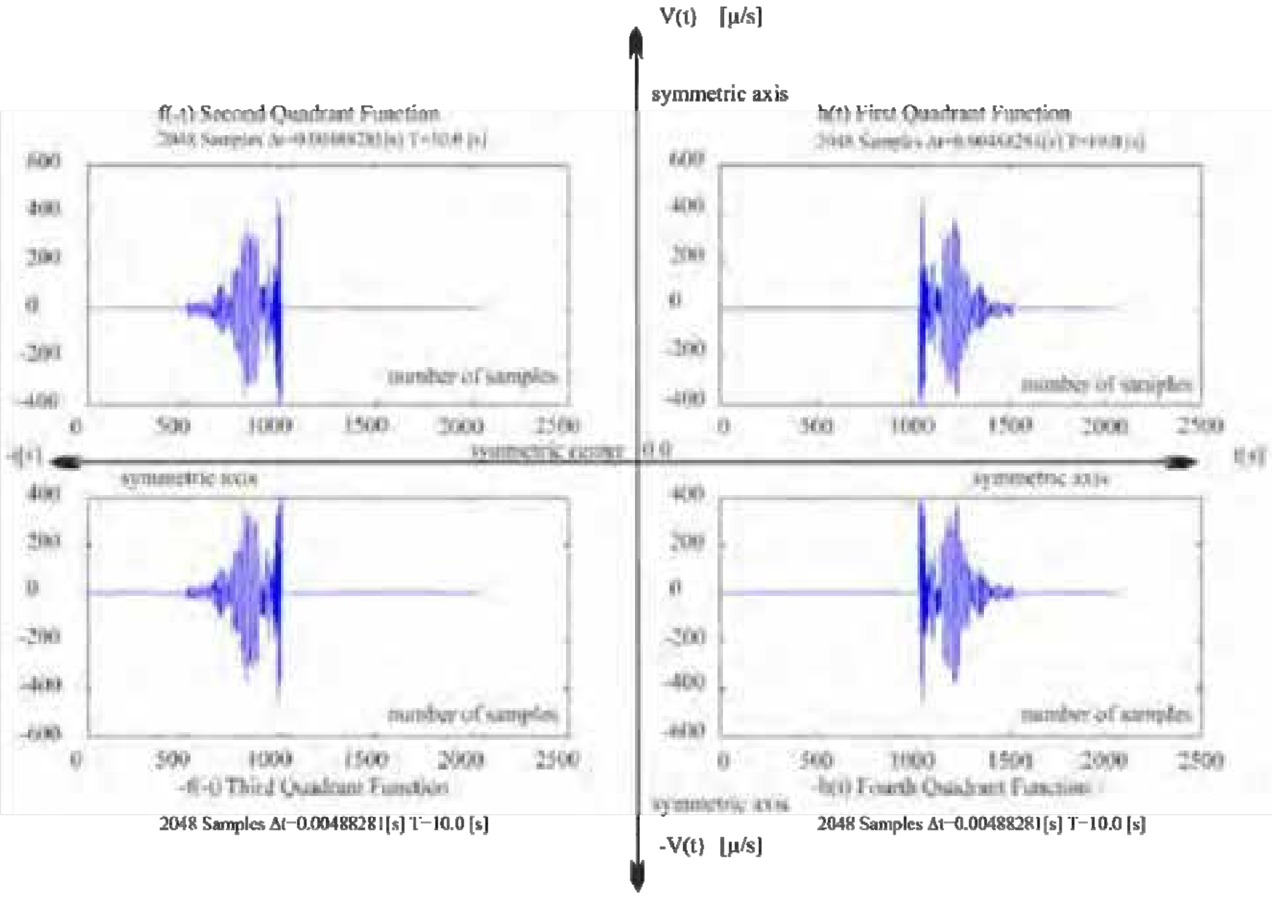

Fig. 2. Quadruple symmetric real functions for the velocities media particles V(t) [μ/s] from fig.1.

- **Theorem 4.** The amplitudes of functions in the first and second quadrants are both positive, while the amplitudes of functions in the third and four quadrants are both negative. The functions under investigation could be of arbitrary amplitudes – negative or positive. The corresponding complex Fourier F(jω) spectra are also of arbitrary type amplitudes - negative or positive.
- **Theorem 5 (Frequency indistinguishable).** Four quadruple symmetric real functions are frequency indistinguishable.

3 FOURIER TRANSFORMABLE FUNCTIONS.

The well known Dirichlet conditions are sufficient for function f(t) in the time domain to be Fourier transformable [6] pp-73. It follows:

3.1 The function f(t) is limited in the absolute value mode:

$$\int_{-\infty}^{\infty} |f(t)|\, dt < \infty \,. \tag{10}$$

3.2 f(t) has finite maxima and minima within any finite interval.

3.3 f(t) has a finite number of discontinuities within any finite interval.

The direct and inverse Fourier transformations are given by:

$$F(j\omega) = \int_{-\infty}^{\infty} f(t) e^{-j\omega t}\, dt \,; \qquad f(t) = \frac{1}{2\pi}\int_{-\infty}^{\infty} F(\omega) e^{j\omega t}\, d\omega \,. \tag{11}$$

4 ODD AND EVEN REPRESENTATIONS.

It is well known that any function in the time domain can be decomposed into an odd and even function [6] pp-75 as follows:

$$f^{common\ function}(t) = s^{even\ function}(t) + c^{odd\ function}(t) = \frac{f^{common\ function}(t) - f^{common\ function}(-t)}{2} + \frac{f^{common\ function}(t) + f^{common\ function}(-t)}{2}. \qquad (12)$$

Theorem 6 (The phenomenon “Symmetry” in the time domain corresponds to the phenomenon “Conjugation” in the frequency domain. The phenomenon “Anti Symmetry” in the time domain corresponds to the phenomenon “Anti Conjugation” in the frequency domain. The simultaneous operation of the Theorems 1 and 3 leads to even and odd decomposition of the Fourier complex spectrum of the common function with length N in the time domain. This result represents spectral function, composed by the equivalent nonzero real and imaginary spectral parts with length N/2 in the frequency domain).

Any real common function in the time domain can be decomposed in a symmetric and anti symmetric components. The Fourier spectrum of the common function:

$$F^{common\ function}(j\omega) = \frac{1}{\sqrt{2\pi}}\int_{-\infty}^{+\infty} f^{common\ function}(t)e^{-i\omega t}\,dt\,, \qquad (13)$$

can be obtained by adding twice real left part $R_e^{even\ left}(\omega)$ of the symmetric component $S^{even\ function}(t)$:

$$S^{even\ function}(j\omega) = \frac{1}{\sqrt{2\pi}}\int_{-\infty}^{+\infty} s^{even\ function}(t)e^{-i\omega t}\,dt = \frac{1}{\sqrt{2\pi}}\int_{-\infty}^{0} s^{even\ function\ left}(t)e^{-i\omega t} + \frac{1}{\sqrt{2\pi}}\int_{0}^{+\infty} s^{even\ function\ right}(t)e^{-i\omega t}\,dt \qquad (14)$$

plus imaginary unit “j” multiply by twice imaginary right part $I_m^{odd\ right}(\omega)$ of anti symmetric component $C^{odd\ function}(t)$:

$$C^{odd\ function}(j\omega) = \frac{1}{\sqrt{2\pi}}\int_{\infty}^{+\infty} c^{odd\ function}(t)e^{-i\omega t}\,dt = \frac{1}{\sqrt{2\pi}}\int_{-\infty}^{0} c^{odd\ function\ left}(t)e^{-i\omega t}\,dt + \frac{1}{\sqrt{2\pi}}\int_{0}^{+\infty} c^{odd\ function\ right}(t)e^{-i\omega t}\,dt \qquad (15)$$

because of linearity of the above mentioned integrals in (14) and (15) and using the popular rule for zero integral from zero integrand function [9]. Than the complex spectra of the common function could be obtained by the following relation:

$$F^{common\ function}(j\omega) = 2\left(R_e^{even\ left}(\omega) + jI_m^{odd\ right}(\omega)\right). \qquad (16)$$

Proof of the Theorem 6.

The Fourier complex spectrum $S^{even\ function}(j\omega)$ of the symmetric component $s^{even\ function}(t)$ of the common function $f^{common\ function}(t)$ can be written as follows:

$$S^{even\ function}(j\omega) = \frac{1}{\sqrt{2\pi}}\int_{-\infty}^{+\infty} s^{even\ function}(t)e^{-i\omega t}\,dt = R_{e}^{left}(\omega) + jI_{m}^{left}(\omega) + R_{e}^{right}(\omega) + jI_{m}^{right}(\omega). \quad (17)$$

Symmetric component could be decomposed as follows:

$$S^{even\ function}(j\omega) = S^{even\ function\ left}(j\omega) + S^{even\ function\ right}(j\omega) \quad (18)$$

$$S^{even\ function\ left}(j\omega) = R_{e}^{left}(\omega) + jI_{m}^{left}(\omega) \quad (19)$$

$$S^{even\ function\ right}(j\omega) = R_{e}^{right}(\omega) + jI_{m}^{right}(\omega). \quad (20)$$

According to (10) from [5] pp-346 for the symmetric function left $S^{even\ function\ left}(j\omega)$ and for the symmetric function right $S^{even\ function\ right}(j\omega)$

$$S^{even\ function\ left}(j\omega) = R_{e}^{left}(\omega) + jI_{m}^{left}(\omega) = \overline{S^{even\ function\ right}(j\omega)} = R_{e}^{left}(\omega) - jI_{m}^{left}(\omega) \quad (21)$$

$$S^{even\ function}(j\omega) = S^{even\ function\ left}(j\omega) + S^{even\ function\ right}(j\omega) = R_{e}^{left}(\omega) + jI_{m}^{left}(\omega) + R_{e}^{left}(\omega) - jI_{m}^{left}(\omega) = 2\,R_{e}^{left}(\omega). \quad (22)$$

The Fourier complex spectrum $C^{odd\ function}(j\omega)$ of the anti symmetric component $c^{odd\ function}(t)$ of the common function $f^{common\ function}(t)$ can be written as follows:

$$C^{odd\ function}(j\omega) = \frac{1}{\sqrt{2\pi}}\int_{-\infty}^{+\infty} c^{odd\ function}(t)e^{-i\omega t}\,dt = R_{e}^{left}(\omega) + jI_{m}^{left}(\omega) + R_{e}^{right}(\omega) + jI_{m}^{right}(\omega). \quad (23)$$

Anti symmetric component could be decomposed as follows:

$$C^{odd\ function}(j\omega) = C^{odd\ function\ left}(j\omega) + C^{odd\ function\ right}(j\omega) \quad (24)$$

$$C^{odd\ function\ left}(j\omega) = R_{e}^{left}(\omega) + jI_{m}^{left}(\omega) \quad (25)$$

$$C^{odd\ function\ right}(j\omega) = R_{e}^{right}(\omega) + jI_{m}^{right}(\omega). \quad (26)$$

According to (10) from [5] pp-346 for the symmetric function left $C^{odd\ function\ left}(j\omega)$ and for the symmetric function right $C^{odd\ function\ right}(j\omega)$:

$$C^{odd\ function\ left}(j\omega)= R_{e}^{left}(\omega)+jI_{m}^{left}(\omega)=\overline{C^{odd\ function\ right}(j\omega)}=-R_{e}^{left}(\omega)+jI_{m}^{left}(\omega) \quad (27)$$

$$C^{odd\ function}(j\omega)=C^{odd\ function\ left}(j\omega)+C^{odd\ function\ right}(j\omega)= \\ R_{e}^{right}(\omega)+jI_{m}^{right}(\omega)-R_{e}^{right}(\omega)+jI_{m}^{right}(\omega)=2\,j\,I_{m}^{right}(\omega). \quad (28)$$

Finally:

$$F^{common\ function}(j\omega)= 2\left(R_{e}^{even\ left}(\omega)+jI_{m}^{odd\ right}(\omega)\right). \quad (29)$$

5 ILLUSTRATIVE NUMERICAL EXAMPLES.

The proof of the Theorem 6 is presented analytically in the paragraph four of the present paper. This proof of the Theorem 6 can be illustrated by the following eight numerical examples. The first example represents common real function of discrete type. The next eight numerical examples are of symmetric or anti symmetric discrete type functions. All examples illustrated the process of even and odd decomposition numerically.

5.1 First Common Function Numerical Example: "Rectangular Half Wave".

Three figures number 3, 4 and 5, show the process of decomposition of common function "Rectangular Half Wave" by eight samples. Figure 3 illustrates decomposition of common function in even and odd components according to [6]. Figure 4 illustrates decomposition of even component in a "Symmetric Wave Component Left" and "Symmetric Wave Component Right" according to relation (17). Figure 5 illustrates decomposition of odd component to "Anti Symmetric Wave Component Left" and "Anti Symmetric Wave Component Right" functions according to relation (23).

Table 1 and Table 2 illustrate the possibility of calculating complex Fourier spectra of the "Rectangular Half Wave" by the relation (28). The initial common function is shown in the row 2 of Table 1. The row 4 of Table 1 shows symmetric component of the initial function and the row 6 of Table 1 shows anti symmetric component of the initial function. The "Even Left Function" from the Theorem 6 is shown in the row 9 of Table 1. The "Odd Right Function" from the Theorem 6 is shown in the row 11 of Table 1.

The coefficients of the complex Fourier spectra of the "Rectangular Half Wave" are shown in the row 14 of Table 1. They are obtained by the function "fft" of MatLab program system [10]. The "Complex coefficients of the ½ event left component of the rectangular half wave" are shown in the row 16 of Table 1. The "Complex coefficients of the ½ odd right component of the rectangular half wave" are shown in row 18 of Table 1. The "Complex coefficients of the ½ event left component + Complex coefficients of the ½ odd right component of the rectangular half wave" are shown in the row 20 of Table 1. The "Complex coefficients of the ½ event left component - Complex coefficients of the ½ odd right component of the rectangular half wave" are shown in the row 22 of Table 1. Finally, the "{Complex coefficients of the ½ event left component + Complex coefficients of the ½ odd right component of the rectangular half wave } + {Complex coefficients of the ½ event left component - Complex coefficients of the ½ odd right component of the rectangular half wave }" are shown in the last row 24 of Table 1. This operation closed the illustration of applying the relation (28) for the numerical example under consideration. The row 24 of Table 1 is identical of the row 14 of Table 1. This is the numerical proof of the numerical example "Rectangular Half Wave". This numerical proof shows, that the complex Fourier spectra calculated by MatLab program system [10] directly and complex Fourier spectra calculated by using the relation (28) are identical.

In addition, Table 2 showing the numerical example under investigation has illustrated the inverse composition of the initial "Rectangular Half Wave". The "Complex coefficients of the ½ event left component of the rectangular half wave" are shown in the row 27 of Table 2. The "Inverse Samples of the ½ event left component of the rectangular half wave – Time Domain" are shown in the row 29 of Table 2. The "Complex coefficients of the ½ odd right component of the rectangular half wave" are shown in the row 32 of Table 2. The "Inverse Samples of the ½ odd right component of the rectangular half wave – Time Domain" are shown in the row 34 of Table 2. The "Complex coefficients of the ½ event left component + Complex coefficients of the ½ odd right component of the rectangular half wave" are shown in the row 37 of Table 2. The "Inverse Samples of the {Complex coefficients of the ½ event left component + Complex coefficients of the ½ odd right component of the rectangular half wave} – Time Domain" are shown in the row 39 of Table 2. The "Complex coefficients of the ½ event left component - Complex coefficients of the ½ odd right component of the rectangular half wave" are shown in the row 42 of

Table 2. The “Inverse Samples of the { Complex coefficients of the ½ event left component - Complex coefficients of the ½ odd right component of the rectangular half wave} – Time Domain” are shown in the row 44 of Table 2. The “Complex coefficients of the { Complex coefficients of the ½ event left component + Complex coefficients of the ½ odd right component of the rectangular half wave } + {Complex coefficients of the ½ event left component -Complex coefficients of the ½ odd right component of the rectangular half wave }” are shown in the row 46 of Table 2. The “Inverse Samples of the { Complex coefficients of the ½ event left component + Complex coefficients of the ½ odd right component of the rectangular half wave } + {Complex coefficients of the ½ event left component -Complex coefficients of the ½ odd right component of the rectangular half wave } – Time Domain” are shown in the row 49 of Table 2. This final numerical result from simultaneous interpretation of Table 1 and Table 2 shows, that the inverse transformation using the relation (28) restore the initial “Rectangular Half Wave” signal in the row 49 of Table 2. This numerical proof of the first numerical example illustrates the statement, that the complex Fourier spectra has been calculated directly for the “Rectangular Half Wave” by MatLab program system [10] and complex Fourier spectra using the relation (28) restores accuracy of the initial time domain signal after inverse discrete Fourier transformation.

The study of complex numerical examples like “Rectangular Half Wave” is possible only with the help of computers, fast Fourier transformation and software systems such as MatLab [10].

The next eight numerical examples are specially selected. They are only symmetric or only anti symmetric. They can be detected and studied more easily, because the appropriate equivalent symmetric or anti symmetric functions can be evaluated directly from the MstLab Command Window.

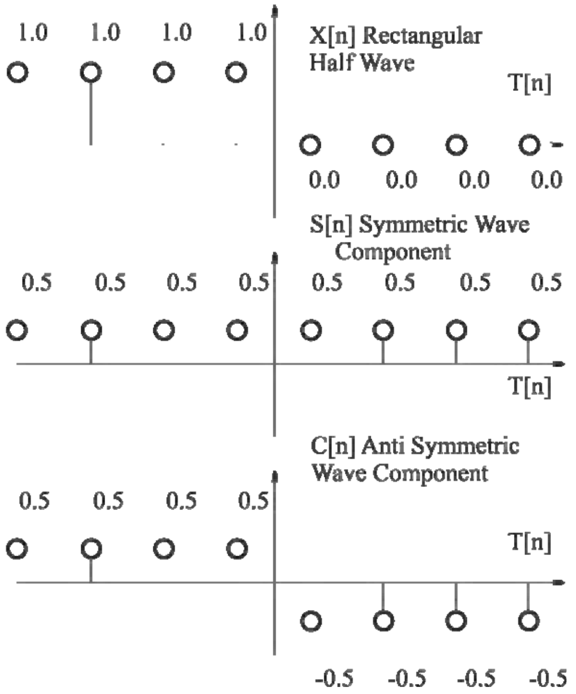

Fig. 3. Even – Odd Decomposition of the “Rectangular Half Wave”

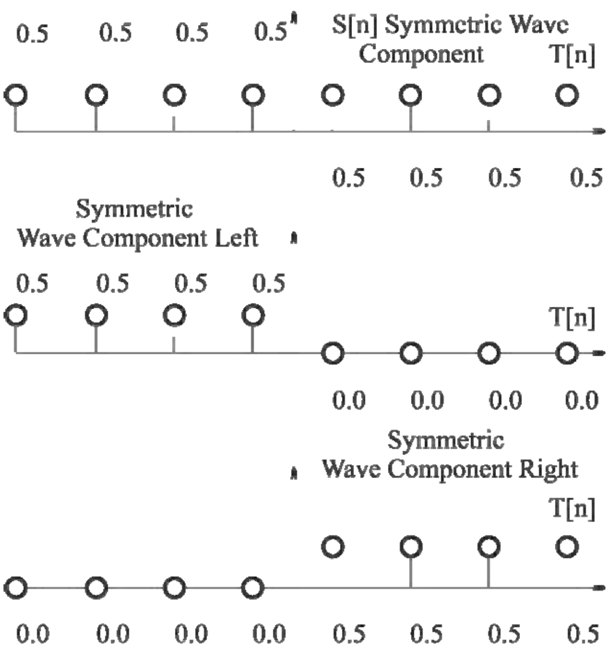

Fig. 4. Decomposition of the symmetric Wave Component to Symmetric Wave Component Left and Symmetric Wave Component Right, According to the relation (19)

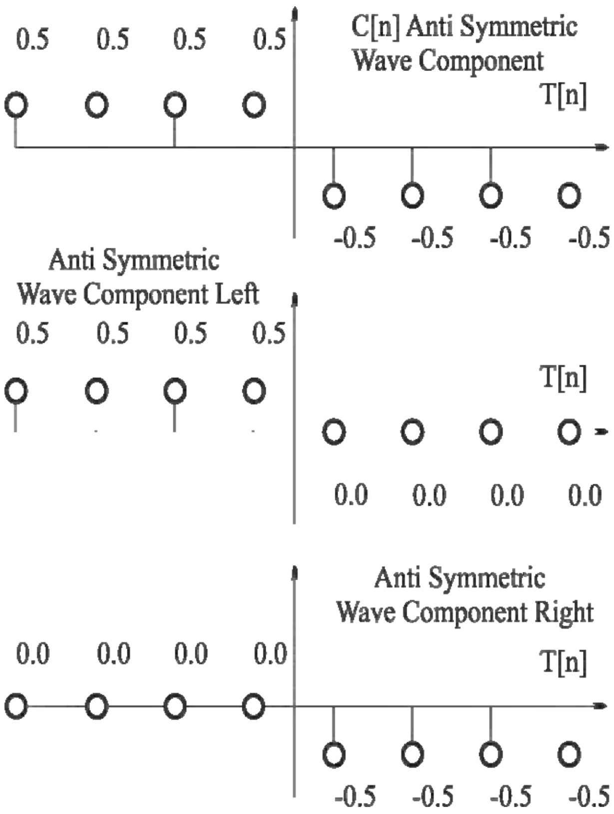

Fig. 5. Decomposition of the anti symmetric Wave Component to Anti Symmetric Wave Component Left and Anti Symmetric Wave Component Right, According to the relation (25)

Table 1. Samples and Fast Fourier Transformation Complex Coefficients of the Rectanqular Half Wave and its Components

N.	Rectangular Half Wave, Symmetric and Anti - symmetric Components, Even Left and Odd Right Functions - Samples							
1	Rectangular Half Wave							
2	1.0	1.0	1.0	1.0	0.0	0.0	0.0	0.0
3	Symmetric Component of the Rectangular Half Wave							
4	0.5	0.5	0.5	0.5	0.5	0.5	0.5	0.5
5	Anti Symmetric Component of the Rectangular Half Wave							
6	0.5	0.5	0.5	0.5	-0.5	-0.5	-0.5	-0.5
7	Six Theorem Functions							
8	Even Left Function							
9	0.5	0.5	0.5	0.5	0.0	0.0	0.0	0.0
10	Odd Right Function							
11	0.0	0.0	0.0	0.0	-0.5	-0.5	-0.5	-0.5
12	Complex Coefficients of Fourier Spectrums							
13	$C_1(Re_1+jIm_1)$	$C_2(Re_2+jIm_2)$	$C_3(Re_3+jIm_3)$	$C_4(Re_4+jIm_4)$	$C_5(Re_5+jIm_5)$	$C_6(Re_6+jIm_6)$	$C_7(Re_7+jIm_7)$	$C_8(Re_8+jIm_8)$
14	4+j0	1-j2.4142	0+j0	1-j0.4142	0+j0	1+j0.4142	0+j0	1+j2.4142
15	Complex coefficients of the ½ event left component of the rectangular half wave							
16	2+j0	0.5 - j1.2071	0+j0	0.5 - j0.2071	0+j0	0.5 + j0.2071	0+j0	0.5 + j1.2071
17	Complex coefficients of the ½ odd right component of the rectangular half wave							
18	-2+j0	0.5 – j1.2071	0+j0	0.5 – j0.2071	0+j0	0.5 + j0.2071	0+j0	0.5 + j1.2071
19	Complex coefficients of the ½ event left component + Complex coefficients of the ½ odd right component of the rectangular half wave							
20	0+j0	1-j2.4142	0+j0	1-j0.4142	0+j0	1+j0.4142	0+j0	1+j2.4142
21	Complex coefficients of the ½ event left component -Complex coefficients of the ½ odd right component of the rectangular half wave							
22	4+j0	0+j0	0+j0	0+j0	0+j0	0+j0	0+j0	0+j0
23	{Complex coefficients of the ½ event left component + Complex coefficients of the ½ odd right component of the rectangular half wave } + {Complex coefficients of the ½ event left component -Complex coefficients of the ½ odd right component of the rectangular half wave }							
24	4+j0	1-j2.4142	0+j0	1-j0.4142	0+j0	1+j0.4142	0+j0	1+j2.4142

Table 2. Fast Fourier Transformation Complex Coefficients and Inverse Samples of the Rectangular Half Wave and its Components

N	Fast Fourier Transformation Complex Coefficients and Inverse Samples of the Components of the Rectangular Half Wave						
25	Complex coefficients of the ½ event left component of the rectangular half wave						
26	$C_1(Re_1+jIm_1)$	$C_2(Re_2+jIm_2)$	$C_3(Re_3+jIm_3)$	$C_4(Re_4+jIm_4)$	$C_5(Re_5+jIm_5)$	$C_6(Re_6+jIm_6)$	$C_7(Re_7+jIm_7)$	$C_8(Re_8+jIm_8)$
27	2+j0	0.5 - j1.2071	0+j0	0.5 - j0.2071	0+j0	0.5 + j0.2071	0+j0	0.5 + j1.2071
28	Inverse Samples of the ½ event left component of the rectangular half wave – Time Domain							
29	0.5	0.5	0.5	0.5	0.0	0.0	0.0	0.0
30	Complex coefficients of the ½ odd right component of the rectangular half wave							
31	$C_1(Re_1+jIm_1)$	$C_2(Re_2+jIm_2)$	$C_3(Re_3+jIm_3)$	$C_4(Re_4+jIm_4)$	$C_5(Re_5+jIm_5)$	$C_6(Re_6+jIm_6)$	$C_7(Re_7+jIm_7)$	$C_8(Re_8+jIm_8)$
32	-2+j0	0.5 - j1.2071	0+j0	0.5 - j0.2071	0+j0	0.5 + j0.2071	0+j0	0.5 + j1.2071
33	Inverse Samples of the ½ odd right component of the rectangular half wave – Time Domain							
34	0.0	0.0	0.0	0.0	-0.5	-0.5	-0.5	-0.5
35	Complex coefficients of the ½ event left component + Complex coefficients of the ½ odd right component of the rectangular half wave							
36	$C_1(Re_1+jIm_1)$	$C_2(Re_2+jIm_2)$	$C_3(Re_3+jIm_3)$	$C_4(Re_4+jIm_4)$	$C_5(Re_5+jIm_5)$	$C_6(Re_6+jIm_6)$	$C_7(Re_7+jIm_7)$	$C_8(Re_8+jIm_8)$
37	0+j0	1-j2.4142	0+j0	1-j0.4142	0+j0	1+j0.4142	0+j0	1+j2.4142
38	Inverse Samples of the {Complex coefficients of the ½ event left component + Complex coefficients of the ½ odd right component of the rectangular half wave} – Time Domain							
39	0.5	0.5	0.5	0.5	-0.5	-0.5	-0.5	-0.5
40	Complex coefficients of the ½ event left component -Complex coefficients of the ½ odd right component of the rectangular half wave							
41	$C_1(Re_1+jIm_1)$	$C_2(Re_2+jIm_2)$	$C_3(Re_3+jIm_3)$	$C_4(Re_4+jIm_4)$	$C_5(Re_5+jIm_5)$	$C_6(Re_6+jIm_6)$	$C_7(Re_7+jIm_7)$	$C_8(Re_8+jIm_8)$
42	4+j0	0+j0	0+j0	0+j0	0+j0	0+j0	0+j0	0+j0
43	Inverse Samples of the {Complex coefficients of the ½ event left component -Complex coefficients of the ½ odd right component of the rectangular half wave} – Time Domain							
44	0.5	0.5	0.5	0.5	0.5	0.5	0.5	0.5
45	Complex coefficients of the {Complex coefficients of the ½ event left component + Complex coefficients of the ½ odd right component of the rectangular half wave} + {Complex coefficients of the ½ event left component -Complex coefficients of the ½ odd right component of the rectangular half wave}							
46	4+j0	1-j2.4142	0+j0	1-j0.4142	0+j0	1+j0.4142	0+j0	1+j2.4142
47	Inverse Samples of the {Complex coefficients of the ½ event left component + Complex coefficients of the ½ odd right component of the rectangular half wave} + {Complex coefficients of the ½ event left component -Complex coefficients of the ½ odd right component of the rectangular half wave} – Time Domain							
48	Initial Rectangular Half Wave							
49	1.0	1.0	1.0	1.0	0.0	0.0	0.0	0.0

16 Samples Symmetric and Anti Symmetric Numerical Examples

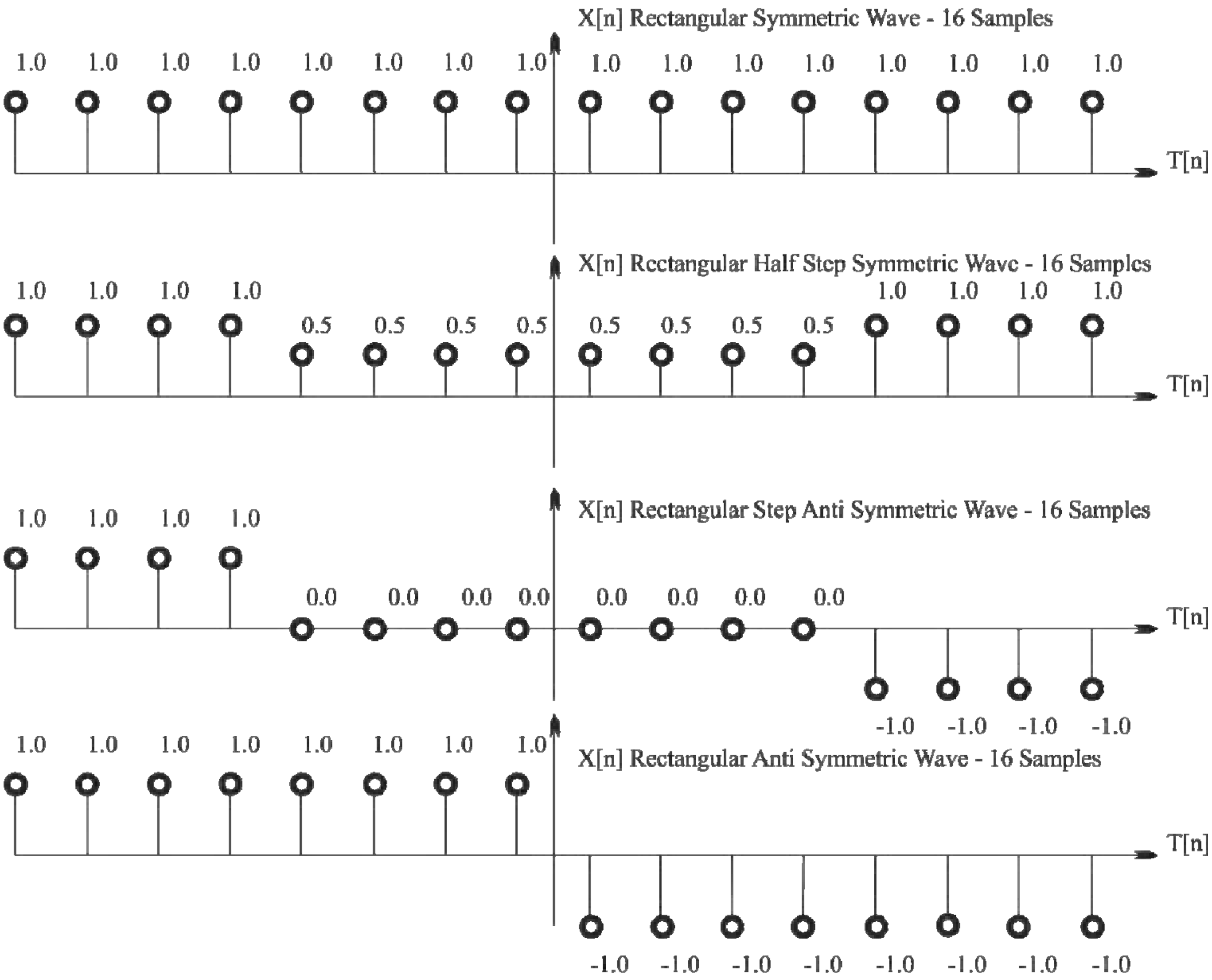

Fig. 6. Symmetric and Anti Symmetric Numerical examples, which illustrate the proof of the Theorem 6.
6.1) Full Rectangular Wave
6.2) Rectangular Half Step Symmetric Wave
6.3) Rectangular Step Anti Symmetric Wave
6.4) Rectangular Full Anti Symmetric wave

The Fourier complex spectra Y9 Octable Triangular Anti Symmetric Wave of the anti symmetric common function for this numerical example can be obtained by summarizing the Fourier complex spectra Y9 Octable Triangular Anti Symmetric Wave Left and the Fourier complex spectra Y9 Octable Triangular Anti Symmetric Wave Right.

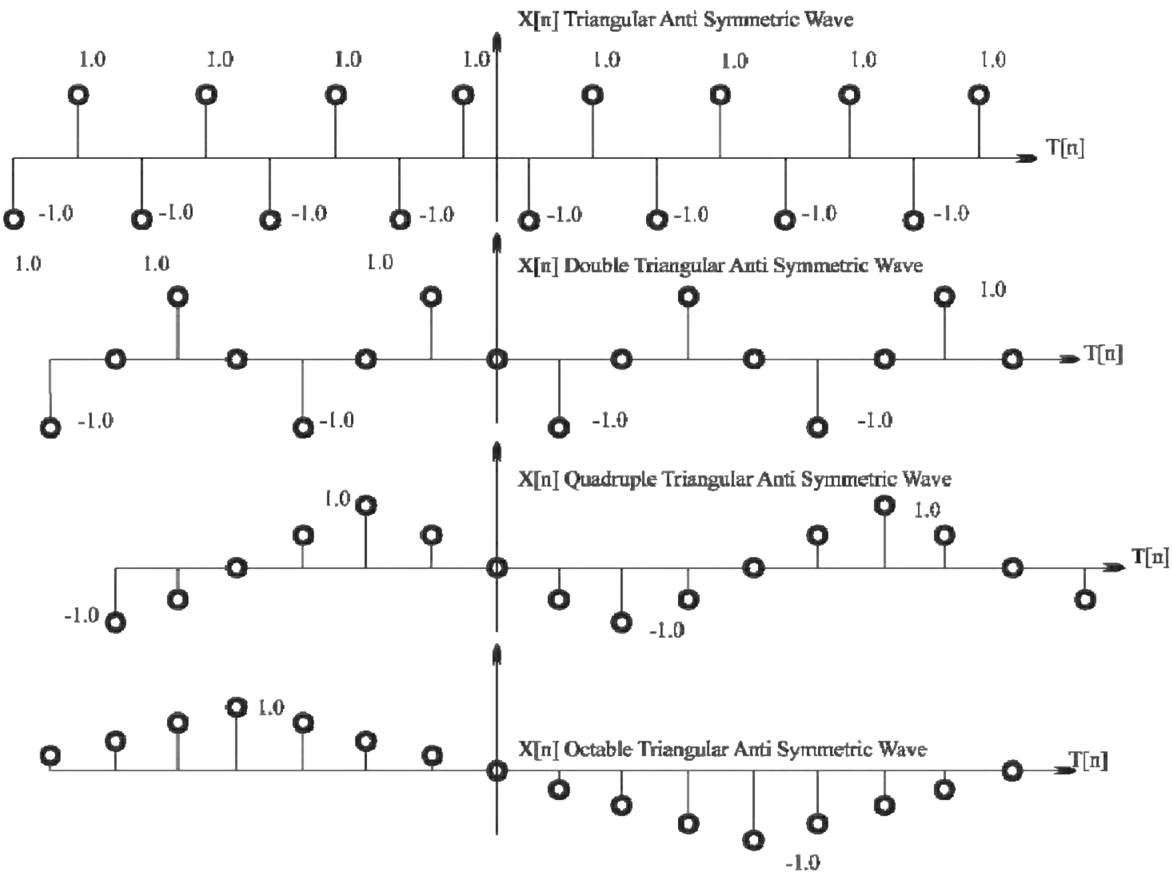

Fig. 7. Anti Symmetric Numerical examples, which illustrate the proof of the Theorem 6.
7.1) Triangular Anti Symmetric Wave
7.2) Double Triangular Anti Symmetric Wave
7.3) Quadruple Triangular Anti Symmetric Wave
7.4) Octable Triangular Anti Symmetric wave

6 CONCLUSIONS

The strategy of spectral even-odd decomposition of the arbitrary real function described in the paper allows constructing complex Fourier spectrum of initial signal with the length N in the time domain base on the equivalent real and imaginary spectral parts with the length N/2 in the frequency domain. The Spectral Even-Odd Decomposition of Arbitrary Real Signals is shown in the figure 8.

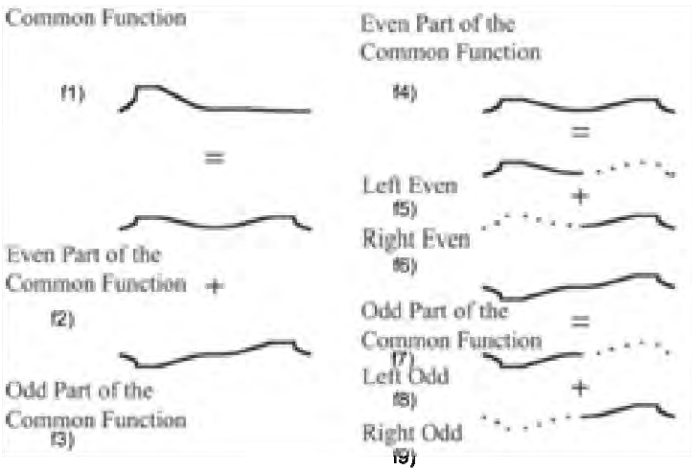

Fig. 8. Spectral Even-Odd Decomposition of Arbitrary Real Signal f1.

In the figure 8 the “black” line corresponds to nonzero values of the corresponding equivalent functions. The “points” line corresponds to zero values of the corresponding equivalent signals. On one hand the function f1 could be obtained by summarizing of functions f2 and f3 according to formulae (12). Function f4 could be obtained by summarizing of functions f5 and f6. Function f7 could be obtained by summarizing of functions f8 and f9. Function f5 could be obtained by replacing the right side of the function f4 with zeros. Function f6 could be obtained by replacing the left side of the function f4 with zeros. Function f8 could be obtained by replacing the right side of the function f7 with zeros. Function f9 could be obtained by replacing the left side of the function f7 with zeros. On the other hand the function f1 could be obtained by summarizing of the functions f5, f6, f8 and f9.

ACKNOWLEDGEMENT

The authors express their acknowledgment to “GPS Control” SA, “Aquapartner” Ltd and “Tokuda broker” Ltd for the financial support of this study.

7 REFERENCES

[1] Philipoff Ph., N.Shopolov, K.Ishtev, P.Dineva, (1997), “Wave Propagation in Multilayered Media”, Pergamon, Nonlinear Analysis, Theory, Methods & Applications, Vol.30, No.4, pp. 2031-2040.

[2] Philipoff Ph., (2003), SH Wave Propagation trough Multilayer Media, Journal of Theoretical and Applied Mechanics N3, pp. 79-98.

[3] Philipoff Ph., Ph.Michaylov, (2007), *“BELENE Nuclear Power Plant Numerical and Experimental Bedrock, Layers and Surface Signals”*, J. Applied Mathematical Modeling, 31 (2007), pp. 1889-1898, Elsevier.

[4] Philipoff Ph., Ph.Michaylov, (2007), *“BELENE” Nuclear Power Plant Numerical and Experimental Free Field Signals*, Siberian Journal Applied Mathematics, RAN – Siberian Branch Novosibirsk, (Сибирский журнал вычислительной математики, РАН, Сиб.отд-ние Новосибирск, том 10, N1, стр. 105-122), v.10, N1, pp. 105-122.

[5] Venelin Jivkov, Philip Philipoff, Anastas Ivanov, Mario Munoz, Galerida Raikova, Mikhail Tatur, Philip Michaylov, (2013), Spectral properties of quadruple symmetric real functions. Applied Mathematics and Computation 221 (2013) pp. 344–350

[6] Alexander Poularikas, (2010), Transforms and Applications for Engineers with Examples and MATLAB, CRC Press is an imprint of Taylor & Francis Group, an Informa business, International Standard Book Number-13: 978-1-4200-8932-5 (Ebook-PDF), statement 3.1 pp-73, statements 3.15 and 3.16 pp-75.

[7] Vasilev G., M. Ivanova, Z. Bonev, (2014), Long in plan buried structures subjected to seismic wave propagation, Mistal Service sas Via U. Bonino, 3, 98100 Messina (Italy), ISBN: 978-88-98161-05-8

[8] Meirovitch Leonard, (1986), Elements of Vibration Analysis, Mc Graw-Hill Book Company, 1986, pp – 559.

[9] Smirnoff, V.I., (1974), Course of Higher Mathematics, v.1, “Nauka”, Moscow, 1974, pp - 225, (in Russian).

[10] MATLAB, <http://www.mathworks.com/products/matlab/>, 2010.

SUMMARY

QUADRUPLE SYMMETRIC REAL SIGNALS SPECTRAL EVEN AND ODD DECOMPOSITION

Venelin JIVKOV
Philip PHILIPOFF

The spectral properties of quadruple symmetric real signals are analyzed in the study. Six number theorems are formulated and proofed analytically in a capacity of central results of the research. Lasted theorem could be used to construct complex Fourier spectrum for arbitrary real function by even – odd decomposition. The theorem is illustrated numerically. The initial signal with length N (analogous values length interval or number of discrete samples) in the time domain is Fourier transformed through two spectral - real and imaginary parts with length N in the frequency domain. The real and imaginary parts of the complex Fourier spectrum of the initial signal, could be obtained by procedure, described in the paper. Spectral parts could be calculated by equivalent functions-signals. Even left and odd right equivalent functions-signals contain N/2 nonzero analogous values or discrete samples. This strategy allows constructing complex Fourier spectrum of the initial signal with length N in the time domain based on equivalent real and imaginary spectral parts with the length N/2 in the frequency domain. The study is an extension and resumé of AMC 221(2013) pp. 344-350.

Key words: Quadruple symmetric real signals, Symmetry - Conjugation relation, Spectral even-odd decomposition

REZIME

SPEKTRALNA DEKOMPOZICIJA ČETVOROSTRUKO SIMETRIČNIH REALNIH SIGNALA PARNIM I NEPARNIM DELOVIMA SIGNALA

Venelin JIVKOV
Philip PHILIPOFF

U ovom radu su analizirane spektralne karakteristike četvorostruko simetričnih realnih signala. Analitički je formulisano i testirano šest teorema kao centralni rezultat istraživanja. Poslednja (šesta) teorema se može koristiti za proračun *Fourier*-ovog spektra proizvoljne realne funkcije dekompozicijom parnim i neparnim delovima signala. Teorema je ilustrovana numerički. Transformacija inicijalnog signala dužine *N* (broj diskretnih vrednosti) iz vremenskog domena u frekventan domen je sprovedena *Fourier*-ovim transformacijama kroz dva spektralna realna i imaginarna dela dužine *N*. Realni i imaginarni deo kompleksnog *Fourier*-ovog spektra inicijalnog signala može se proračunati primenom ekvivalentnih funkcija (signala). Leve parne i desne neparne ekvivalentne funkcije (signali) sadrže *N*/2 nenulte analogne vrednosti ili diskretne uzorke. Ova strategija omogućava izgradnju kompleksnog *Fourier*-ovog spektra, inicijalnog signala dužine *N* u vremenskom domenu, ekvivalentnim realnim i imaginarnim spektralnim delovima dužine *N*/2 u frekventnom domenu. Studija bi mogla da se posmatra kao nastavak i rezime istraživanja (*Jivkov et all*, 2013).

Ključne reči: četvorostruko simetrični realni signal, relacija (odnos) simetrija - konjugacija, spektralna dekompozicija parnim i neparnim delovima signala

IN MEMORIAM

Profesor dr **SRĐAN VENEČANIN**, dipl.inž.građ.
1930-2016

Profesor dr Srđan Venečanin, diplomirani inženjer građevinarstva, zauvek nas je napustio 15. maja 2016. godine u Beogradu. Rođen je 22. aprila 1930. godine u Beogradu. Osnovnu školu i gimnaziju završio je u Beogradu. Građevinski fakultet završio je u Beogradu, gde je i doktorirao 1983. godine. Specijalizaciju je završio u Roterdamu u Holandiji 1970. godine. Radio je u Vojno-tehničkom institutu i u „Mašinoprojektu" u Beogradu. Godine 1960. izabran je u zvanje asistenta, na Građevinskom fakultetu u Beogradu. Od 1984. do 1991. radio je u zvanju docenta na predmetu Betonski mostovi (BM). Od 1991. godine je redovni profesor na Univerzitetu u Novom Sadu, Građevinskom fakultetu Subotica, gde je predavao Betonske mostove i Tehnologiju betona, sve do odlaska u penziju 1997. godine. Poglavlje armirano betonski (AB) mostovi u Tehničaru 5, Građevinska knjiga, 1987. str. 1137-1179, je korišćeno u nastavi predmeta Betonski mostovina na više Grеđevinskih fakulteta u našoj Zemlji.

Osim problemima betonskih konstrukcija, naročito mostova, bavio se problemima trajnosti betona pod temperaturnim dejstvima, posebno u vrućim klimatima Srednjeg istoka. Bio je član Američkog instituta za beton (ACI), Društva za beton (Concrete Sociate – Engleska) i Međunarodnog udruženja za mostove i visoke zgrade (IABSE–Cirih). Valja pomenuti da je bio aktivan član i „Recognized Member", više od 15 godina Komiteta 201 – Trajnost betona, i član Komiteta 343 – Projektovanje BM i 345 – Izgradnja i održavanje BM (ACI i IABSE). Bio je ACI Komiteta 201 za trajnost betona.

Njegova naučna delatnost nastavlja se intenzivnim radom pri izradi doktorske disertacije na temu: „Uticaj termičke nekompatibilnosti betona na njegovu čvrstoću" pod mentorstvom akademika profesora Đorđa Lazarevića. Analitički deo njegovog doktorata zasnivao se na opsežnim eksperimentima obavljenim u laboratoriji Instituta za materijale i konstrukcije Građevinskog fakulteta u Beogradu i u laboratoriji Vojno-tehničkog instituta u Beogradu. Eksperimentima je pokazano da pri izboru agregata kod betonskih konstrukcija izloženih atmosferskim uticajima mora da se vodi računa o tome da se koeficijent termičke dilatacije (KTD) agregata ne razlikuje mnogo od KTD cementnog tela. Pokazano je da je izbor adekvatnog krečnjačkog agregata naročito važan u područjima gde su temperaturna kolebanja velika, pogotovo u vrućim klimatima Srednjeg istoka, Afrike, Indije i tako dalje.

Njegovi publikovani i saopšteni radovi obuhvataju sledeće oblasti: Istraživanje termičkog ponašanja i trajnosti betonskih konstrukcija; Istraživanja racionalnih rešenja mostova; Istraživanja oštećenja i reparatura betonskih konstrukcija; Radovi iz oblasti regulative za probleme definisanja opterećenja mostova i konstruisanja armiranobetonskih ploča u konstrukcijama.

Radovi u vezi s problemima trajnosti betona BM, pod temperaturnim opterećenjima, štampani su u više desetina domaćih i inostranih stručnih i naučnih časopisa i u saopštenjima s naučnih skupova. Ovi radovi predstavljaju značajan doprinos oblastima termičkog ponašanja i trajnosti betonskih konstrukcija i našli su široku primenu i publikovanje u zemlji i inostranstvu.

Preko dvadeset radova štampao je u uglednim naučnim i stručnim časopisima u svetu. Među publikovanim radovima su i oni pisani za naš časopis. Posebnu pažnju svetske naučne javnosti privukli su radovi štampani u uglednim naučnim časopisima, ali i njegova usmena izlaganja na engleskom jeziku u Nemačkoj (Eslinen), Francuskoj (Versaj), Kanadi (Otava), Iraku (Bagdad), Libiji (Tripoli), Finskoj (Espu) i drugde. Posebno se ističu, sa zapaženim odjekom – velikim brojem citata, radovi u kojima je jedini autor:

Influence of Temperature on Deterioration of Concrete in the Middle East; Concrete, Vol. 11, 8 (1977), 31–32;

Thermal Incompatibility of Concrete Components and Thermal Properties of Carbonate Rocks; ACI Materials Journal (USA), Nov-Dec. (1990), 602–607;

Early Deterioration of Concrete Bridge Slabs Due to the Effects of Concrete Strength Reduction and Compressive Overstress; Structural Engineering Review, Vol. 4, 3 (Pergamon Press 1992), 203–209.

Ovi su radovi citirani više od 40 puta samo prema Science Citation Index-u, kao i mnogo puta u drugim inostranim i domaćim časopisima, magistarskim i doktorskim tezama i knjigama. Profesor A. M. Neville sa Univerziteta u Lidsu, Velika Britanija, u svom poslednjem (petom) izdanju knjige „Properties of Concrete – Svojstva betona“ citira njegove radove. Iako po prirodi veoma tih i skroman, s ponosom je pominjao ovaj podatak kojim je, za nas koji znamo značaj ovog dometa, afirmisao našu sredinu i zemlju koju je na naučnom polju, neretko, uspešno reprezentovao.

Pored naučnog i nastavnog rada bavio se i projektovanjem, sanacijama i stručnim konsultacijama. Izvedeni projekti: Studentski dom kulture na Novom Beogradu sa ljuskom oblika hiperboličnog paraboloida prednapregnutog po ivicama, čime su izbegnute deformacije koje se javljaju kod ostalih sličnih izvedenih ljuski. Po njegovim projektima izvedena su i tri mosta od prednapregnutog betona u Crnoj Gori na reci Zeta kod Nikšića, sanacija mostova od prednapregnutog betona na prilazima Pančevačkom mostu preko Dunava, kao i sanacija mosta u Pirotu preko reke Nišave. Za most od prednapregnutog betona preko reke Vrbas u Banjaluci (sa S. Rankovićem) projektant je idejnog rešenja. Učestvovao je u stručnim konsultacijama prilikom gradnje hidroelektrane „Đerdap“, koje su održavane na srpskoj i rumunskoj obali. Uvršten je u knjigu „Who's who in Computational Science and Engineering“, izdanje štampano u Velikoj Britaniji za godinu 2005–2006.

Penzionisan je u zvanju redovnog profesora Univerziteta u Novom Sadu, Građevinskog fakulteta Subotica 1997. godine.

Iz prikaza izuzetno bogate stručne, naučne i nastavne delatnosti vidi se da je prof. dr Srđan Venečanin, dipl. inž. građevine, dao značajan doprinos oblasti tehnologije betona i betonskih mostova. Biće upamćen kao izuzetno plodan istraživač, stručnjak i pedagog. On je svojim rezultatima i njihovim odjekom stekao veliki ugled, ne samo u našoj zemlji, već i u inostranstvu. Njegova smrt je veliki gubitak ne samo za porodicu, već i za sve nas koji smo ga poznavali i radili s njim.

Juna, 2016. godine

Radomir Folić i
Aleksandar Prokić

UPUTSTVO AUTORIMA*

Prihvatanje radova i vrste priloga

U časopisu Građevinski materijali i konstrukcije štampaće se neobjavljeni radovi ili članci i konferencijska saopštenja sa određenim dopunama ili bez dopuna. prema odluci Redakcionog odbora. a samo izuzetno uz dozvolu prethodnog izdavača prihvatiće se i objavljeni rad. Vrste priloga autora i saradnika koji će se štampati su: originalni naučni radovi. prethodna saopštenja. pregledni radovi. stručni radovi. konferencijska saopštenja (radovi sa naučno-stručnih skupova). kao i ostali prilozi kao što su: prikazi objekata i iskustava - primeri. diskusije povodom objavljenih radova i pisma uredništvu. prikazi knjiga i zbornika radova. kao i obaveštenja o naučno-stručnim skupovima.

Originalni naučni rad je primarni izvor naučnih informacija i novih ideja i saznanja kao rezultat izvornih istraživanja uz primenu adekvatnih naučnih metoda. Dobijeni rezultati se izlažu kratko. jasno i objektivno. ali tako da poznavalac problema može proceniti rezultate eksperimentalnih ili teorijsko numeričkih analiza i tok razmišljanja. tako da se istraživanje može ponoviti i pri tome dobiti iste ili rezultate u okvirima dopuštenih odstupanja. kako se to u radu navodi.

Prethodno saopštenje sadrži prva kratka obaveštenja o rezultatima istraživanja ali bez podrobnih objašnjenja. tj. kraće je od originalnog naučnog rada. U ovu kategoriju spadaju i diskusije o objavljenim radovima ako one sadrže naučne doprinose.

Pregledni rad je naučni rad koji prikazuje stanje nauke u određenoj oblasti kao plod analize. kritike i komentara i zaključaka publikovanih radova o kojima se daju svi neophodni podaci pregledno i kritički uključujući i sopstvene radove. Navode se sve bibliografske jedinice korišćene u obradi tematike. kao i radovi koji mogu doprineti rezultatima daljih istraživanja. Ukoliko su bibliografski podaci metodski sistematizovani. ali ne i analizirani i raspravljeni. takvi pregledni radovi se klasifikuju kao stručni pregledni radovi.

Stručni rad predstavlja koristan prilog u kome se iznose poznate spoznaje koje doprinose širenju znanja i prilagođavanja rezultata izvornih istraživanja potrebama teorije i prakse. On sadrži i rezultate razvojnih istraživanja.

Konferencijsko saopštenje ili rad sopšten na naučno-stručnom skupu koji mogu biti objavljeni u izvornom obliku ili ih autor. u dogovoru sa redakcijom. bitno preradi i proširi. To mogu biti naučni radovi. naročito ako su sopštenja po pozivu Organizatora skupa ili sadrže originalne rezultate prvi put objavljene. pa ih je korisno uz određene dopune učiniti dostupnim široj stručnoj javnosti. Štampaće se i stručni radovi za koje Redakcioni odbor oceni da su od šireg interesa.

Ostali prilozi su prikazi objekata. tj. njihove konstrukcije i iskustava-primeri u građenju i primeni različitih materijala. diskusije povodom objavljenih radova i pisma uredništvu. prikazi knjiga i zbornika radova. kao i obaveštenja o naučno-stručnim skupovima.

Autori uz rukopis predlažu kategorizaciju članka. Svi radovi pre objavljivanja se recenziraju. a o prihvatanju za publikovanje o njihovoj kategoriji konačnu odluku donosi Redakcioni odbor.

Da bi se ubrzao postupak prihvatanja radova za publikovanje. potrebno je da autori uvažavaju Uputstva za pripremu radova koja su navedena u daljem tekstu.

Uputstva za pripremu rukopisa

Rukopis otkucati jednostrano na listovima A-4 sa marginama od 31 mm (gore i dole) a 20 mm (levo i desno). u Wordu fontom Arial sa 12 pt. Potrebno je uz jednu kopiju svih delova rada i priloga. dostaviti i elektronsku verziju na navedene E-mail adrese. ili na CD-u. Autor je obavezan da čuva jednu kopiju rukopisa kod sebe zbog eventualnog oštećenja ili gubitka rukopisa.

Od broja 1/2010. prema odluci Upravnog odbora Društva i Redakcionog odbora. radovi sa pozitivnim recenzijama i prihvaćeni za štampu. publikovaće se na srpskom i engleskom jeziku.

Svaka stranica treba da bude numerisana. a optimalni obim članka na jednom jeziku. je oko 16 stranica (30000 slovnih mesta) uključujući slike. fotografije. tabele i popis literature. Za radove većeg obima potrebna je saglasnost Redakcionog odbora.

Naslov rada treba sa što manje reči (poželjno osam. a najviše do jedanaeset) da opiše sadržaj članka. U naslovu ne koristiti skraćenice ni formule. U radu se iza naslova daju ime i prezime autora. a titule i zvanja. kao iime institucije u podnožnoj napomeni. Autor za kontakt daje telefone. faks i adresu elektronske pošte. a za ostale autore poštansku adresu.

Uz sažetak (rezime) od oko 150 do 200 reči. na srpskom i engleskom jeziku daju se ključne reči (do deset). To je jezgrovit prikaz celog članka i čitaocima omogućuje uvid u njegove bitne elemente.

Rukopis se deli na poglavlja i potpoglovlja uz numeraciju. po hijerarhiji. arapskim brojevima. Svaki rad ima uvod. sadržinu rada sa rezultatima. analizom i zaključcima. Na kraju rada se daje popis literature.

Kod svih dimenzionalnih veličina obavezna je primena međunarodnih SI mernih jedinica.

Formule i jednačine treba pisati pažljivo vodeći računa o indeksima i eksponentima. Autori uz izraze u tekstu definšu simbole redom kako se pojavljuju. ali se može dati i posebna lista simbola u prilogu.

Prilozi (tabele. grafikoni. sheme i fotografije) rade se u crno-beloj tehnici. u formatu koji obezbeđuje da pri smanjenju na razmere za štampu. po širini jedan do dva stupca (8cm ili 16.5cm). a po visini najviše 24.5cm. ostanu jasni i čitljivi. tj. da veličine slova i brojeva budu najmanje 1.5mm. Originalni crteži treba da budu kvalitetni i u potpunosti pripremljeni za presnimavanje. Mogu biti i dobre. oštre i kontrastne fotokopije. Koristiti fotogrfije. u crno-beloj tehnici. na kvalitetnoj hartiji sa oštrim konturama. koje omogućuju jasnu reprodukciju. Skraćenice u prilozima koristiti samo izuzetno uz obaveznu legendu. Prilozi se posebno označavaju arapskim brojevima. prema redosledu navođenja u tekstu. Objašnjenje tabela daje se u tekstu.

Potrebno je dati spisak svih skraćenica korišćenih u tekstu.

U popisu literature na kraju rada daju se samo oni radovi koji se pominju u tekstu. Citirane radove treba prikazati po azbučnom redu prezimena prvog autora. Literaturu u tekstu označiti arapskim brojevima u uglastim zagradama. kako se navodi i u Popisu citirane literature. napr [1]. Svaki citat u tekstu mora se naći u Popisu citirane literature i obrnuto svaki podatak iz Popisa se mora navesti u tekstu.

U Popisu literature se navode prezime i inicijali imena autora. zatim potpuni naslov citiranog članka. iza toga sledi ime časopisa. godina izdavanja i početna i završna stranica (od - do). Za knjige iza naslova upisuje se ime urednika (ako ih ima). broj izdanja. prva i poslednja stranicapoglavlja ili dela knjige. ime izdavača i mesto objavljivanja. ako je navedeno više gradova navodi se samo prvi po redu. Kada autor citirane podatke ne uzima iz izvornog rada. već ih je pronašao u drugom delu. uz citat se dodaje «citirano prema...». Neobjavljeni članci mogu se pominjati u tekstu kao «usmeno saopštenje»

Autori su odgovorni za izneseni sadržaj i moraju sami obezbediti eventualno potrebne saglasnosti za objavljivanje nekih podataka i priloga koji se koriste u radu.

Ukoliko rad bude prihvaćen za štampu. autori su dužni da. po uputstvu Redakcije. unesu sve ispravke i dopune u tekstu i prilozima.

Za detaljnija tehnička uputstva za pripremu rukopisa autori se mogu obratiti Redakcionom odboru časopisa.

Rukopisi i prilozi objavljenih radova se ne vraćaju. Sva eventualna objašnjenja i uputstva mogu se dobiti od Redakcionog odbora.

Radovi se mogu slati i na e-mail: folic@uns.ac.rs ili miram@uns.ac.rs i dimk@ptt.rs

Veb sajt Društva i časopisa: www.dimk.rs

* **Uputstvo autorima je modifikovano i treba ga u pripremi radova slediti.**

Izdavanje časopisa "Građevinski materijali i konstrukcije" finansijski su pomogli:

INŽENJERSKA KOMORA SRBIJE

REPUBLIKA SRBIJA
MINISTARSTVO PROSVETE, NAUKE I TEHNOLOŠKOG RAZVOJA

UNIVERZITET U BEOGRADU
GRAĐEVINSKI FAKULTET

DEPARTMAN ZA GRAĐEVINARSTVO I GEODEZIJU
FAKULTET TEHNIČKIH NAUKA NOVI SAD

INSTITUT IMS AD, BEOGRAD

UNIVERZITET CRNE GORE
GRAĐEVINSKI FAKULTET - PODGORICA